Acta Universitatis Agriculturae Sueciae

Doctoral Thesis No. 2025:40
Faculty of Forest Sciences

Making better use of sample data: estimation of plant abundance and associated uncertainties

Léna Gozé

Making better use of sample data: estimation of plant abundance and associated uncertainties

Léna Gozé
Faculty of Forest Sciences
Department of Forest Resource Management
Umeå

SWEDISH UNIVERSITY
OF AGRICULTURAL
SCIENCES

DOCTORAL THESIS
Umeå 2025

Acta Universitatis Agriculturae Sueciae
2025:40

Cover: Arctic starflower (*Lysimachia europaea*) (photo by Jenny Svennås-Gillner, SLU, 2015)

ISSN 1652-6880
ISBN (print version) 978-91-8046-475-8
ISBN (electronic version) 978-91-8046-525-0
https://doi.org/10.54612/a.3a4d2oki20
© 2025 Léna Gozé, https://orcid.org/0000-0001-8974-1996
Swedish University of Agricultural Sciences, Department of Forest Resource Management, Umeå, Sweden

Print: SLU Grafisk service, Uppsala 2025

Making better use of sample data: estimation of plant abundance and associated uncertainties

Abstract

Environmental monitoring has become increasingly important in the current context of global ecological change. More directives and reporting guidelines are issued, hence the need for additional methods for exploiting data from environmental monitoring programmes in order to obtain relevant information about the current state of forests and landscapes. National monitoring programmes, such as the Swedish National Forest Inventory and the National Inventory of Landscapes in Sweden, are core infrastructures for describing and analysing state and change in terrestrial ecosystems. These programmes have large, but not fully exploited potential as a basis for basic and applied research. This thesis aims to develop and apply novel tools for analysing presence/absence (P/A) data from environmental monitoring programmes. Although the area of spatial statistics has been extensively studied, the issue of relating P/A data to plant abundance is an underdeveloped field that needs further attention. The primary goal of this thesis is thus to estimate plant abundance both locally and across large regions for various species. Such plant abundance estimators are derived through models for spatial distribution of plants, by using inhomogeneous point process models that are capable of modelling various categories of point patterns across the landscape, taking geographical covariate information into account. The methods are applied to data collected in the field as well as simulated data to assess the performance of the estimators of plant abundance and associated estimators of uncertainty. The results are promising and show the potential of P/A data in environmental analyses. Another objective of this thesis is to provide reliable estimators of uncertainty in different contexts, with a particular study that takes into account several sources of uncertainty when applying model-based inference (Paper IV). That study shows that the variance of a predictor is a fairly good approximation of uncertainty in large-area surveys, whereas other components come into play when the study area is decreased.

Keywords: Presence/absence data, plant density, model-based inference, generalised linear models, forest inventory data, spatial point processes, uncertainty analysis

Effektivare användning av stickprovsdata: skattning av planttäthet och tillhörande osäkerhet

Sammanfattning

Miljöövervakning har fått allt större betydelse i samband med globala miljöförändringar. Ett ökande antal direktiv och rapporteringskrav utfärdas, vilket kräver utveckling av metoder som stärker användandet av data från miljöövervakningsprogram och som ger relevant information om statusen för skogar och landskap. Nationella övervakningsprogram, som Riksskogstaxeringen och Nationell Inventering av Landskapet i Sverige (NILS), fungerar som viktiga infrastrukturer för att beskriva och analysera tillstånd och förändringar som sker i miljön. Dessa program representerar stora men underutnyttjade möjligheter som bas för grundläggande och avancerad forskning. Det primära målet med denna avhandling är att skapa och implementera nya verktyg för att analysera närvaro-/frånvaro-data (N/F-data) som härrör från miljöövervakningsprogram. Även om området för rumslig statistik har utforskats i stor utsträckning, kvarstår utmaningar med att koppla N/F-data till planttäthet, vilket motiverar ytterligare studier. Ett syfte med denna avhandling är därför att skatta planttäthet både lokalt och över större geografiska regioner för olika arter baserat på N/F-data. Planttäthet skattas via modeller för den rumsliga fördelningen av växter, med ickehomogena punktprocessmodeller som kan ta hänsyn till olika typer av punktmönster över landskapet, samt genom att integrera geografisk kovariatinformation i beräkningarna. För att utvärdera skattningar av planttäthet och tillhörande osäkerhet i skattningar tillämpas metoderna på såväl faktiska fältdata som simulerade data. Resultaten är lovande och belyser potentialen hos N/F-data inom miljöanalys. Ett annat mål med avhandlingen är att ta fram tillförlitliga skattningar av osäkerhet i olika sammanhang, med en specifik studie som behandlar olika osäkerhetskällor inom modellbaserad inferens (papper IV). Den studien visar att för t.ex. en predikterad mängd biomassa ger variansen en bra approximation av osäkerhet vid storskaliga undersökningar, medan andra komponenter kan få större betydelse ifall studieområdet är mindre.

Nyckelord: Närvaro- och frånvarodata, planttäthet, modellbaserad inferens, generaliserade linjära modeller, skoglig inventering, punktprocesser, osäkerhetsanalys

Contents

List of publications

This thesis is based on the work contained in the following papers, referred to by Roman numerals in the text:

I. Gozé, L., Ekström, M., Wallerman, J., Dahlgren, J., Jonsson, B. G., Sandring, S., & Ståhl, G. Large-area estimation of plant density using presence/absence data and binary regression, and a correlation test of the binary regression model (manuscript).

II. Gozé, L., Ekström, M., Sandring, S., Jonsson, B. G., Wallerman, J., & Ståhl, G. (2024). Estimation of plant density based on presence/absence data using hybrid inference. Ecological Informatics, 80, 102377. https://doi.org/10.1016/j.ecoinf.2023.102377

III. Ekström, M., Gozé, L., Sandring, S., Jonsson, B. G., Wallerman, J., & Ståhl, G. Estimation of parameters in inhomogeneous Neyman-Scott processes using presence/absence data (submitted).

IV. Ståhl, G., Gozé, L., Papucci, E., Gobakken, T., Saarela, S., Healey, S. P., Yang, Z., Ekström, M., Kellner, J., Hou, Z., Xu, Q., Ørka, H. O., Næsset E. , McRoberts, R. E. A closer look at uncertainties in forest ecosystem surveys using remotely sensed data and model-based inference (submitted).

Paper II is published open access.

The contribution of Léna Gozé to the papers included in this thesis was as follows:

I. Wrote a major part of the main draft, performed the analyses and simulations and contributed to the theoretical developments.

II. Wrote the main draft, performed the analyses and simulations and contributed to the theoretical developments.

III. Performed analyses and simulations, contributed critically to the main draft and contributed to the theoretical developments.

IV. Performed the simulation study and produced the results, contributed critically to the main draft.

List of figures

Abbreviations

ACL	Actual Confidence Level
AGB	Aboveground Biomass
ALS	Airborne Laser Scanning
EU	European Union
GEDI	Global Ecosystem Dynamics Investigation
GLM	Generalised Linear Model
i.i.d.	independent and identically distributed
LGCP	Log-Gaussian Cox Process
MSE	Mean Squared Error
NFAM	National Forest Attribute Map
NFI	National Forest Inventory
NILS	National Inventory of Landscapes in Sweden
NSP	Neyman-Scott Process
p.d.f.	Probability distribution function
P/A	Presence/Absence
PPP	Poisson Point Process
RS	Remote Sensing
SRS	Simple Random Sampling
USA	United States of America

1. Introduction

1.1 Motivation

Vegetation monitoring has long played a central role in the study of ecosystem processes (Elzinga et al. 1998; Bonham 2013). In the context of the current environmental crisis, the study of plant populations is more important than ever as part of ecological assessments, including biodiversity quantification, tracking of threatened or invasive species, and evaluation of restoration effectiveness. In particular, it is of interest to understand the current state of plant populations and communities and how they evolve with time. Plant occurrence and abundance are good indicators of biodiversity status and can be used to evaluate state and change that are relevant for ecosystem function and resilience. In this thesis, emphasis is made on non-tree vegetation in Papers I, I and III, and on vegetation in a broader sense (in the form of biomass) in Paper IV.

Legal directives (e.g., the EU's Habitats Directive (Commission of the European Communities 2003); or the EU's Biodiversity and Forestry strategies (The European Commission 2020, 2021)) were instituted and require the regularity of reports of vegetation characteristics. Hence, one of the primary objectives is to estimate the number of plants (i.e., plant abundance) in forests.

Environmental monitoring programs such as the Swedish National Forest Inventory (NFI, Fridman et al. 2014) and the National Inventory of Landscapes in Sweden (NILS, Ståhl et al. 2011a) perform different types of inventories in order to collect data on the current state of forests and landscapes in the entirety of Sweden. Similar programs exist in other countries (Tomppo et al. 2010). These infrastructures have large, but not fully exploited potential for performing environmental analyses. Therefore, this thesis aims at developing new methods to make better use of the largely untapped data in the environmental monitoring programmes' databases, with an emphasis on presence/absence (P/A) data.

Monitoring data can be gathered in several ways. For instance, using sample plots is a widespread method to register information on plants in the field (Gregoire & Valentine 2007). Sample plots, generally of circular shape (although they can also be of, e.g., quadratic shape), are placed in a region of interest according to some sampling design. Then, registrations and

measurements are made at individual plot level. Sampling designs can be quite simple, like simple random sampling (SRS) or systematic sampling (Thompson 2012), or take more aspects into consideration, like spatially balanced sampling (Grafström et al. 2012; Grafström & Matei 2018). Other methods to make measurements in the field include distance and line transect methods (see Bonham (2013) for an overview).

1.2 How to register plant information?

The basis for vegetation monitoring is well established, but fundamental problems remain. Trees are relatively easy to count and monitor, but this is far from being the case for ground vegetation (Elzinga et al. 1998). How to correctly define a plant individual? The definition differs depending on the kind of plant under study (Bonham 2013). In addition, some plants grow in numbers so high that it is no simple task to count them accurately, not to mention species with clonal growth pattern, or clustering. All these reasons could explain why so many inventories rely on alternatives to counting plant individuals.

There are several alternatives to simple count data. Vegetation cover estimation is relatively common in vegetation studies and inventory programmes (Godínez-Alvarez et al. 2009; Bonham 2013). However, this method is impacted by a phenomenon called observer judgement bias (Gallegos Torell & Glimskär 2009). Surveyors might interpret cover percentage differently, and it is difficult to derive reasonably accurate estimates of plant cover with only the naked eye. This is similar to what could happen with counting plants. Some surveyors could miss individuals, especially if the plants are numerous in a given sample plot. Traditional cover estimates through ocular assessment are prone to significant observer errors, and hence estimates may vary between surveys. This entails a serious risk that results from monitoring are misinterpreted and may result in reported changes that have not occurred in reality. Potentially equally problematic is the fact that the observer-generated variation in cover estimates can become so large that trends are missed due to low power in analyses – in theory, even when there is no bias. As highlighted by Ståhl (2003), these spurious conclusions need to be avoided, stressing the importance of developing improved methods that limit observer bias.

An alternative to vegetation cover estimation is the point intercept method, where a thin device is used to assess what species cover randomly selected points (Rochefort et al. 2013). The proportion of points where the species occurs is used as a measure of plant cover, but since the device cannot be made infinitesimally thin, the methods will usually overestimate cover (Ståhl 2003). Point intercept methods are less prone to judgement bias than ocular assessments, but require large samples and are time-consuming and costly to conduct (Ringvall et al. 2005).

A simpler, cost-effective alternative to all the methods mentioned above is P/A sampling (Elzinga et al. 1998). All that is required with this kind of survey is to verify whether a specific species is present in a given sample plot. In case the species of interest is present, the surveyor enters "1", otherwise they enter "0". No accurate counts or cover estimation are necessary, hence the advantage of the method cost- and time-wise (Ståhl et al. 2017). In addition, the method is less susceptible to surveyor judgement bias compared to the aforementioned types of survey (Ringvall et al. 2005). All the surveyor needs to know is how the species looks like. On the other hand, P/A sampling presents several challenges. For example, P/A data usually do not provide direct information on plant density (defined as the mean number of individuals per unit area, usually square metres or hectares), and plant occurrence frequencies are difficult to interpret due to their dependence on spatial occurrence patterns and plot size (Ståhl et al. 2017). Hence, one of the main motivations for the present thesis is to find new ways to make use of P/A data to obtain information related to plant density, based on model assumptions regarding the spatial distribution of plant individuals. The very same question has been continually studied, recently by, e.g., Fithian et al. (2015), Ståhl et al. (2017, 2020), Gelfand & Shirota (2019) and Ekström et al. (2020). Earlier references are presented in the next subsection.

1.3 Modelling plant locations and estimating plant density: earlier developments

The concept of frequency, which is closely linked to the concept of density, was first used by Raunkiaer in 1909 (English translation in Raunkiaer (1934)). That researcher observed the presence of plant species in a number of sample plots placed in an area of interest. Plant frequency is then defined

as the number of sample plots where the species is present divided by the total number of sample plots.

However, plant frequency estimates are dependent on the spatial distribution of individuals. Poisson point process (PPP) models are often used, explicitly or implicitly, to model locations of plants and other species. PPP models consider the plant locations as randomly distributed and independent of each other. A closely related point process is the binomial point process, where the point locations are considered random but the process will always generate a fixed number of points (Baddeley et al. 2016).

Works that attempt to find suitable ways to estimate plant density from P/A data assuming random populations date back from at least the start of the twentieth century, with the pioneering article by Arrhenius (1921). There, the author considered P/A data under a binomial point process and estimated the number of species in an area of interest. Later, Kylin (1926) derived a formula for the expected proportion of sampling plots in which the species would be absent, assuming individuals are randomly distributed in the study area. Under the same assumption, Blackman (1935) stated that if the percentage of absence is known then the density can be deduced. In the discussion of the same article by Bartlett, an estimate of the probability of absence in a plot was derived, followed by an estimator for the density as well as a corresponding estimate of variance, based on plant occurrence proportions. Bartlett further stated that the most efficient plot size for density estimation corresponds to around 20% absence of the species under study (Bartlett 1948). Aberdeen (1958) developed a formula that links sample plot size, plant size, plant density and frequency under the assumption of a PPP for plant positions and SRS for the sampling design. Later, Greig-Smith (1983) proposed a model that describes the relationship between frequency and density when plant individuals are randomly distributed. Swindel (1983) determined the optimal size and number of plots to estimate density from P/A data when the plant locations are supposed to be at random. Later, Ståhl et al. (2020) estimated plant density from P/A data with an explicit assumption about a homogeneous PPP in the special case where sample plot sizes vary.

However, plant individuals are rarely randomly distributed (Bonham 2013). Additional assumptions might be needed, as some plant patterns exhibit spatial dependence. Clustered patterns began to be studied around the second half of the twentieth century, although the following studies did not

necessarily handle P/A data. Thomas (1949) proposed a method to estimate density for clustered plant populations based on abundance data. The (generalised) Thomas process was named in recognition of Thomas' contribution (Diggle et al. 1976). A little later, Neyman & Scott (1952) studied clustering of galaxies, although the model developed therein has also been applied to model clustered plant populations (e.g., Batista & Maguire 1998; Ogata 2020). Neyman and Scott also gave their names to a type of clustered point process, and the generalised Thomas process is actually a special case of Neyman-Scott process (NSP). A list of all special subcases of Neyman-Scott processes that have been studied around that time is provided by Guttorp & Thorarinsdottir (2012). During the same decade, Pielou (1957) studied the effect of plot size when estimating parameters from a Neyman-Scott and a Thomas process.

Another type of Neyman-Scott cluster process that is sometimes used for the modelling of clustering in plant populations is the Matérn cluster process (Matérn 1960, 1986), that differs from the generalised Thomas process regarding the distribution of plants in the clusters. Matérn focused on applications of point processes in forestry. Applications of Matérn cluster processes in forest studies include Fleischer et al. (2006), Eichhorn (2010) and Ekström et al. (2020). Out of these references, only the latter presented estimators of expected plant density using P/A data.

Other models for plant populations have also been applied for studying associated properties. One of the most popular models for plant abundance is the negative binomial model, especially when plants are known to exhibit clustering. He & Gaston (2000, 2007) proposed a method for estimating plant abundance based on occurrence data based on the assumption that plant abundance follows a negative binomial distribution. Similarly, Hwang & He (2011) showed how to estimate plant abundance based on P/A maps using a Gamma-Poisson model, which is a generalisation of the negative binomial model. However, the method presented in He & Gaston (2000) tends to overestimate species abundance (Conlisk et al. 2007). In addition, the negative binomial model does not appear to be very suitable for studying plant populations (Holt et al. 2002; Gaston et al. 2011), especially since only two known homogeneous point processes produce the negative binomial distribution for plot abundances, and both of them are extreme cases (Daley & Vere-Jones 2008). For an overview of applications of the negative binomial model in ecology, see Stoklosa et al. (2022). Some other studies,

such as Chang & Huang (2024), used techniques such as kernel estimation to estimate plant abundance from P/A data under several population assumptions. Holt et al. (2002) provided an overview of other models to model plant abundance and density from P/A data.

1.4 Use of additional data in the modelling

In for example Ståhl et al. (2020) or Ekström et al. (2020), the intensity of the point process, defined as the expected number of points per unit area (Baddeley et al. 2016), was supposed to be constant at every point of the region of interest (i.e., homogeneous). However, this is an oversimplification of the reality in most cases. Plant density is known to vary depending on environmental factors such as soil moisture, ambient humidity, chemical composition in the soil, tree cover, and many more (Schulze et al. 2019). As a consequence, it would be an advantage to take such factors into account when modelling abundance and deriving estimates of plant density, in order to make the latter more accurate. Thus, it is suitable to introduce explanatory variables, also called covariates, in the point process models (that are thus called inhomogeneous point process models) and the generalised linear models (GLMs, McCullagh 1989) implied by the point processes. Based on available knowledge, no previous study has suggested large-area estimators of plant density from P/A data and inhomogeneous PPPs, including corresponding variance estimators; nor has any study presented estimators of plant density based on P/A data and inhomogeneous NSPs.

There exists several possible sources for obtaining covariates, either from field surveys or from remote sensing (RS). Covariates from field surveys are collected by surveyors when they visit the different sample plots in a specific region of interest. On the one hand, the main advantage of field covariate registrations is that they usually are very thorough since a lot of environmental aspects are taken into account. On the other hand, a major drawback of auxiliary data taken locally at plot level is that they are generally not available in the whole region of interest. Another consequence is that it is not possible to apply the standard model-based framework if only field-based covariate data are used (Ståhl et al. 2016). This drawback can be counteracted by using RS covariate data, also called “wall-to-wall” data, since they are available for any point of the region of interest. Nowadays, such remotely-sensed covariate information for modelling is currently

increasing in amount, resolution and quality (e.g., Kangas et al. 2018; Dubayah et al. 2022). Moreover, some of them are being made available at short intervals of time (Lindgren et al. 2021). Remotely-sensed covariate data such as airborne laser scanning (ALS) are made less frequently but contain a plethora of useful information on vegetation sites that can be used for modelling (Lidberg et al. 2020). The availability and ready-to-use nature of this kind of covariate information has made the modelling of species abundance depending on environmental factors easier compared to yesteryear.

Another factor that could potentially contribute to the improvement of species modelling is the increasing availability of presence data offered by citizen science data, i.e. spontaneous, voluntary species registrations made outside of structured monitoring programmes and research projects. Most of citizen data are in the form of presence-only data, i.e. only the presence of species is registered. Such data can be used in connection with P/A data from planned surveys to create a more incorporating framework (Fithian et al. 2015; Bradter et al. 2018; Gelfand & Shirota 2019; Mäkinen et al. 2024). However, one should keep in mind that such modelling offers substantial challenges, mostly because of preferential bias, where observers tend to focus on the species they know or appreciate and usually make observations at easily accessible sites (Robinson et al. 2018; Johnston et al. 2020, 2023; Cretois et al. 2021).

The maximum entropy method (shortened as MaxEnt, Phillips et al. (2017)), first mentioned by Jaynes (1957) in a more global context, is equivalent to a regression model based on an inhomogeneous PPP (Renner & Warton 2013), except for the intercept. It has become extremely popular in ecology (e.g., Dudík et al. 2005), although it is rather used with presence-only data instead of P/A data and is often applied uncritically (Royle et al. 2012).

For modelling binary response data, GLMs can be used with an appropriate choice of link function (Mehtätalo & Lappi 2020). In ecology, the most commonly chosen link function is the logit link, which leads to the logistic regression model (see, e.g., Wintle et al. 2005; Foody 2008; Pellissier et al. 2013; Sipek et al. 2022). However, Baddeley et al. (2010) warn that the logistic regression model might not be appropriate when tessellating the region of interest if plant locations are considered as a realisation of an inhomogeneous PPP. On the other hand, binary regression models with

complementary log-log link are not affected by this issue (Baddeley et al. 2010), hence their use in Paper I where a cell grid is used to tessellate the area of interest. See Fortin et al. (2008), Lindenmayer et al. (2009), Yee & Dirnböck (2009), Fithian et al. (2015) or Fiorentin et al. (2019) for other examples of ecological studies based on P/A data and a complementary log-log link function.

1.5 Other considerations

In papers I, II and III, model-based inference is used, which implies that the variable under study is considered as random. Hence, the plant density is considered as a random variable. However, to facilitate the derivations, the expected value of the plant density, which is fixed, is estimated instead of the actual plant density being predicted. Not much is lost by making this adjustment, since the relative difference between the actual and expected values for the plant density are small in large-area surveys if the model used is approximately correct (Ståhl et al. 2016).

Instead of focusing on specific plant species and P/A data, one could register continuous variables, for example aboveground biomass (AGB). Biomass is the variable under study in Paper IV. AGB, or its density, can be estimated by field data (Næsset et al. 2016) or coupled with ALS methods, for example via the Global Ecosystem Dynamics Investigation (GEDI, Dubayah et al. 2022).

Whenever an estimation is made, uncertainty comes into play and must be taken into account. Reporting of estimates usually comprises associated measures of uncertainty, for example variance estimates, mean squared error (MSE) values, or confidence intervals. Indeed, errors can come from different sources, such as the mathematical modelling, the map products produced by remote sensing tools, or the measurements done in the field. In this thesis, it is supposed that the covariate and field data (including the P/A registrations) are devoid of errors, although this is a simplification of reality.

A large number of studies utilising model-based inference use solely the variance of the predictor of the target variable as a measure of uncertainty. Some studies (e.g., McRoberts et al. 2018) suggest that the variance estimator alone can be a sufficient estimator to quantify uncertainty in large-area surveys. However, the variance estimator alone does not take into account all the potential sources of error, largely because it does not directly

factor in the fact that the true value of the target variable is a random variable. A more thorough measure to estimate uncertainty is the MSE, which takes into account the variance and model bias of the predictor, the variance of the true value and the covariance between the predicted and true value. Thus, in-depth uncertainty assessments in model-based inference should use the MSE rather than the variance of the predictor (Cassel et al. 1977). Estimating different components in a broadened uncertainty analysis is the main subject of Paper IV.

2. Aims and objectives

The main objective of this thesis is to propose new ways to make better use of sample data in assessing characteristics of plant populations. A particular emphasis is made on P/A data, which are believed to have an underexploited potential. By proposing new methods and models to facilitate the use of this kind of data, it is believed that researchers and monitoring programmes will be able to get more extensive understanding of the data they are working with, and increase the possibilities of interpretation as well as analytic capacities.

More specifically, the use of model-based and hybrid inference in relation to inhomogeneous spatial point processes and P/A data is investigated in order to estimate plant density taking environmental factors into account. Corresponding variance estimators are also derived.

Additionally, a widened uncertainty analysis is performed in one of the articles, where the variance is one of the components of the MSE formula when model-based inference is used and AGB is the target variable. The extent of the error components in the MSE formula is studied in different subcases.

The specific objectives for each of the papers were as follows:

1. To develop a model-based method in combination with P/A data collected in the field, remotely-sensed covariate data and inhomogeneous PPP in order to derive large-area estimates of expected plant density for a selection of plant species, as well as corresponding estimators of variance, and to apply a residual-based test to test whether the derived GLM implied by the inhomogeneous PPP model has independent response variables given the covariates (**Paper I**);
2. To develop a method that makes use of hybrid-based inference together with P/A data and covariate data collected in the field and inhomogeneous PPP in order to obtain large-area estimates of expected plant density for a selected species, as well as corresponding estimators of variance (**Paper II**);
3. To develop a method that makes use of model-based inference jointly with P/A data collected in the field, remotely-sensed covariate data and inhomogeneous NSPs in order to estimate parameters from the process and to get local estimates of

expected plant density for some selected species, as well as corresponding estimators of variance (**Paper III**);

4. To widen the uncertainty analysis in a model-based framework, and thus to investigate the extent of the different components of the MSE formula in a model-based inference framework, using simulated data and biomass as the target variable (**Paper IV**).

3. Material and Methods

3.1 Data

3.1.1 Field data

Data collected from four different locations were used in the papers contained in this thesis, including a field study that was performed especially for Paper III. For the other papers, data were collected for other purposes, such as registrations as part of forest inventories and monitoring.

For Papers I and II, the data were collected in Northern Sweden, more precisely in the Lappland region of Norrbotten County (Fig. 1). In Paper I, the data, collected during the years 2011 to 2013, originated from the permanent plots of the Swedish NFI (Fridman et al. 2014). The P/A data in the study were originally available for 293 plots. Other covariates related to field and terrain properties were also registered as part of the survey. P/A data for *Luzula pilosa* (L.) Willd. (hairy woodrush), and *Lysimachia europaea* (L.) U. Manns & Anderb. (arctic starflower) were used.

In Paper II, the variable of interest was P/A data of *Vaccinium vitis-idaea* L. (lingonberry). Two samples, both from the Swedish NFI, were considered in the study. The first sample, called S_1, consisted of the centres of the small vegetation plots included in permanent plots in the Lappland region of Norrbotten during the years 2008 to 2012. Sample S_1 had a size n_1 equal to 724 plots. Cluster sampling was used to obtain the second sample, called S_2. This sample had a size of $n_2 = 111$ tract centres, which corresponds to 1132 temporary sample plots in total.

In Paper III, the data were collected in the forest connected to the SLU field station at Kulbäcksliden (Västerbotten County, Sweden, Fig. 2) during the month of September 2022. In total, P/A data for 559 sets of concentric circular plots were obtained (Fig. 3). P/A data for the following plant species were recorded: *L. pilosa, Maianthemum bifolium* (L.) F.W. Schmidt (false lily of the valley), and *L. europaea*.

Concerning Paper IV, the data were collected in the field in Liwale District in Southeast Tanzania, originally as part of another study (Næsset et al. 2016). The sample survey in Tanzania was conducted according to a systematic single-stage cluster design. Each of the 11 clusters consisted of

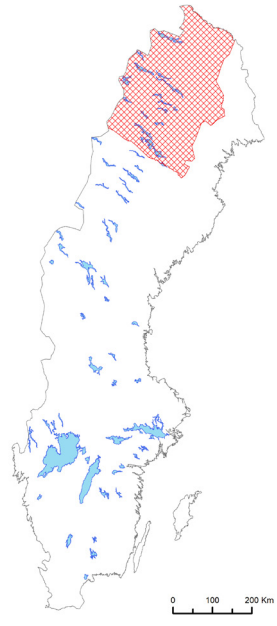

Figure 1. Position of the Lappmark region of Norrbotten County in Sweden.

eight plots, forming an L-shape. The circular plots had a radius of 15 metres, and the data were collected in 2014. AGB was calculated for each tree and then summed at sample plot level. Several tree measurements (for example diameter at breast height) were also conducted on the plots. Data that mimic conditions in Western USA (Saarela et al. 2025) were also used in Paper IV.

3.1.2 Remote sensing data

For papers I, II and III, covariates were obtained from several forest raster map products: the SLU Forest Map (Reese et al. 2003; Wallerman et al. 2021), the National Forest Attribute Map (NFAM, Nilsson et al. 2017), and a soil moisture map produced by Ågren et al. (2021).The SLU Forest Map is made of raster maps of the Swedish forest state, generated from satellite images using the Swedish NFI sample plots as reference data. A similar method was used in the NFAM to create forest raster maps from airborne laser scanning data collected in Sweden between 2009 and 2016. The soil moisture map by Ågren et al. (2021) was derived from terrain indices generated from a national ALS digital elevation model and environmental features.

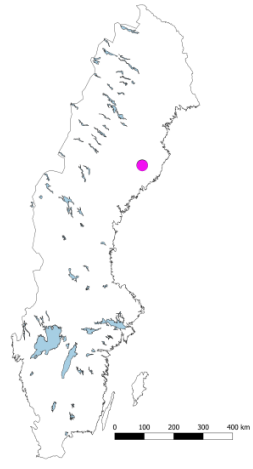

Figure 2. Map of Sweden showing the position of the Kulbäcksliden research park.

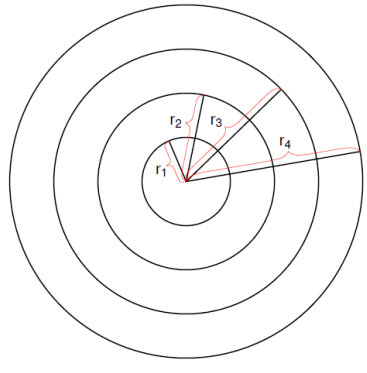

Figure 3. Example of a plot design with four concentric circular sample plots.

For Paper IV, the remotely sensed data came from different sources, the first one being ALS (or GEDI (Dubayah et al. 2022) in the case with simulated USA data), and the other one being satellite image data from the Landsat 8 sensor. The Western USA data were obtained through copula modelling (Ene et al. 2013) based on RS data available from a previous study (Saarela et al. 2025).

3.2 Estimation frameworks

3.2.1 Model-based inference

Model-based inference relies on model assumptions rather than sampling designs. The values that are linked to the elements in the population of interest are realisations of random variables (Ståhl et al. 2016). The realisations come from a so-called superpopulation model that attributes new values to every population unit (in particular values of the response variable) every time it is run. When model-based inference is applied to real data, it is assumed that the real population is a realisation of an invisible, unknown superpopulation model (Cassel et al. 1977). Alternatively, if model-based inference is applied as part of a simulation study, it is relatively easy to make realisations out of a superpopulation model since the latter is assumed to be known. Covariates that originate from, e.g., RS can be used as auxiliary data when creating a model based on a realisation of the superpopulation model. Inference is then based on this model, and estimators of fixed quantities are constructed (alternatively, predictions of random variables are made). In this thesis, model-based inference is used in Papers I, III and IV, as well as partially in Paper II.

Examples of application of model-based inference in forestry include Askne et al. (2013), in which AGB was estimated with models that include RS auxiliary data; Hou et al. (2017), that estimated firewood volume while relying on auxiliary data; Saarela et al. (2018), that developed a hierarchical model-based framework for the estimation of biomass based on ALS and GEDI data; and Mukhopadhyay et al. (2024), that predicted AGB based on GLMs and computed associated prediction intervals. Contrary to the aforementioned studies, that focus on AGB or volume estimation, Papers I, II and III are among the rare ones (including, e.g., Ekström et al. (2020)) that used model-based inference and plant P/A data as a response variable.

3.2.2 Design-based inference

Design-based inference relies on specific sampling designs. Contrary to model-based inference, the randomness in design-based inference comes from the sampling process, while the population is assumed to be fixed. The sample is random for each realisation, while the population parameters (for example the population total or population mean) do not vary. Estimations of population parameters are then made based on these samples, using so-

called design-based estimators. The probability of inclusion of each unit in the sample must be known. In this thesis, design-based inference is used partially in Paper II.

Examples of applications of design-based inference in forestry include Fattorini et al. (2019), Marcelli et al. (2019) and Di Biase et al. (2022), that concentrate on estimating diverse forest attributes. The latter study focused on the estimation of several plant indicators, including plant presence.

3.2.3 Hybrid inference

Hybrid inference is a mixture of both model-based and design-based inference. Two samples are involved in the process. The first sample is used to fit a model, and thus covariate data (that do not need to be wall-to-wall but only available at field plot level) as well as response data are needed. The second sample, which is a sample of covariate data and on which the model fitted on the first sample is applied, is used exclusively to estimate a population parameter, for example expected plant density or biomass per hectare in an entire region. Thus, while covariate data at plot level are required even for the second sample, no response data are needed. Inclusion probabilities for all sampling units in the second sample need to be known, since most of the design-based estimators, for example the Horvitz-Thompson estimator (Horvitz & Thompson 1952), involve inclusion probabilities of some sort.

The term "hybrid" inference was first introduced in an article by Corona et al. (2014) about estimation of standing wood volume in Italy, even if the method itself was already in use before (for example in Ståhl et al. (2011)). Most applications of hybrid inference in forestry concern biomass estimation and prediction. For example, Ståhl et al. (2011) and Gobakken et al. (2012) used a hybrid inference framework to estimate biomass based on ALS sample data in a Norwegian county. A similar study, based in North America, was performed by Margolis et al. (2015). Likewise, Bullock et al. (2023) used GEDI data in combination with NFI data to estimate biomass in Paraguay. Prediction of biomass based on hybrid inference has also been done for larger regions, for example by Saarela et al. (2022), using GEDI data. McRoberts et al. (2019) used that type of inference to compare forest biomass estimates at different resolutions in the USA. Hybrid inference has also been applied to estimate growing stock volume in Finland (Saarela et al. 2015) and Spain (Condés & McRoberts 2017). Hybrid inference can also be

used with mixed-effects models (e.g., Fortin et al. 2016). Note that all the aforementioned studies used hybrid inference through models with a continuous response variable, contrary to Paper II where the response variable was binary. Based on available knowledge, Paper II is the first study that involves GLMs in hybrid inference.

3.3 Spatial point processes

Spatial point processes are, as the name indicates, processes that randomly generate points in space (Møller & Waagepetersen 2003). Spatial point processes are generally denoted by capital letters, such as $\mathbf{X}$. In the following, a point pattern generated by a spatial point process $\mathbf{X}$ will be denoted by $\mathbf{x}$. $\mathbf{x}$ is a set of points $\mathbf{x}_i$, $i = 1, \dots, n$, in the two-dimensional space $\mathbb{R}^2$. It can be written as

$$\mathbf{x} = \{\mathbf{x}_1, \mathbf{x}_2, \dots, \mathbf{x}_n\}.$$

Let U be a region of $\mathbb{R}^2$. The subset that consists of the points generated by $\mathbf{x}$ that fall in U is denoted by $\mathbf{x} \cap U$.

The intensity of a point process, which can be defined as the average number of points per unit area (Baddeley et al. 2016), will be denoted by λ. Examples of spatial point processes studied in this thesis are presented below.

3.3.1 Poisson point processes

Homogeneous PPPs are sometimes called Complete Spatial Randomness (Baddeley et al. 2016). They fulfil two main properties: first, the homogeneity property, which states that the points have no preference for any spatial location, and thus that the intensity of the process is constant in the whole region of interest. A homogeneous PPP verifies the independence property as well. The latter states that the positions of points do not impact each other. In short, point locations are independent of each other. When the process is inhomogeneous, the homogeneity property is not respected anymore and λ varies, for example, depending on external factors such as environmental covariates. However, the process still fulfils the independence property.

Let $\boldsymbol{\beta}$ denote a vector of model coefficients and denote its transpose by $\boldsymbol{\beta}^{\mathrm{T}}$. Let $\boldsymbol{z}(\boldsymbol{u})$ denote the vector of covariate data, of size q, at location $\boldsymbol{u}$. The intensity of a PPP (Baddeley et al. 2010) can be modelled as

$$\lambda(\boldsymbol{u}) = \exp\left(\boldsymbol{\beta}^{\mathrm{T}}\boldsymbol{z}(\boldsymbol{u})\right), \boldsymbol{u} \in U \subset \mathbb{R}^2, \quad (1)$$

as in Paper II. This implies that the expected total number of plants in region U is

$$\Lambda(\boldsymbol{\beta}) = \int_U \lambda(\boldsymbol{u}) d\boldsymbol{u} = \int_U \exp\left(\boldsymbol{\beta}^{\mathrm{T}}\boldsymbol{z}(\boldsymbol{u})\right). \quad (2)$$

In case a grid tessellation over U is used, as in Paper I, the intensity of the PPP in cell $i, i = 1, \ldots, N$, can be expressed as

$$\lambda_i = \exp\left(\boldsymbol{\beta}^{\mathrm{T}}\boldsymbol{z}_i\right), \quad (3)$$

where $\boldsymbol{z}_i$ denotes the covariate vector in grid cell i, assuming that the covariate vector inside a cell is constant. Then, the expected total number of plants in U can be expressed as

$$\Lambda = a_P \sum_{i=1}^{N} \exp\left(\boldsymbol{\beta}^{\mathrm{T}}\boldsymbol{z}_i\right), \quad (4)$$

where a_P is the size of the cells tessellating U.

3.3.2 Neyman-Scott processes

NSPs are part of a larger family of point processes called cluster processes (Baddeley et al. 2016). Cluster processes involve two mechanisms: the first one generates points (called parent points) according to a given process (e.g., a PPP) in the region of interest. Subsequently, a second process creates points (also called offspring points) around each and every parent point. Parent points are then removed to produce the realisation of the cluster process. Clustered point processes have the potential to mimic reality pretty well when it comes to plant locations, since offspring plants usually grow in clusters around some parent plant (Schulze et al. 2019). In fact, this kind of model might be more appropriate than PPP models to model plant populations since random populations seldom exist in nature, although individual species in most plant communities may be randomly scattered (Bonham 2013).

The unobserved parent points in NSPs follow a PPP with a given intensity τ. Each parent point will produce a cluster of offspring points, and these clusters will be independent and identically distributed (i.i.d.) (Baddeley et al. 2016). Offspring points are generated by another point process and are independent within a cluster. The point process that generates the offspring points has an average number of points per cluster μ. The intensity of the NSP as a whole thus becomes $\tau\mu$.

Some NSPs are characterised by a positive third parameter, γ, that refers to the size of the clusters (e.g., their radius). In that case, for each parent point $\mathbf{x}_i \in \mathbb{R}^2$, the offspring points $\boldsymbol{y}_{ij} \in \mathbb{R}^2$ are i.i.d. with a spatial offspring probability density $f_\gamma(\boldsymbol{y} - \mathbf{x}_i)$ that depends on γ.

There are several ways to make the above process inhomogeneous. In this thesis (as well as in Paper III), the method proposed by Waagepetersen (2007) is applied. For a parent point at location $\mathbf{x}_i$, the offspring follow a PPP with intensity $\mu(\boldsymbol{u})f_\gamma(\boldsymbol{u} - \mathbf{x}_i),\ \boldsymbol{u} \in \mathbb{R}^2$. The mean number of points in the clusters μ varies according to environmental covariates, while the intensity of the parent process τ stays constant. More precisely,

$$\mu(\boldsymbol{u}) = \exp\left(\beta_0 + \sum_{i=1}^{q-1} \beta_i z_i(\boldsymbol{u})\right), \tag{5}$$

where each $z_i(\boldsymbol{u})$ denotes an environmental spatial covariate from vector $z(\boldsymbol{u})$, $i = 1, \ldots, q-1$. Other methods to make a NSP inhomogeneous are mentioned in subsection 7.2.

If $f_\gamma(\boldsymbol{u})$ is a uniform density function in a disc of radius γ, then the point process can be seen as an inhomogeneous Matérn cluster process. If, instead, $f_\gamma(\boldsymbol{u})$ is the density function of an isotropic Gaussian distribution $N(0, \gamma^2 I)$, where γ is a standard deviation parameter and I is the identity matrix, then the point process can be seen as an inhomogeneous generalised Thomas cluster process. The inhomogeneous Matérn cluster process is studied in Paper III, while both Matérn and Thomas are used as subcases in Paper I, where non-Poisson processes were generated to investigate the power of the correlation tests.

3.3.3 Other cluster processes

NSPs are not the only examples of processes that generate clustered patterns. For example, the log-Gaussian Cox process (LGCP), which is also employed in Paper I during the simulation study, is part of this family. Cox processes are basically PPPs with a random intensity function (Baddeley et al. 2016), the latter varying depending on unobservable external factors (and possible environmental covariates). No offspring and parent points are involved in the process, contrary to Neyman-Scott cluster processes. A LGCP is a Cox process whose driving intensity is of the form

$$\Lambda(\boldsymbol{u}) = \exp G(\boldsymbol{u}),$$

where $G(\boldsymbol{u})$ is a Gaussian random field.

4. Estimation of plant density based on spatial point processes and P/A data

4.1 Using inhomogeneous Poisson point processes

Both Paper I and Paper II make use of inhomogeneous PPP and P/A data for obtaining estimates of expected plant density and associated variance estimators within large regions. The difference between these two papers is that a tessellation of the study area U is used in conjunction with wall-to-wall covariate date for Paper I, while Paper II makes use of hybrid inference where the covariate data come from sampling plots in U. Paper I makes use of tessellation cells, while circular field plots are the main sampling units in Paper II (cluster sampling is also studied in that paper). For the sake of simplicity, it is supposed henceforth that all grid cells or circular plots are entirely inside the region of interest U. In Paper II, this is not necessarily the case and a buffer is used around U to mitigate potential edge effects (Gregoire & Valentine 2007).

Let N_i denote the number of plants in grid cell i or in circular plot i (called unit i henceforth) in U. Assume that the area of every unit is constant and equal to a_P. If the values of the covariate vector $\boldsymbol{z}_i$ are assumed to be constant within unit i, then the expected number of plants in unit i can be expressed as

$$E(N_i) = a_P \lambda_i,$$

with λ_i as defined in (3). N_i is Poisson distributed, which implies that the probability of presence in unit i can be expressed as

$$p_i = 1 - P(N_i = 0) = 1 - \exp\left(-a_P \exp\left(\boldsymbol{\beta}^{\mathrm{T}} \boldsymbol{z}_i\right)\right).$$

It follows that the loglikelihood for the binary response variables Y_i (that denote presence or absence of plant individuals in unit i) becomes the loglikelihood of a complementary log-log regression model (Baddeley et al. 2010) with an offset equal to the log of the area of unit i

$$\log(-\log(1 - p_i)) = \log(a_P) + \boldsymbol{\beta}^{\mathrm{T}} \boldsymbol{z}_i. \qquad (6)$$

The estimator of the model parameter vector $\boldsymbol{\beta}$, denoted $\widehat{\boldsymbol{\beta}}$, is obtained from the model above.

In Paper I, there is no need for a second sample since the covariates are available in the entirety of the region of interest. Thus, the expected plant density in U can be expressed as

$$R_U = \frac{\Lambda}{Na_P},$$

with Λ defined as in (4). Note that R_U is the expected total number of plants in U divided by the total area of U, which follows from the definition of the density. R_U can be estimated by

$$\hat{R}_U = \frac{\widehat{\Lambda}}{Na_P} = \frac{1}{N}\sum_{i=1}^{N} \exp\left(\widehat{\boldsymbol{\beta}}^{\mathrm{T}}\boldsymbol{z}_i\right), \tag{7}$$

where $\widehat{\Lambda}$ is the estimator of Λ, obtained by replacing $\boldsymbol{\beta}$ by $\widehat{\boldsymbol{\beta}}$ in (4).

The next step is to derive the associated variance of $\hat{R}_U$ and its estimator. Using the computation rules of the variance, it follows that $\mathrm{Var}\left(\hat{R}_U\right) = (Na_P)^{-2}\mathrm{Var}(\widehat{\Lambda})$. Let n denote the sample size. For estimating the variance of Λ, one may use the fact that for large samples and under mild conditions, $\widehat{\boldsymbol{\beta}}$ is asymptotically normally distributed, i.e.

$$n^{\frac{1}{2}}\left(\widehat{\boldsymbol{\beta}} - \boldsymbol{\beta}\right) \xrightarrow{D} N_q(0, \boldsymbol{\Sigma}),$$

where N_q designates the q-variate normal distribution. The covariance matrix $\boldsymbol{\Sigma}$ (whose definition can be seen in Paper I) is assumed to be positive definite (Sen & Singer 1993). This implies that $\widehat{\boldsymbol{\beta}}^{\mathrm{T}}\boldsymbol{z}_i$ is approximately normally distributed with mean $\boldsymbol{\beta}^{\mathrm{T}}\boldsymbol{z}_i$ and variance $n^{-1}\boldsymbol{z}_i^{\mathrm{T}}\Sigma\boldsymbol{z}_i$. It follows that

$$\mathrm{Var}(\widehat{\Lambda}) \approx a_P^2 \sum_{i=1}^{N}\sum_{j=1}^{N}\left[\exp\left(\frac{\boldsymbol{z}_i^T\boldsymbol{\Sigma}\boldsymbol{z}_j}{n} - 1\right)\right]\exp\left(\boldsymbol{\beta}^{\mathrm{T}}(\boldsymbol{z}_i + \boldsymbol{z}_j) + \frac{\boldsymbol{z}_i^{\mathrm{T}}\boldsymbol{\Sigma}\boldsymbol{z}_i + \boldsymbol{z}_j^{\mathrm{T}}\boldsymbol{\Sigma}\boldsymbol{z}_j}{2n}\right),$$

which is estimated by replacing $\boldsymbol{\beta}$ by $\widehat{\boldsymbol{\beta}}$ and $\boldsymbol{\Sigma}$ by $\widehat{\boldsymbol{\Sigma}}$ (see Paper I for details).

Now, the variance of $\hat{R}_U$ can be estimated by

$$\hat{\sigma}_U^2 = \frac{1}{N^2}\sum_{i=1}^{N}\sum_{j=1}^{N}\left[\exp\left(\frac{\boldsymbol{z}_i^{\mathrm{T}}\widehat{\boldsymbol{\Sigma}}\boldsymbol{z}_j}{n} - 1\right)\right]\exp\left(\widehat{\boldsymbol{\beta}}^{\mathrm{T}}(\boldsymbol{z}_i + \boldsymbol{z}_j) + \frac{\boldsymbol{z}_i^{\mathrm{T}}\widehat{\boldsymbol{\Sigma}}\boldsymbol{z}_i + \boldsymbol{z}_j^{\mathrm{T}}\widehat{\boldsymbol{\Sigma}}\boldsymbol{z}_j}{2n}\right).$$

The above method can be applied when one has access to wall-to-wall covariate data that cover the entire region of interest U. However, this might not be the case in every study. In such cases, hybrid inference may be preferred (as in Paper II), and additional steps are required to obtain estimators of expected plant density and associated variance estimators.

Let f be the joint probability density function (p.d.f.) for the plot centres in sample S_2, and $f_i(\boldsymbol{u})$ the marginal p.d.f. for plot centre $\boldsymbol{u}_i$ in S_2, $i = 1, \ldots, n_2$. The inclusion density function is

$$\pi(\boldsymbol{u}) = \sum_{i=1}^{n_2} f_i(\boldsymbol{u}), \tag{8}$$

and can be considered as a local measure of the number of sample points to be selected per unit area (Cordy 1993). The generalised Horvitz-Thompson estimator of the expected number of plants in U is then given by

$$\widehat{\Lambda}(\boldsymbol{\beta}) = \sum_{i=1}^{n_2} \frac{\lambda(\boldsymbol{u}_i)}{\pi(\boldsymbol{u}_i)} = \sum_{i=1}^{n_2} \frac{\exp(\boldsymbol{\beta}^{\mathrm{T}}\boldsymbol{z}_i)}{\pi(\boldsymbol{u}_i)}, \tag{9}$$

where $\pi(\boldsymbol{u})$ is given by (8) and $\lambda(\boldsymbol{u}_i)$ is the average expected intensity in sample plot i with centre $\boldsymbol{u}_i$. If the covariate data are supposed to be constant in sample plot i, then $\lambda(\boldsymbol{u}_i)$ is the same as $\lambda(\boldsymbol{u})$ as defined in (1), with $\boldsymbol{z}(\boldsymbol{u}) = \boldsymbol{z}_i$, $\boldsymbol{z}_i$ being equal to the value of the covariate vector in sample plot i. Since the parameter vector $\boldsymbol{\beta}$ is usually unknown, $\widehat{\Lambda}(\widehat{\boldsymbol{\beta}})$ is used as an estimator of the expected number of plants instead.

It is of necessity to know the area of U, or to estimate that area, to get an estimate of the expected plant density. In case the area of U is known (denote this area by a_U), the expected density in U is expressed as

$$R(\boldsymbol{\beta}) = \frac{\Lambda(\boldsymbol{\beta})}{a_U},$$

where $\Lambda(\boldsymbol{\beta})$ is defined in (2). This expected density can be estimated by

$$\hat{R}(\widehat{\boldsymbol{\beta}}) = \frac{\widehat{\Lambda}(\widehat{\boldsymbol{\beta}})}{a_U},$$

where $\widehat{\Lambda}(\boldsymbol{\beta})$ is defined in (9). The case where a_U is unknown and estimated is presented in detail in Paper II.

In order to get an estimate of the variance of $\widehat{\Lambda}(\boldsymbol{\beta})$, the Sen-Yates-Grundy variance formula defined in Cordy (1993) is applied (see Paper II). Let

$$\Delta(\boldsymbol{u}, \boldsymbol{u}') = \pi(\boldsymbol{u})\pi(\boldsymbol{u}') - \pi(\boldsymbol{u}, \boldsymbol{u}') \text{ and } \pi(\boldsymbol{u}, \boldsymbol{u}') = \sum_{i \in I_n} \sum_{j \in J_{n,i}} f_{ij}(\boldsymbol{u}, \boldsymbol{u}'),$$

the latter being the pairwise inclusion density function with $I_n = \{1, \dots, n_2\}, J_{n,i} = \{1, \dots, n_2\} \backslash \{i\}$, and f_{ij} is the joint p.d.f. of $\boldsymbol{u}_i$ and $\boldsymbol{u}_j$. According to Cordy (1993), if $\pi(\boldsymbol{u})$ and $\pi(\boldsymbol{u}, \boldsymbol{u}')$ are strictly positive for all $(\boldsymbol{u}, \boldsymbol{u}') \in U$, an unbiased estimator of $\mathrm{Var}(\widehat{\Lambda}(\boldsymbol{\beta}))$ is given by

$$\widehat{\mathrm{Var}}\left(\widehat{\Lambda}(\boldsymbol{\beta})\right) = \frac{1}{2} \sum_{i \in I_n} \sum_{j \in J_{n,i}} \frac{\Delta(\boldsymbol{u}_i, \boldsymbol{u}_j)}{\pi(\boldsymbol{u}_i, \boldsymbol{u}_j)} \left(\frac{\exp(\boldsymbol{\beta}^{\mathrm{T}}\boldsymbol{z}_i)}{\pi(\boldsymbol{u}_i)} - \frac{\exp(\boldsymbol{\beta}^{\mathrm{T}}\boldsymbol{z}_j)}{\pi(\boldsymbol{u}_j)} \right)^2.$$

When the model coefficients are unknown, $\boldsymbol{\beta}$ is estimated by $\widehat{\boldsymbol{\beta}}$ and an estimate of the variance of $\widehat{\Lambda}(\widehat{\boldsymbol{\beta}})$ can be written as

$$\widehat{\mathrm{Var}}\left(\hat{\Lambda}(\hat{\boldsymbol{\beta}})\right) = \frac{1}{2}\sum_{i\in I_n}\sum_{\substack{j\in J_{n,i}\\ q\quad q}} \frac{\Delta(\boldsymbol{u}_i,\boldsymbol{u}_j)}{\pi(\boldsymbol{u}_i,\boldsymbol{u}_j)}\left(\frac{\exp(\hat{\boldsymbol{\beta}}^{\mathrm{T}}\boldsymbol{z}_i)}{\pi(\boldsymbol{u}_i)} - \frac{\exp(\hat{\boldsymbol{\beta}}^{\mathrm{T}}\boldsymbol{z}_j)}{\pi(\boldsymbol{u}_j)}\right)^2 + \sum_{k=1}^{q}\sum_{l=1}^{q} \widehat{\mathrm{Cov}}_{S_1}(\hat{\beta}_k,\hat{\beta}_l)\,\hat{v}_k\hat{v}_l,$$

with

$$\hat{v}_k = \sum_{i=1}^{n_2} \frac{1}{\pi(\boldsymbol{u}_i)}\lambda^{(k)}(\mathbf{u}_i)\,,$$

where $\hat{\beta}_k$ denotes the kth component of the $\hat{\boldsymbol{\beta}}$ vector and

$$\lambda^{(k)}(\boldsymbol{u}_i) = \frac{\partial\lambda(\boldsymbol{u}_i)}{\partial\hat{\beta}_k} = z_{ik}\exp(\hat{\boldsymbol{\beta}}^{\mathrm{T}}\boldsymbol{z}_i),$$

with z_{ik} denoting the kth component of $\boldsymbol{z}_i$.

Then, it follows that the variance estimator of the estimator of expected plant density with known area a_U is

$$\widehat{Var}\left(\hat{R}(\hat{\boldsymbol{\beta}})\right) = \frac{\widehat{Var}(\hat{\Lambda}(\hat{\boldsymbol{\beta}}))}{a_U^2}.$$

A variance estimator in the case where the area a_U is unknown is given in Paper II.

4.2 Using inhomogeneous Neyman-Scott processes

In Paper III, plant locations are supposed to be generated by cluster point processes, in particular Matérn cluster processes. A design with sampling plots is applied, and the inference is based on the plant registrations (more specifically, P/A data of plants) done within these sampling plots. The estimation of the parameters of the inhomogeneous NSP cannot be done in the same way as in Papers I and II, i.e. a binary regression model cannot be used. It will be shown below that a multinomial regression model is used to estimate the parameter vector $\boldsymbol{\theta} = (\tau, \beta_0, \dots, \beta_{q-1}, \gamma)$. For a Matérn cluster processes, τ denotes the intensity of the parent process, $\mu(\boldsymbol{u})$ is defined as in (5) as a function of a parameter vector $\boldsymbol{\beta} = (\beta_0, \dots, \beta_{q-1})$, and γ denotes the cluster radius parameter.

It is necessary to know about the disposition of plots in a given sampling design in order to calculate the probabilities of presence in the different plots (or in the different configurations of plots). The following design with concentric circular plots, used in Paper III, can be taken as an example (see

Fig. 3). The use of sampling designs with concentric plots when spatial patterns are to be expected is recommended by Morrison et al. (1995). Assume that there are n sets of (concentric) plots $C_{i,j}, i = 1, \dots, n,\ j = 1, \dots, k$. Suppose that the n sets of concentric plots are so far apart that the point patterns within these sets can reasonably be considered as independent. In main plot i, the jth innermost circle $C_{i,j}$ has a radius $r_j, j = 1, \dots, k$. Let $B_{i,1} = C_{i,1}$ and $B_{i,j} = C_{i,j} \backslash C_{i,j-1}, i = 1, \dots, n, j = 2, \dots, k$, and let $N_{C_{i,k}}$ denote the number of plants in plot $C_{i,k}$. A survey of such set of plots is done from the innermost plot outwards, and is over as soon as a plant is encountered on one of the $B_{i,j}$s or if no plants at all are registered in the k concentric circular plots. Thus, the events corresponding to this survey are the following:

$$A_{i,0} = \{\text{absence in } C_{i,k}\} = \{N_{C_{i,k}} = 0\},$$
$$A_{i,1} = \{\text{presence in } C_{i,1}\} = \{N_{C_{i,1}} > 0\},$$
$$A_{i,j} = \{\text{presence in } B_{i,j} \text{ but not in } C_{i,j-1}\} = \{N_{C_{i,j-1}} = 0 \text{ and } N_{B_{i,j}} > 0\},$$

for $i = 1, \dots, n$ and $j = 2, \dots, k$.

Let $I_{i,j}$ be the indicator of the event $A_{i,j}$ and $\pi_{i,j}(\boldsymbol{\theta})$ the associated probabilities for every $A_{i,j}$, computed using Theorem 1 in Paper III. Set Y_i equal to j if the event $A_{i,j}$ occurs, $i = 1, \dots, n$. The variable Y_i then becomes the dependent variable in a multinomial regression model (cf. Amemiya 1985), for which

$$P\{Y_i = j\} = P\{A_{i,j}\} = \pi_{i,j}(\boldsymbol{\theta}).$$

Let $\boldsymbol{\theta}_0$ denote the true value of $\boldsymbol{\theta}$. This parameter vector is estimated by maximum likelihood. The maximum likelihood estimator $\widehat{\boldsymbol{\theta}}$ of $\boldsymbol{\theta}_0$ is any parameter vector in $\Theta = \{\boldsymbol{\theta} = (\tau, \beta_0, \dots, \beta_{q-1}, \gamma)^{\mathrm{T}} : \tau, \gamma > 0\}$ that maximises the log-likelihood function

$$l(\boldsymbol{\theta}) = \sum_{i=1}^{n} \sum_{j=0}^{k} I_{i,j} \log \pi_{i,j}(\boldsymbol{\theta}).$$

By standard arguments (cf. Rao 1973; Amemiya 1985),

$$i_{rsn}(\boldsymbol{\theta}) = E_{\boldsymbol{\theta}}\left[\frac{\partial l(\boldsymbol{\theta})}{\partial \theta_r} \frac{\partial l(\boldsymbol{\theta})}{\partial \theta_s}\right] = \sum_{i=1}^{n} \sum_{j=0}^{k} \frac{1}{\pi_{i,j}(\boldsymbol{\theta})} \frac{\partial \pi_{i,j}(\boldsymbol{\theta})}{\partial \theta_r} \frac{\partial \pi_{i,j}(\boldsymbol{\theta})}{\partial \theta_s},$$

where $\theta_1 = \tau, \theta_k = \beta_{k-2}, k = 2, \dots, q+1, \theta_{q+2} = \gamma$. Let $I_n(\boldsymbol{\theta}) = (i_{rsn}(\boldsymbol{\theta}))$. It is assumed that the limiting matrix $\lim_{n \to \infty} n^{-1} I_n(\boldsymbol{\theta}) = I(\boldsymbol{\theta})$ exists, is finite and positive definite (Sen & Singer 1993). The maximum likelihood

estimator $\widehat{\boldsymbol{\theta}}$ is supposed to be consistent and asymptotically normally distributed, i.e.

$$n^{\frac{1}{2}}\left(\widehat{\boldsymbol{\theta}}-\boldsymbol{\theta}_0\right) \xrightarrow{D} N(0,[I(\boldsymbol{\theta}_0)]^{-1}). \tag{10}$$

Let $i^{rsn}(\boldsymbol{\theta}), r, s = 1,2,\dots,q+2$, denote the elements of the inverse of the matrix $I_n(\boldsymbol{\theta})$. An approximate 95% confidence interval for the individual parameters θ_r is given by

$$\hat{\theta}_r \pm 1.96\sqrt{i^{rrn}\left(\widehat{\boldsymbol{\theta}}\right)}, r = 1,2,\dots,q+2. \tag{11}$$

An approximate confidence interval can also be constructed for the intensity $\lambda_{\boldsymbol{\theta}}(\boldsymbol{u}) = \tau\mu(\boldsymbol{u}) = \tau\exp(\beta_0 + \sum_{i=1}^{q-1}\beta_i z_i(\boldsymbol{u}))$ of the point process at a spatial location $\boldsymbol{u}$. By (10) and the delta-method (e.g., Shao 2003),

$$n^{\frac{1}{2}}\left(\lambda_{\widehat{\boldsymbol{\theta}}}(\boldsymbol{u}) - \lambda_{\boldsymbol{\theta}_0}(\boldsymbol{u})\right) \xrightarrow{D} N\left(0, \nabla\lambda_{\boldsymbol{\theta}_0}(\boldsymbol{u})^{\mathrm{T}}[I(\boldsymbol{\theta}_0)]^{-1}\nabla\lambda_{\boldsymbol{\theta}_0}(\boldsymbol{u})\right),$$

where $\nabla\lambda_{\boldsymbol{\theta}}(\boldsymbol{u})$ denotes the gradient, i.e., the vector formed by the partial derivatives $\frac{\partial\lambda_{\boldsymbol{\theta}}(\boldsymbol{u})}{\partial\theta_r}, r = 1,\dots,q+2$. Then, an approximate 95% confidence interval for the intensity at a given spatial location $\boldsymbol{u}$ is given by

$$\lambda_{\widehat{\boldsymbol{\theta}}}(\boldsymbol{u}) \pm 1.96\sqrt{\sum_{r=1}^{q+1}\sum_{s=1}^{q+1} i^{rsn}\left(\widehat{\boldsymbol{\theta}}\right)\left.\frac{\partial\lambda_{\boldsymbol{\theta}}(\boldsymbol{u})}{\partial\theta_r}\right|_{\widehat{\boldsymbol{\theta}}}\left.\frac{\partial\lambda_{\boldsymbol{\theta}}(\boldsymbol{u})}{\partial\theta_s}\right|_{\widehat{\boldsymbol{\theta}}}}. \tag{12}$$

The estimated standard errors for the estimators $\hat{\theta}_r$ and $\lambda_{\widehat{\boldsymbol{\theta}}}(\boldsymbol{u})$ are provided by the square root expressions of (11) and (12), respectively.

4.3 Assessing the models

There is no guarantee that the regression models presented in 4.1 and 4.2 are directly applicable. These models, that are implied by their respective types of point processes, need to be evaluated for suitability. First, standard methods for model selection and validation of the regression models were applied. In addition, in Paper I, the correlation between the residuals in the fitted model (6) was investigated. If spatial correlation was found between the paired residuals (obtained from the paired observations in the sampling design in Fig. 4), this indicated that the assumption of independence of the response variables—given the covariates—in the binary regression model (6), as implied by the inhomogeneous PPP model, was violated. This would then make the underlying hypothesis of inhomogeneous PPP invalid. The

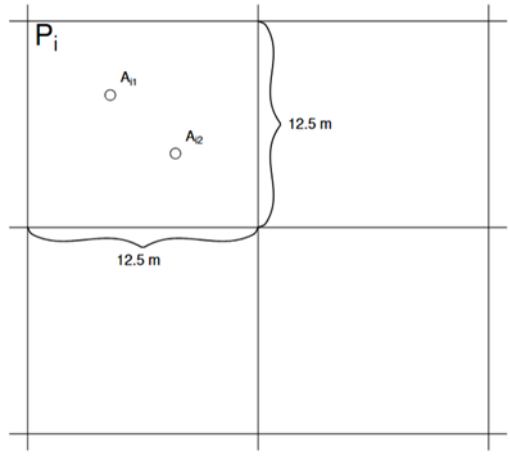

Figure 4. Disposition of the paired vegetation plots in a pixel, based on the design used in the Swedish NFI.

regression model residuals that were studied were the Pearson, working and randomised quantile residuals (Dunn & Smyth 1996, 2018). Additionally, the Pearson and Spearman correlation coefficients were the coefficients that were studied.

In Paper III, randomised quantile residuals as defined in Trijoulet et al. (2023) were used to evaluate the fitted multinomial regression models.

4.4 Simulation studies

Simulation studies are an essential part of this thesis. Indeed, Monte Carlo simulations are convenient in order to evaluate the performance of the developed estimators and their estimators of variance. They are also practical to investigate the actual significance levels (i.e., the percentage of times the null hypothesis is rejected when the data are generated according to the null hypothesis) and the power (i.e., the percentage of times the null hypothesis is rejected when the data are generated according to the alternative hypothesis) of the tests. All the simulations in this thesis were performed in R (R Core Team 2025).

In Paper I, simulation studies were conducted in order to investigate the power and actual significance levels of the correlation tests. The actual significance levels should ideally be close to the nominal significance level,

i.e. 0.05 as it was set, and the power should be close to 1 the more the studied point processes differ from an inhomogeneous PPP (e.g., when investigating processes that produce strong clustering). Different point processes were generated: log-Gaussian Cox, Matérn cluster and Thomas processes. The parameters for these processes were adjusted to express different strength of clustering. A GLM was then fitted on the P/A data coming from the generated point data and the covariates associated with each sample plot under the assumption that the process was generated by an inhomogeneous PPP, which was then used to produce residuals to use for the considered tests.

In Paper II, simulations were performed in order to evaluate the performance of the derived density estimators and their associated variance estimators. This was done for two cases, both when the area of the region of interest was known and when it was unknown. Covariates were created artificially based on the ones that were included in the *V. vitis-idaea* model. P/A data were generated from an inhomogeneous PPP for each replicate. The plot centres for samples S_1 and S_2 were randomly selected for each replicate. A model was then created on S_1 and model coefficients $\widehat{\boldsymbol{\beta}}$ were estimated. Then, the expected plant density and corresponding variance were estimated based on S_2.

In Paper III, the main objective of the simulation study was to verify the performance of the parameter estimators and their associated variance estimators. This involved computing the actual confidence level (ACL) of the derived confidence intervals for the individual parameters included in vector $\boldsymbol{\theta}$. The ACL should ideally be close to the nominal confidence level, set to 95% for this study. The design used during the Monte Carlo study was the design with concentric circles presented in subsection 3.1, with 6 concentric circular plots. Realisations of Matérn cluster processes were generated and maximum likelihood estimates of $\boldsymbol{\theta}_0$ were produced. The models investigated were the ones for the 3 plant species introduced in subsection 3.1, with covariates based on the actual covariates in the study area. The intensity of the process when the covariate was equal to its ith sample quartile, $i = 1,2,3$, was estimated, and the performance of these intensity estimators was also evaluated.

5. Estimation of the components of the MSE based on simulations

In Papers I to III, the measure of uncertainty was uniquely the variance estimator for the estimator of expected plant density. However, it can be of interest to investigate a more thorough measure of uncertainty in some cases, if each of the components of said measure of uncertainty can be estimated. The MSE can be applied as a measurement of uncertainty when model-based inference is used. The MSE gives an expression for the expected squared deviation between predicted and actual values, and takes several relevant uncertainty factors into consideration, in addition to the variance of the estimator/predictor.

Let Y be the (random) targeted response variable (e.g., AGB measurement in ton/ha) and $\hat{Y}$ be its predictor. In the model-based inference case, the MSE of the predictor is expressed as

$$\mathrm{MSE}(\hat{Y}) = \mathrm{Var}(\hat{Y}) + \mathrm{Bias}^2(\hat{Y}) + \mathrm{Var}(Y) - 2\mathrm{Cov}(\hat{Y}, Y),$$

where $\mathrm{Var}(\hat{Y})$ is the variance of the predictor, $\mathrm{Bias}(\hat{Y}) = \mathrm{E}(\hat{Y} - Y)$ is the model bias of the predictor, $\mathrm{Var}(Y)$ is the variance of the target variable and $\mathrm{Cov}(\hat{Y}, Y)$ is the covariance of the target variable and its predictor.

In a number of model-based studies that make use of remotely sensed data, the formula of the MSE is believed to be used wrongly (Ståhl et al. 2024). Indeed, some studies use the design-based version of the MSE formula instead of the model-based version. In other words, the variance of the target variable, the model bias and the covariance term are omitted. However, these terms can be non-negligible in some cases. Looking at the magnitude of each term of the model-based MSE in different cases is the main objective of Paper IV.

For large areas, the MSE can reasonably be approximated by the variance of the predictor solely (McRoberts et al. 2018). This is not the case anymore when the area of study is small, as can be seen in the results of Paper IV.

Paper IV relied entirely on simulations. For each combination of study area (Tanzania or USA) and RS data source (ALS/GEDI or Landsat 8), a proxy of the superpopulation model was estimated and applied to generate a large number of population realisations. For each population and field data sample size, a new prediction model was created based on a fixed systematic sample, and the biomass density predicted for the target area. Thus, for each

replicate, a true and a predicted biomass density values were obtained. Based on these, all the terms constituting the MSE formula could be empirically estimated.

In order to make the simulations more realistic, a spatial autocorrelation structure was introduced. It was applied to the error terms in the superpopulation model. The strength of the spatial autocorrelation could be controlled (no autocorrelation, mild autocorrelation, moderate autocorrelation and strong autocorrelation), and several subcases were examined. The benchmark case in the simulations had moderate autocorrelation and a sample size of 150 cells.

6. Results from the empirical data studies and simulations

6.1 Large-area estimation of plant density using presence/absence data and binary regression, and correlation tests of the binary regression model (Paper I)

The results were separated into two categories for this paper. First, an application with field data was conducted, and then a simulation study was performed to evaluate the performance of the proposed estimators and associated variance estimators.

A model was first constructed on field data, i.e. P/A data of *L. europaea* and *L. pilosa*, in the Lappland region of Norrbotten county in Sweden. Both binary regression models based on data from these species passed the correlation test at the 5% significance level. Both models contained two explanatory variables: the first model, for *L. europaea*, comprised the proportion of tree stem volume of deciduous trees and basal area; whereas the second model, for *L. pilosa*, comprised the basal area-weighted mean tree DBH and an index of soil moisture. The expected plant density was estimated for both species in the region of interest. The estimate of expected plant density, as defined in (7), was 0.111 individuals per square metres for *L. europaea* and 0.054 individuals per square metres for *L. pilosa*. The associated estimated variances were respectively 0.00125 and 0.00052.

In the Monte Carlo simulation study, the variant with the Pearson residuals and Pearson correlation test was the one that produced the largest power, whereas the variant with randomised quantile residuals was the one that produced actual significance levels closer to the nominal level of 5%. It was clear that the larger the sample, the higher the power. The power increased monotonously for the LGCP with increasing standard deviation parameter from 0 to 3, whereas it increased and then decreased with the two types of NSPs (i.e., Matérn cluster and generalised Thomas) with increasing cluster size. It was also apparent that when the distance between the vegetation plots in a same pair was reduced, the power of the test increased (as can be seen in Fig. 5).

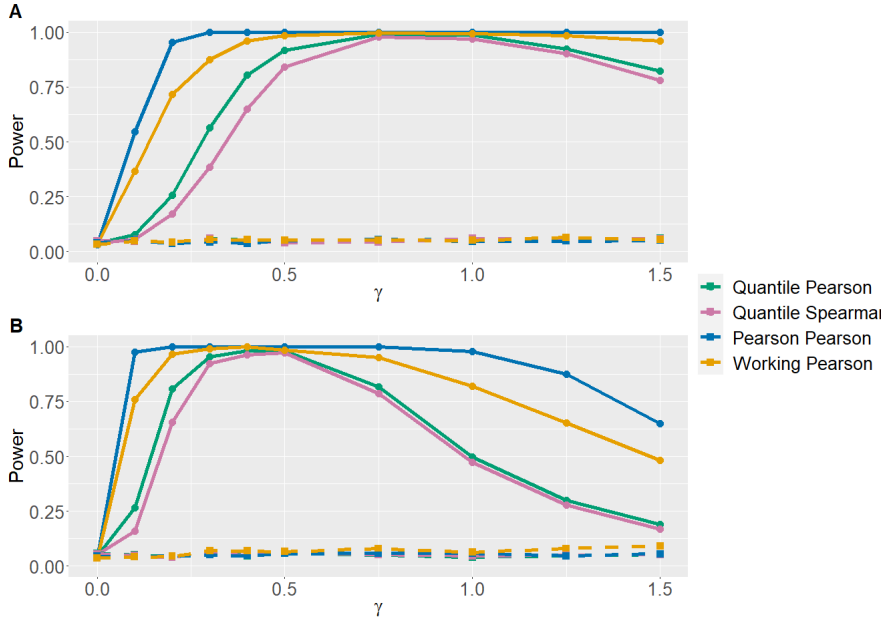

Figure 5. Examples of power curves, with Matérn and Thomas processes, for different types of residuals (quantile, Pearson, working) and correlation coefficients (Pearson, Spearman), with varying γ. The curves with solid lines represent the cases with a distance of 0.62 metres between the plot centres, and the curves with dashed lines represent the cases with a distance of 5 metres between the plot centres.

6.2 Estimation of plant density based on presence/absence data using hybrid inference (Paper II)

The results were separated into two categories for this paper as well, in the same way as in Paper I. A model was first constructed based on real data, i.e. P/A data of *V. vitis-idaea* in the Lappland region of Norrbotten county in Sweden. The model comprised two explanatory variables: the number of tree stems per hectare, and an indicator variable indicating whether the soil was humid or wet. The density of *V. vitis-idaea* was estimated to be approximately 7.5 individuals per square metre in the whole Lappland region of Norrbotten county. If only the areas consisting of productive forests were considered, this estimated density increased to approximately 9.7 individuals per square metre. The associated estimated variances were respectively 0.209 and 0.411.

A Monte Carlo study was also performed to see whether these estimators and associated variance estimators performed satisfactorily. In both cases with known and unknown area, the estimator of expected density presented slight negative bias and the associate variance estimators showed small bias (see Paper II).

6.3 Estimation of parameters in inhomogeneous Neyman-Scott processes using presence/absence data (Paper III)

There were two parts in the results section in this paper as well. Models were first created on field data collected in the Kulbäcksliden research park in Västerbotten County, Sweden. Three species were selected to apply the proposed method: *M. bifolium*, *L. pilosa* and *L. europaea*. Only one covariate variable was used for each model. All the models passed the Shapiro-Wilk test of normality based on the model residuals, and the parameters for the underlying NSPs were estimated. Local estimates of plant density when the covariate was equal to specific, meaningful values were also provided in the article. The estimated process intensities (as well as the associated 95% confidence interval) when the covariates equal their sample median values were respectively 0.052 (0.034, 0.071), 0.11 (0.063, 0.17) and 0.026 (0.018, 0.035) for *M. bifolium*, *L. pilosa* and *L. europaea*.

In the Monte Carlo study, it was apparent that the (mean and median) biases and standard deviations of the estimators decreased as the sample size increased. For the largest sample size considered, the biases were very small and the ACLs were pretty close to the nominal level of 95%. However, for the smallest sample size considered, the ACLs were notably lower than the nominal level 95% for several parameters and estimates of plant density. The standard error estimators exhibited some biases, but they were not severe for any of the sample sizes considered.

6.4 A closer look at uncertainties in forest ecosystem surveys using remotely sensed data and model-based inference (Paper IV)

In the simulation study of Paper IV, several cases were investigated. In the first case, variability due to study area size was studied. The sample size was

held constant at 150 cells, while the study area (i.e. the area where the models are applied) varied between very small area, small area, intermediate area and very large area (the whole grid). The main observation from that subcase was that the variance of the true value decreased with study area size, whereas the other components of the MSE did not appear to be particularly affected (Fig. 6). A particularly interesting observation when the area of application was the entire grid was that the MSE was smaller than the variance of the predictor due to the non-negligible covariance term.

The second case was variability due to field sample size. The study area was the whole grid in both regions, and the field sample size varied between 50, 150 and 500 sample units. This change in sample size principally affected the variance of the predictor (Fig. 7). More specifically, the larger the sample, the smaller the variance of the predictor.

The third case was variability due to spatial autocorrelation of the error terms. The sample size was set to 150 sample units, the study area was set to the whole grid, and the strength of the autocorrelation varied between no autocorrelation, mild autocorrelation, moderate autocorrelation and strong autocorrelation. The results showed that both the variance of the true value and the covariance term increased significantly with the strength of spatial autocorrelation (Fig. 8). A similar change occurred for the variance of the predictor, albeit less obviously. However, this had the effect of decreasing the MSE with autocorrelation strength, mostly because of the covariance term.

The fourth case was the effect of model transfer on the components of the MSE. The model constructed on Tanzania data was applied on USA data and vice versa. Significant model bias occurred in both cases, and the squared model bias component made up for approximately 95% of the total MSE. This can be explained by strong extrapolation that occurs when applying a model from one region to another, since these regions might not have the same range for the target variable.

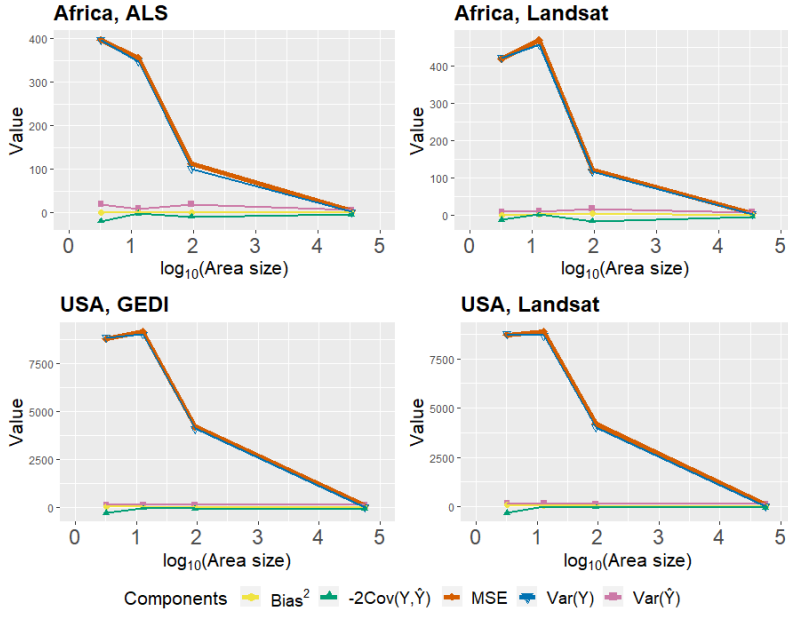

Figure 6. Effect of area size on the different MSE components in the different areas of study and for each kind of RS data.

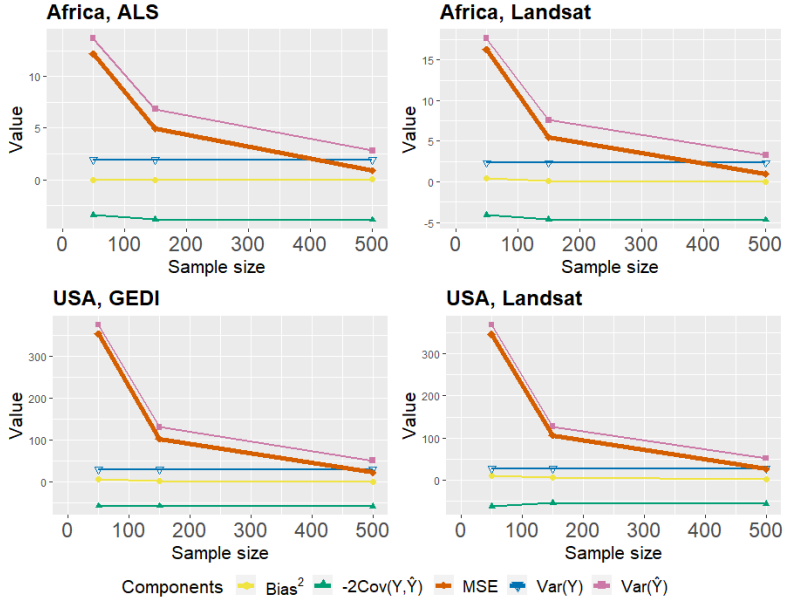

Figure 7. Effect of sample size on the different MSE components in the different areas of study and for each kind of RS data.

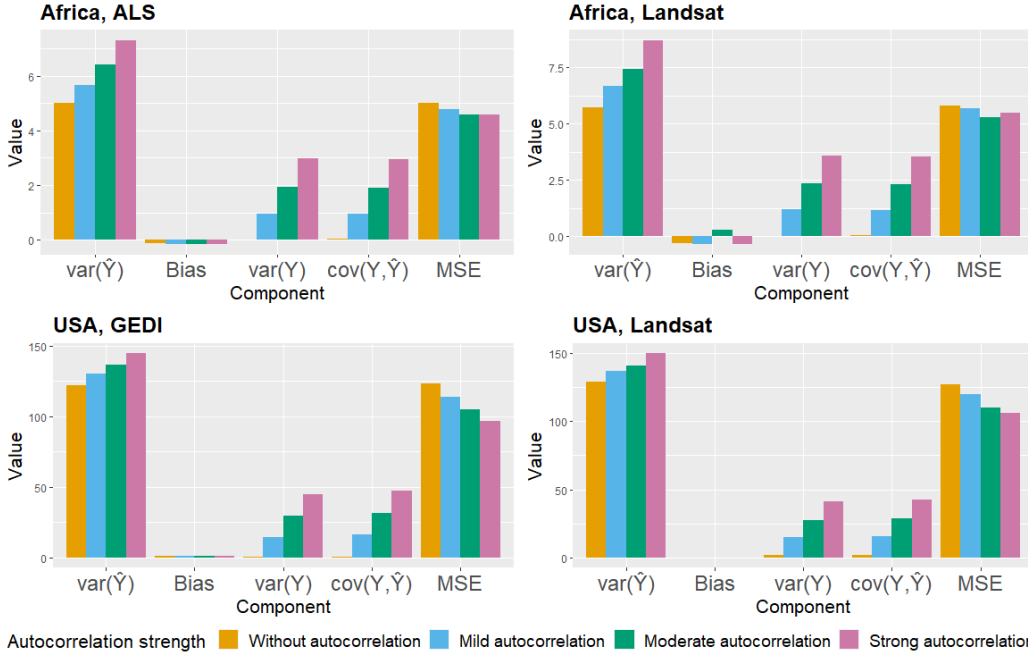

Figure 8. Effect of autocorrelation strength on the different MSE components in the different areas of study and for each kind of RS data.

7. Discussion and future research

7.1 Some reflections and conclusions

In this thesis, several methods intended for application in ecological research and environmental monitoring programmes were developed. A particular emphasis was made on P/A data, which are oftentimes registered as part of these programmes but are only occasionally used in analyses. The methods presented in this thesis for estimating plant density from P/A data show versatility, since they can be adapted to different assumptions regarding plant populations (more precisely, plant locations) and different types of covariate information (wall-to-wall or at plot sample level). The results were promising but additional research is needed.

P/A data are known for being hard to interpret (Ståhl et al. 2017). It is difficult to get ecologically valuable measurements directly from P/A data (for example total cover area or number of plants per hectare), and the occurrence proportions obtained from P/A data analyses are usually comparable only within monitoring inventories as long as the sample plot sizes are the same. In this thesis, several methods that mitigate these aspects have been presented. Inhomogeneous point process models, i.e. point process models that take environmental covariates into account, were used to model plant positions. These point process models imply GLMs that create a link between these environmental covariates and P/A data of plants. Based on these GLMs, estimates of plant density can be obtained locally and in large regions when P/A data are registered at sample plot level. Thus, if the assumed point process model is approximately correct, the proposed methodology provides estimates of plant density that are more easily interpretable than, for example, occurrence proportions. Such estimates can be used for state and trend analyses, as well as for reporting by environmental monitoring programmes within the scope of the habitat directives mentioned in Section 1.

In a way, this thesis can be seen as an argument for the more frequent use of P/A data in environmental monitoring analyses. The cost- and time-effectiveness of P/A sampling, in combination with the readily-available nature of RS data, can be reasonable arguments in favour of the wide-spreading of GLMs with binary response variables in ecology, especially for environmental analyses. This thesis has hopefully demonstrated that model-

based and hybrid inference can be used efficiently to derive meaningful and construable characteristics of plant populations – in particular, plant density and abundance – using spatial models to represent the locations of plants as well as P/A data in connection with auxiliary environmental data.

One should keep in mind that inference from model-based estimators always rely on some model assumptions, and these should be tested. Different ways to assess the GLMs implied by the underlying spatial point process models have been suggested in this thesis. The tests presented herein, as well as in Papers I and III, are based on model residuals. Randomised quantile residuals appear to be useful for assessing binary regression models, although their randomness could cause problems in the correlation tests. Indeed, as stated in Paper I, the test statistic and associated p-value will vary each time the test is run, even for the exact same values of response variable and covariate data. Moreover, it has been shown in the simulation study in Paper I that the test variant with Pearson residuals is more powerful than the one making use of randomised quantile residuals, although the actual significance levels for the former variant were a little less satisfactory.

One relevant observation with regard to environmental monitoring programmes based on the analyses in Paper I is that the method developed within would detect deviations from random populations better if the distance between the plots in a same pair of vegetation plots would be decreased to its minimum possible without any overlap occurring (in case such a sampling design is used, for example in the Swedish NFI). This aspect could be taken into account for future planning in the monitoring programmes.

The derived estimators and corresponding variance estimators in Papers I, II and III were evaluated through Monte Carlo simulations. The results indicated that these estimators performed relatively well, with only slight bias and reasonable orders of magnitude for the variance estimates, particularly when the sample size increased. In addition, the confidence intervals in Paper III were relatively narrow for the larger sample sizes considered, which shows that the method used therein is rather precise.

In Papers I and II, some estimates of expected density for several plant species in an entire region of Sweden were produced. However, it is difficult to see if these values are reasonably accurate, since there exists no reference data to compare with. In spite of that, these values do not appear to be too far-fetched, since for example *V. vitis-idaea* is a relatively common plant

species in the whole of Sweden, and thus relatively high densities are to be expected.

An important aspect to take into consideration when performing plant surveys is to decide what constitutes a presence registration for a given species. In other words, it has to be decided what part of the plant is sufficient for the plant to be considered as present on a sample plot. In Paper III, presence is recorded if a predetermined part of the plant is located on the vegetation plot (i.e., their root points), as advised by, e.g., Cain & Castro (1959), whereas in Papers I and II, presence was recorded if any part of the plant was located in the vegetation plot. As a consequence, the plot radii needed to be adjusted in the calculations by adding a presumed average radius for the plant, in accordance with Ståhl et al. (2017).

In Paper IV, the MSE and its different components were estimated in a model-based context. The results showed that the variance of the estimator (or predictor) is not the only component that can be significant, especially in small-area surveys. In the latter case, the variance of the true value of the variable under study can be largely influential. Moreover, if a spatial autocorrelation structure exists, the covariance between the predicted value and the true value can impact the MSE and contribute to it negatively. Model bias can be an issue if one applies a model to another region compared to where said model was constructed. Thus, the conclusion is that one should be aware of other uncertainty components than the variance of the predictor when performing model-based inference. This conclusion has consequences for Papers I, II and III, as will be explained in subsection 7.2.

The models presented in Papers I, II and III contain at most two explanatory variables. As a consequence, these models can be considered too simplistic, and can be criticised for failing to capture the complexity of the environment and the different processes within it that can affect the presence of plants at a given location. It would have been interesting to consider models with more explanatory variables, although this might necessitate an increase of the sample size as well. However, the methods presented in these papers are computationally demanding, and the complexity rises when the number of explanatory variables increases, especially in Paper III. Hence, future attempts at such modelling should take computer efficiency as a factor.

7.2 Ideas for future research

An interesting area to look further into is the estimation of change of plant density between two time points in case plant data are assumed to be generated from inhomogeneous point processes. Ståhl et al. (2017) have already studied this issue for homogeneous PPP. Modelling of P/A data from two different point processes are needed: one from the process at the first time point and another one at the second time point. If the time between the two considered time points is long enough, these two processes can be considered independent, and then the extension from the methods in, e.g., Paper I can be relatively straightforward. However, if this time interval is relatively short, then the two point processes will probably be dependent, and adjustments would be needed in the modelling.

In Paper II, hybrid inference is applied to data that are supposed to be realisations of an inhomogeneous PPP. It could be feasible to develop the method for other kinds of point processes as well, not least Neyman-Scott cluster processes, that is to expand the methods presented in Paper III to obtain an estimator of expected plant density in an entire region.

In Paper III, inhomogeneity in the NSPs was introduced by letting μ vary by environmental covariates. The idea followed from Waagepetersen (2007). Nevertheless, this is far from being the only way to make a NSP inhomogeneous. Baddeley et al. (2016) make the intensity of the parent process, τ, vary with covariates. Other methods to include non-homogeneity in cluster processes include second order intensity reweighted stationarity (Baddeley et al. 2000), which is another way to make μ vary through thinning the offspring points. This is similar to dependent thinning (Prokešová 2010). Other methods make γ vary. Such examples include inhomogeneous space-location dependent scaling (in which τ varies as well (Hahn et al. 2003)) or the "growing clusters" approach developed in (Mrkvička 2014). In the latter, μ varies as well. It would be interesting to expand the methods derived in Paper III by applying these other techniques to make NSPs inhomogeneous, as well as different other types of NSPs such as Thomas processes, although this would complicate the numerical calculations.

Takashina et al. (2018) propose a framework to estimate abundance from count data using SRS and cluster sampling while making assumptions about an underlying homogeneous Thomas process. An area of interest could be to develop the method presented therein so that it takes into account inhomogeneous point processes as well. Several other models already exist

to estimate population abundance or density based on abundance data. Design-based methods that make use of, e.g., adaptive cluster sampling have been used to estimate abundance for rare plant species that are known to grow in clusters, using, for example, a Horvitz-Thompson estimator as in Philippi (2005). Abrahamson et al. (2011) compared the performance of several sampling designs, including adaptive cluster sampling, to estimate understory plant abundance.

The measure of uncertainty in Papers I, II and III is solely the variance of the estimator of the variable of interest. However, it has been shown in Paper IV that other uncertainty components (that constitute the formula for the MSE) can be significant in model-based studies. Moreover, the MSE is more suitable as a measurement of uncertainty compared to the variance of the estimator/predictor alone, since it takes into account the deviation between the true and estimated/predicted value. A problem is that it seems to be difficult to estimate the model bias for the cases studies in Papers I, II and III, since there are no registrations of plant abundance available at sample plot level. Instead, the bias is estimated by a simulation study. Likewise, a possible further development of the studies regarding plant density can be to specify predictors for actual plant density at regional level and perform simulations similar to the ones conducted in Paper IV for a wider uncertainty analysis of the estimations of plant density.

In the simulation study in Paper IV, the biomass values in each cell were supposed to be strictly positive. This is not always the case in reality, where some areas, even inside forests, can have an absence of biomass (for example in Næsset et al. (2016)). Further simulations would be needed where zero values can be accepted, for example by adopting a two-part modelling approach (Duan et al. 1983), where the 0-data are first generated from a specific model (e.g., a logistic regression model), and then the non-0 data are generated according to another model, e.g., a GLM (cf. Min & Agresti 2002).

There is a growing need for methods that integrate multiple data types into a single analytical framework. Over the past decade, initial efforts have been made to combine unbiased P/A data from structured monitoring programs with abundant presence-only data from citizen science sources; see, e.g., Fletcher et al. (2019) for a review. Using an inhomogeneous PPP model for multispecies data, Fithian et al. (2015) propose pooling presence-only and P/A data to simultaneously estimate and correct for the sampling bias affecting the presence-only data. A key assumption of their model is that

the sampling bias is consistent across all species considered. Under these assumptions, they argue that unbiased or nearly unbiased estimates of plant density can be obtained for all species, including rare ones. Pacifici et al. (2017), Gelfand & Shirota (2019), and Ahmad Suhaimi et al. (2021) developed similar frameworks that also account for spatial dependence. However, because these models do not incorporate a multispecies setting, they are less suitable for rare species.

References

Aberdeen, J. (1958). The effect of quadrat size, plant size, and plant distribution on frequency estimates in plant ecology. *Australian Journal of Botany*, 6 (1), 47–58. https://doi.org/10.1071/BT9580047

Abrahamson, I.L., Nelson, C.R. & Affleck, D.L. (2011). Assessing the performance of sampling designs for measuring the abundance of understory plants. *Ecological Applications*, 21 (2), 452–64. https://doi.org/10.1890/09-2296.1

Ågren, A.M., Larson, J., Paul, S.S., Laudon, H. & Lidberg, W. (2021). Use of multiple LIDAR-derived digital terrain indices and machine learning for high-resolution national-scale soil moisture mapping of the Swedish forest landscape. *Geoderma*, 404. https://doi.org/10.1016/j.geoderma.2021.115280

Ahmad Suhaimi, S.S., Blair, G.S. & Jarvis, S.G. (2021). Integrated species distribution models: A comparison of approaches under different data quality scenarios. *Diversity and Distributions*, 27 (6), 1066–1075. https://doi.org/10.1111/ddi.13255

Amemiya, T. (1985). *Advanced Econometrics*. Harvard University Press, Cambridge.

Arrhenius, O. (1921). Species and area. *Journal of Ecology*, 9, 95–99. https://doi.org/10.2307/2255763

Askne, J., Fransson, J., Santoro, M., Soja, M. & Ulander, L. (2013). Model-Based Biomass Estimation of a Hemi-Boreal Forest from Multitemporal TanDEM-X Acquisitions. *Remote Sensing*, 5 (11), 5574–5597. https://doi.org/10.3390/rs5115574

Baddeley, A., Berman, M., Fisher, N.I., Hardegen, A., Milne, R.K., Schuhmacher, D. & Shah, R. (2010). Spatial logistic regression and change-of-support in poisson point processes. *Electronic Journal of Statistics*, 4, 1151–1201. https://doi.org/10.1214/10-EJS581

Baddeley, A., Rubak, E. & Turner, R. (2016). *Spatial Point Patterns: Methodology and Applications with R*. CRC Press, Boca Raton. https://doi.org/10.1201/b19708

Baddeley, A.J., Møller, J. & Waagepetersen, R. (2000). Non- and semi-parametric estimation of interaction in inhomogeneous point patterns. *Statistica Neerlandica*, 54 (3), 329–350. https://doi.org/10.1111/1467-9574.00144

Bartlett, M.S. (1948). Determination of Plant Densities. *Nature*, 162 (4120), 621. https://doi.org/10.1038/162621a0

Batista, J.L.F. & Maguire, D.A. (1998). Modeling the spatial structure of topical forests. *Forest Ecology and Management*, 110 (1–3), 293–314. https://doi.org/10.1016/S0378-1127(98)00296-5

Blackman, G.E. (1935). A study by statistical methods of the distribution of species in grassland associations. *Annals of Botany*, os-49 (4), 749–777. https://doi.org/10.1093/oxfordjournals.aob.a090534

Bonham, C.D. (2013). *Measurements for Terrestrial Vegetation: Second Edition*. Wiley, New York. https://doi.org/10.1002/9781118534540

Bradter, U., Mair, L., Jönsson, M., Knape, J., Singer, A. & Snäll, T. (2018). Can opportunistically collected Citizen Science data fill a data gap for habitat suitability models of less common species? *Methods in Ecology and Evolution*, 9 (7), 1667–1678. https://doi.org/10.1111/2041-210X.13012

Bullock, E., Healey, S., Yang, Z., Acosta, R., Villalba, H., Insfran, K., Melo, J., Wilson, S., Duncanson, L., Naesset, E., Armston, J., Saarela, S., Stahl, G., Patterson, P. & Dubayah, R. (2023). Estimating aboveground biomass density using hybrid statistical inference with GEDI lidar data and Paraguay's national forest inventory. *Environmental Research Letters*, 18 (8). https://doi.org/10.1088/1748-9326/acdf03

Cain, S.A. & Castro, G.M.O. (1959). *Manual of Vegetation Analysis*. Harper, New York.

Cassel, C.M., Särndal, C.E. & Wretman, J.H. (1977). *Foundations of inference in survey sampling*. John Wiley & Sons.

Chang, Y.-M. & Huang, Y.-C. (2024). Estimating Species Abundance from Presence–Absence Maps by Kernel Estimation. *Journal of Agricultural, Biological and Environmental Statistics*, 29 (4), 812–830. https://doi.org/10.1007/s13253-023-00589-4

Commission of the European Communities (2003). Council directive 92/43/EEC of 21 May 1992 on the conservation of natural habitats and of wild fauna and flora.

Condés, S. & McRoberts, R.E. (2017). Updating national forest inventory estimates of growing stock volume using hybrid inference. *Forest Ecology and Management*, 400, 48–57. https://doi.org/10.1016/j.foreco.2017.04.046

Conlisk, E., Conlisk, J. & Harte, J. (2007). The impossibility of estimating a negative binomial clustering parameter from presence-absence data: A comment on He and Gaston. *American Naturalist*, 170 (4), 651–654. https://doi.org/10.1086/521339

Cordy, C.B. (1993). An extension of the Horvitz-Thompson theorem to point sampling from a continuous universe. *Statistics and Probability*

Letters, 18 (5), 353–362. https://doi.org/10.1016/0167-7152(93)90028-H

Corona, P., Fattorini, L., Franceschi, S., Scrinzi, G. & Torresan, C. (2014). Estimation of standing wood volume in forest compartments by exploiting airborne laser scanning information: Model-based, Design-based, And hybrid perspectives. *Canadian Journal of Forest Research*, 44 (11), 1303–1311. https://doi.org/10.1139/cjfr-2014-0203

Cretois, B., Simmonds, E., Linnell, J., van Moorter, B., Rolandsen, C., Solberg, E., Strand, O., Gundersen, V., Roer, O. & Rod, J. (2021). Identifying and correcting spatial bias in opportunistic citizen science data for wild ungulates in Norway. *Ecology and Evolution*, 11 (21), 15191–15204. https://doi.org/10.1002/ece3.8200

Daley, D.J. & Vere-Jones, D. (2008). *An introduction to the theory of point processes (2nd ed.).* Springer Verlag, New York.

Di Biase, R., Marcelli, A., Franceschi, S., Bartolini, A. & Fattorini, L. (2022). Design-based mapping of plant species presence, association, and richness by nearest-neighbour interpolation. *Spatial Statistics*, 51. https://doi.org/10.1016/j.spasta.2022.100660

Diggle, P., Besag, J. & Gleaves, J. (1976). Statistical Analysis of Spatial Point Patterns by Means of Distance Methods. *Biometrics*, 32 (3), 659–667. https://doi.org/10.2307/2529754

Duan, N., Manning, W.G.Jr., Morris, C.N. & Newhouse, J.P. (1983). A comparison of alternative models for the demand for medical care (Corr: V2 P413). *Journal of Business and Economic Statistics*, 1, 115–126. https://doi.org/10.2307/1391852

Dubayah, R., Armston, J., Healey, S.P., Bruening, J.M., Patterson, P.L., Kellner, J.R., Duncanson, L., Saarela, S., Ståhl, G., Yang, Z., Tang, H., Blair, J.B., Fatoyinbo, L., Goetz, S., Hancock, S., Hansen, M., Hofton, M., Hurtt, G. & Luthcke, S. (2022). GEDI launches a new era of biomass inference from space. *Environmental Research Letters*, 17 (9). https://doi.org/10.1088/1748-9326/ac8694

Dudík, M., Schapire, R.E. & Phillips, S.J. (2005). Correcting sample selection bias in maximum entropy density estimation. *Proceedings of Advances in Neural Information Processing Systems*, 2005. 323–330

Eichhorn, M. (2010). Pattern reveals process: spatial organisation of a Kamchatkan stone birch forest. *Plant Ecology & Diversity*, 3 (3), 281–288. https://doi.org/10.1080/17550874.2010.528804

Ekström, M., Sandring, S., Grafström, A., Esseen, P.A., Jonsson, B.G. & Ståhl, G. (2020). Estimating density from presence/absence data in

clustered populations. *Methods in Ecology and Evolution*, 11 (3), 390–402. https://doi.org/10.1111/2041-210X.13347

Elzinga, C.L., Salzer, D.W. & Willoughby, J.W. (1998). *Measuring and Monitoring Plant Populations. BLM Technical Reference 1730-1.* BLM National Applied Resource Sciences Center, Denver.

Ene, L.T., Næsset, E. & Gobakken, T. (2013). Model-based inference for k-nearest neighbours predictions using a canonical vine copula. *Scandinavian Journal of Forest Research*, 28 (3), 266–281. https://doi.org/10.1080/02827581.2012.723743

Fattorini, L., Di Biase, R., Giuliarelli, D., Marcheselli, M., Pisani, C. & Corona, P. (2019). Mapping the diversity of forest attributes: a design-based approach. *Canadian Journal of Forest Research*, 49 (2), 190–197. https://doi.org/10.1139/cjfr-2018-0204

Fiorentin, L., Bonat, W., Pelissari, A., Machado, S., Téo, S. & Orso, G. (2019). Generalized Linear Models for Tree Survival in Lobolly Pine Plantations. *Cerne*, 25 (4), 347–356. https://doi.org/10.1590/01047760201925042649

Fithian, W., Elith, J., Hastie, T. & Keith, D.A. (2015). Bias correction in species distribution models: Pooling survey and collection data for multiple species. *Methods in Ecology and Evolution*, 6 (4), 424–438. https://doi.org/10.1111/2041-210X.12242

Fleischer, F., Eckel, S., Schmid, I. & Kazda, M. (2006). Point process modelling of root distribution in pure stands of Fagus sylvatica and Picea abies. *Canadian Journal of Forest Research*, 36 (1), 227–237. https://doi.org/10.1139/X05-232

Fletcher, R.J., Hefley, T.J., Robertson, E.P., Zuckerberg, B., McCleery, R.A. & Dorazio, R.M. (2019). A practical guide for combining data to model species distributions. *Ecology*, 100 (6). https://doi.org/10.1002/ecy.2710

Foody, G.M. (2008). Refining predictions of climate change impacts on plant species distribution through the use of local statistics. *Ecological Informatics*, 3 (3), 228–236. https://doi.org/10.1016/j.ecoinf.2008.02.002

Fortin, M., Bédard, S., DeBlois, J. & Meunier, S. (2008). Predicting individual tree mortality in northern hardwood stands under uneven-aged management in southern Quebec, Canada. *Annals of Forest Science*, 65 (2). https://doi.org/10.1051/forest:2007088

Fortin, M., Manso, R. & Calama, R. (2016). Hybrid estimation based on mixed-effects models in forest inventories. *Canadian Journal of Forest Research*, 46 (11), 1310–1319. https://doi.org/10.1139/cjfr-2016-0298

Fridman, J., Holm, S., Nilsson, M., Nilsson, P., Ringvall, A.H. & Ståhl, G. (2014). Adapting National Forest Inventories to changing requirements - The case of the Swedish National Forest Inventory at the turn of the 20th century. *Silva Fennica*, 48 (3). https://doi.org/10.14214/sf.1095

Gallegos Torell, Å. & Glimskär, A. (2009). Computer-aided calibration for visual estimation of vegetation cover. *Journal of Vegetation Science*, 20 (6), 973–983. https://doi.org/10.1111/j.1654-1103.2009.01111.x

Gaston, K.J., He, F., Maguran, A. & McGill, B. (2011). Species occurrence and occupancy. *Biological diversity: frontiers in measurement and assessment*, 141–151

Gelfand, A.E. & Shirota, S. (2019). Preferential sampling for presence/absence data and for fusion of presence/absence data with presence-only data. *Ecological Monographs*, 89 (3). https://doi.org/10.1002/ecm.1372

Gobakken, T., Næsset, E., Nelson, R., Bollandsås, O., Gregoire, T., Ståhl, G., Holm, S., Orka, H. & Astrup, R. (2012). Estimating biomass in Hedmark County, Norway using national forest inventory field plots and airborne laser scanning. *Remote Sensing of Environment*, 123, 443–456. https://doi.org/10.1016/j.rse.2012.01.025

Godínez-Alvarez, H., Herrick, J.E., Mattocks, M., Toledo, D. & Van Zee, J. (2009). Comparison of three vegetation monitoring methods: Their relative utility for ecological assessment and monitoring. *Ecological Indicators*, 9 (5), 1001–1008. https://doi.org/10.1016/j.ecolind.2008.11.011

Grafström, A., Lundström, N.L.P. & Schelin, L. (2012). Spatially Balanced Sampling through the Pivotal Method. *Biometrics*, 68 (2), 514–520. https://doi.org/10.1111/j.1541-0420.2011.01699.x

Grafström, A. & Matei, A. (2018). Spatially Balanced Sampling of Continuous Populations. *Scandinavian Journal of Statistics*, 45 (3), 792–805. https://doi.org/10.1111/sjos.12322

Gregoire, T.G. & Valentine, H.T. (2007). *Sampling strategies for natural resources and the environment*. Chapman & Hall/CRC Press, Boca Raton.

Greig-Smith, P. (1983). *Quantitative Plant Ecology, 3rd Edition*. University of California Press.

Guttorp, P. & Thorarinsdottir, T.L. (2012). What Happened to Discrete Chaos, the Quenouille Process, and the Sharp Markov Property? Some History of Stochastic Point Processes. *International Statistical Review*, 80 (2), 253–268. https://doi.org/10.1111/j.1751-5823.2012.00181.x

Hahn, U., Jensen, E., van Lieshout, M. & Nielsen, L. (2003). Inhomogeneous spatial point processes by location-dependent scaling. *Advanced in Applied Probability*, 35 (2), 319–336. https://doi.org/10.1239/aap/1051201648

He, F. & Gaston, K.J. (2000). Estimating species abundance from occurrence. *American Naturalist*, 156 (5), 553–559. https://doi.org/10.1086/303403

He, F. & Gaston, K.J. (2007). Estimating abundance from occurrence: An underdetermined problem. *American Naturalist*, 170 (4), 655–659. https://doi.org/10.1086/521340

Holt, A.R., Gaston, K.J. & He, F. (2002). Occupancy-abundance relationships and spatial distribution: A review. *Basic and Applied Ecology*, 3 (1), 1–13. https://doi.org/10.1078/1439-1791-00083

Horvitz, D.G. & Thompson, D.J. (1952). A Generalization of Sampling Without Replacement from a Finite Universe. *Journal of the American Statistical Association*, 47 (260), 663–685. https://doi.org/10.1080/01621459.1952.10483446

Hou, Z., Xu, Q., McRoberts, R., Greenberg, J., Liu, J., Heiskanen, J., Pitkänen, S. & Packalen, P. (2017). Effects of temporally external auxiliary data on model-based inference. *Remote Sensing of Environment*, 198, 150–159. https://doi.org/10.1016/j.rse.2017.06.013

Hwang, W.H. & He, F. (2011). Estimating abundance from presence/absence maps. *Methods in Ecology and Evolution*, 2 (5), 550–559. https://doi.org/10.1111/j.2041-210X.2011.00105.x

Jaynes, E.T. (1957). Information Theory and Statistical Mechanics. *Physical Review*, 106 (4), 620–630. https://doi.org/10.1103/PhysRev.106.620

Johnston, A., Matechou, E. & Dennis, E. (2023). Outstanding challenges and future directions for biodiversity monitoring using citizen science data. *Methods in Ecology and Evolution*, 14 (1), 103–116. https://doi.org/10.1111/2041-210X.13834

Johnston, A., Moran, N., Musgrove, A., Fink, D. & Baillie, S. (2020). Estimating species distributions from spatially biased citizen science data. *Ecological Modelling*, 422. https://doi.org/10.1016/j.ecolmodel.2019.108927

Kangas, A., Astrup, R., Breidenbach, J., Fridman, J., Gobakken, T., Korhonen, K.T., Maltamo, M., Nilsson, M., Nord-Larsen, T., Næsset, E. & Olsson, H. (2018). Remote sensing and forest inventories in Nordic countries – roadmap for the future. *Scandinavian Journal of Forest Research*, 33 (4), 397–412. https://doi.org/10.1080/02827581.2017.1416666

Kylin, H. (1926). Uber Begriffsbildung und Statistik in der Pflanzensociologie. *Botaniska notiser*, ii. (81)

Lidberg, W., Nilsson, M. & Agren, A. (2020). Using machine learning to generate high-resolution wet area maps for planning forest management: A study in a boreal forest landscape. *Ambio*, 49 (2), 475–486. https://doi.org/10.1007/s13280-019-01196-9

Lindenmayer, D.B., Welsh, A., Donnelly, C., Crane, M., Michael, D., Macgregor, C., McBurney, L., Montague-Drake, R. & Gibbons, P. (2009). Are nest boxes a viable alternative source of cavities for hollow-dependent animals? Long-term monitoring of nest box occupancy, pest use and attrition. *Biological Conservation*, 142 (1), 33–42. https://doi.org/10.1016/j.biocon.2008.09.026

Lindgren, N., Olsson, H., Nyström, K., Nyström, M. & Ståhl, G. (2021). Data Assimilation of Growing Stock Volume Using a Sequence of Remote Sensing Data from Different Sensors. *Canadian Journal of Remote Sensing*, 48 (2), 127–143. https://doi.org/10.1080/07038992.2021.1988542

Mäkinen, J., Merow, C. & Jetz, W. (2024). Integrated species distribution models to account for sampling biases and improve range-wide occurrence predictions. *Global Ecology and Biogeography*, 33 (3), 356–370. https://doi.org/10.1111/geb.13792

Marcelli, A., Corona, P. & Fattorini, L. (2019). Design-based estimation of mark variograms in forest ecosystem surveys. *Spatial Statistics*, 30, 27–38. https://doi.org/10.1016/j.spasta.2019.02.002

Matérn, B. (1960). Spatial variation. *Meddelanden Fran Statens Skogsforskningsinstitut*, 49 (5), 1–144. https://res.slu.se/id/publ/125179

Matérn, B. (1986). *Spatial variation. Lecture notes in statistics 36*. Springer Verlag.

McCullagh, P. (1989). *Generalized Linear Models*. 2nd ed. Springer US.

McRoberts, R., Næsset, E., Gobakken, T., Chirici, G., Condés, S., Hou, Z., Saarela, S., Chen, Q., Ståhl, G. & Walters, B. (2018). Assessing components of the model-based mean square error estimator for remote sensing assisted forest applications. *Canadian Journal of Forest Research*, 48 (6), 642–649. https://doi.org/10.1139/cjfr-2017-0396

McRoberts, R.E., Næsset, E., Liknes, G.C., Chen, Q., Walters, B.F., Saatchi, S. & Herold, M. (2019). Using a Finer Resolution Biomass Map to Assess the Accuracy of a Regional, Map-Based Estimate of Forest Biomass. *Surveys in Geophysics*, 40 (4), 1001–1015. https://doi.org/10.1007/s10712-019-09507-1

Mehtätalo, L. & Lappi, J. (2020). *Biometry for Forestry and Environmental Data : With Examples in R*. Chapman and Hall/CRC, Boca Raton.

Min, Y. & Agresti, A. (2002). Modeling Nonnegative Data with Clumping at Zero: A Survey. *Journal of the Iranian Statistical Society*, 1 (1–2), 7–33

Møller, J. & Waagepetersen, R. P., R. (2003). *Statistical Inference and Simulation for Spatial Point Processes*. CRC Press.

Morrison, D.A., Le Brocque, A.F. & Clarke, P.J. (1995). An assessment of some improved techniques for estimating the abundance (frequency) of sedentary organisms. *Vegetatio*, 120 (2), 131–145. https://doi.org/10.1007/BF00034343

Mrkvička, T. (2014). Distinguishing Different Types of Inhomogeneity in Neyman–Scott Point Processes. *Methodology and Computing in Applied Probability*, 16 (2), 385–395. https://doi.org/10.1007/s11009-013-9365-4

Mukhopadhyay, R., Ekström, M., Lindberg, E., Persson, H., Saarela, S. & Nilsson, M. (2024). Computation of prediction intervals for forest aboveground biomass predictions using generalized linear models in a large-extent boreal forest region. *Forestry*, cpae006, 1–11. https://doi.org/10.1093/forestry/cpae006

Næsset, E., Ørka, H.O., Solberg, S., Bollandsås, O.M., Hansen, E.H., Mauya, E., Zahabu, E., Malimbwi, R., Chamuya, N., Olsson, H. & Gobakken, T. (2016). Mapping and estimating forest area and aboveground biomass in miombo woodlands in Tanzania using data from airborne laser scanning, TanDEM-X, RapidEye, and global forest maps: A comparison of estimated precision. *Remote Sensing of Environment*, 175, 282–300. https://doi.org/10.1016/j.rse.2016.01.006

Neyman, J. & Scott, E. (1952). A Theory of the Spatial Distribution of Galaxies. *Astrophysical Journal*, 116 (1), 144–163. https://doi.org/10.1086/145599

Nilsson, M., Nordkvist, K., Jonzén, J., Lindgren, N., Axensten, P., Wallerman, J., Egberth, M., Larsson, S., Nilsson, L., Eriksson, J. & Olsson, H. (2017). A nationwide forest attribute map of Sweden predicted using airborne laser scanning data and field data from the National Forest Inventory. *Remote Sensing of Environment*, 194, 447–454. https://doi.org/10.1016/j.rse.2016.10.022

Ogata, Y. (2020). Cluster analysis of spatial point patterns: posterior distribution of parents inferred from offspring. *Japanese Journal of Statistics and Data Science*, 3 (1), 367–390. https://doi.org/10.1007/s42081-019-00065-9

Pacifici, K., Reich, B.J., Miller, D.A.W., Gardner, B., Stauffer, G., Singh, S., McKerrow, A. & Collazo, J.A. (2017). Integrating multiple data sources in species distribution modeling: A framework for data fusion. *Ecology*, 98 (3), 840–850. https://doi.org/10.1002/ecy.1710

Pellissier, V., Bergès, L., Nedeltcheva, T., Schmitt, M., Avon, C., Cluzeau, C. & Dupouey, J. (2013). Understorey plant species show long-range spatial patterns in forest patches according to distance-to-edge. *Journal of Vegetation Science*, 24 (1), 9–24. https://doi.org/10.1111/j.1654-1103.2012.01435.x

Philippi, T. (2005). Adaptive Cluster Sampling for Estimation of Abundances within Local Populations of Low-Abundance Plants. *Ecology*, 86 (5), 1091–1100. https://doi.org/10.1890/04-0621

Phillips, S.J., Anderson, R.P., Dudík, M., Schapire, R.E. & Blair, M.E. (2017). Opening the black box: an open-source release of Maxent. *Ecography*, 40 (7), 887–893. https://doi.org/10.1111/ecog.03049

Pielou, E. (1957). The Effect of Quadrat Size on the Estimation of the Parameters of Neyman and Thomas Distributions. *Journal of Ecology*, 45 (1), 31–47. https://doi.org/10.2307/2257075

Prokešová, M. (2010). Inhomogeneity in Spatial Cox Point Processes – Location Dependent Thinning Is Not the Only Option. *Image Analysis & Stereology*, 29 (3). https://doi.org/10.5566/ias.v29.p133-141

R Core Team (2025). R: A Language and Environment for Statistical Computing. R Foundation for Statistical Computing. https://www.R-project.org/

Rao, C.R. (1973). *Linear statistical Inference and its Applications*. Wiley, New York.

Raunkiaer, C. (1934). *The life forms of plants and statistical plant geography; being the collected papers of C. Raunkiaer. The life forms of plants and statistical plant geography; being the collected papers of C. Raunkiaer.*. Oxford: Clarendon Press.

Reese, H., Nilsson, M., Pahlén, T.G., Hagner, O., Joyce, S., Tingelöf, U., Egberth, M. & Olsson, H. (2003). Countrywide Estimates of Forest Variables Using Satellite Data and Field Data from the National Forest Inventory. *Ambio*, 32 (8), 542–548. https://doi.org/10.1579/0044-7447-32.8.542

Renner, I.W. & Warton, D.I. (2013). Equivalence of MAXENT and Poisson Point Process Models for Species Distribution Modeling in Ecology. *Biometrics*, 69 (1), 274–281. https://doi.org/10.1111/j.1541-0420.2012.01824.x

Ringvall, A., Petersson, H., Ståhl, G. & Lämås, T. (2005). Surveyor consistency in presence/absence sampling for monitoring vegetation in a boreal forest. *Forest Ecology and Management*, 212 (1–3), 109–117. https://doi.org/10.1016/j.foreco.2005.03.002

Robinson, O., Ruiz-Gutierrez, V. & Fink, D. (2018). Correcting for bias in distribution modelling for rare species using citizen science data. *Diversity and Distributions*, 24 (4), 460–472. https://doi.org/10.1111/ddi.12698

Rochefort, L., Isselin-Nondedeu, F., Boudreau, S. & Poulin, M. (2013). Comparing survey methods for monitoring vegetation change through time in a restored peatland. *Wetlands Ecology and Management*, 21 (1), 71–85. https://doi.org/10.1007/s11273-012-9280-4

Royle, J., Chandler, R., Yackulic, C. & Nichols, J. (2012). Likelihood analysis of species occurrence probability from presence-only data for modelling species distributions. *Methods in Ecology and Evolution*, 3 (3), 545–554. https://doi.org/10.1111/j.2041-210X.2011.00182.x

Saarela, S., Grafström, A., Ståhl, G., Kangas, A., Holopainen, M., Tuominen, S., Nordkvist, K. & Hyyppä, J. (2015). Model-assisted estimation of growing stock volume using different combinations of LiDAR and Landsat data as auxiliary information. *Remote Sensing of Environment*, 158, 431–440. https://doi.org/10.1016/j.rse.2014.11.020

Saarela, S., Healey, S.P., Yang, Z., Roald, B.-E., Patterson, P.L., Gobakken, T., Næsset, E., Hou, Z., McRoberts, R.E. & Ståhl, G. (2025). A Separable Bootstrap Variance Estimation Algorithm for Hierarchical Model-Based Inference of Forest Aboveground Biomass Using Data From NASA's GEDI and Landsat Missions. *Environmetrics*, 36 (1). https://doi.org/10.1002/env.2883

Saarela, S., Holm, S., Healey, S., Andersen, H., Petersson, H., Prentius, W., Patterson, P., Næsset, E., Gregoire, T. & Ståhl, G. (2018). Generalized Hierarchical Model-Based Estimation for Aboveground Biomass Assessment Using GEDI and Landsat Data. *Remote Sensing*, 10 (11). https://doi.org/10.3390/rs10111832

Saarela, S., Holm, S., Healey, S.P., Patterson, P.L., Yang, Z., Andersen, H.E., Dubayah, R.O., Qi, W., Duncanson, L.I., Armston, J.D., Gobakken, T., Næsset, E., Ekström, M. & Ståhl, G. (2022). Comparing frameworks for biomass prediction for the Global Ecosystem Dynamics Investigation. *Remote Sensing of Environment*, 278. https://doi.org/10.1016/j.rse.2022.113074

Schulze, E.-D., Beck, E., Buchmann, N., Clemens, S., Müller-Hohenstein, K. & Scherer-Lorenzen, M. (2019). *Plant Ecology, Second Edition*. 926. https://doi.org/10.1007/978-3-662-56233-8

Sen, P.K. & Singer, J.M. (1993). *Large sample methods in statistics: An introduction with applications*. Chapman & Hall, New York.

Shao, J. (2003). *Mathematical Statistics*. Springer Verlag, New York.

Sipek, M., Horvat, E., Kosic, I. & Sajna, N. (2022). Presence of Alien Prunus Serotina and Impatiens Parviflora in Lowland Forest Fragments in NE Slovenia. *Sumarski List*, 146 (5–6), 215–224. https://doi.org/10.31298/sl.146.5-6.4

Ståhl, G. (2003). Presence/absence sampling as a substitute for cover assessment in vegetation monitoring. *Advances in Forest Inventory for Sustainable Forest Management and Biodiversity Monitoring*, 137–142

Ståhl, G., Allard, A., Esseen, P.A., Glimskär, A., Ringvall, A., Svensson, J., Sundquist, S., Christensen, P., Torell, Å.G., Högström, M., Lagerqvist, K., Marklund, L., Nilsson, B. & Inghe, O. (2011a). National Inventory of Landscapes in Sweden (NILS)-scope, design, and experiences from establishing a multiscale biodiversity monitoring system. *Environmental Monitoring and Assessment*, 173 (1–4), 579–595. https://doi.org/10.1007/s10661-010-1406-7

Ståhl, G., Ekström, M., Dahlgren, J., Esseen, P.A., Grafström, A. & Jonsson, B.G. (2017). Informative plot sizes in presence-absence sampling of forest floor vegetation. *Methods in Ecology and Evolution*, 8 (10), 1284–1291. https://doi.org/10.1111/2041-210X.12749

Ståhl, G., Ekström, M., Dahlgren, J., Esseen, P.-A., Grafström, A., Jonsson, B.-G. & Molofsky, J. (2020). Presence–absence sampling for estimating plant density using survey data with variable plot size. *Methods in Ecology and Evolution*, 11 (4), 580–590. https://doi.org/10.1111/2041-210x.13348

Ståhl, G., Gobakken, T., Saarela, S., Persson, H.J., Ekström, M., Healey, S.P., Yang, Z., Holmgren, J., Lindberg, E., Nyström, K., Papucci, E., Ulvdal, P., Ørka, H.O., Næsset, E., Hou, Z., Olsson, H. & McRoberts, R.E. (2024). Why ecosystem characteristics predicted from remotely sensed data are unbiased and biased at the same time – and how this affects applications. *Forest Ecosystems*, 11. https://doi.org/10.1016/j.fecs.2023.100164

Ståhl, G., Holm, S., Gregoire, T.G., Gobakken, T., Næsset, E. & Nelson, R. (2011b). Model-based inference for biomass estimation in a LiDAR sample survey in Hedmark county, Norway. *Canadian Journal of Forest Research*, 41 (1), 96–107. https://doi.org/10.1139/X10-161

Ståhl, G., Saarela, S., Schnell, S., Holm, S., Breidenbach, J., Healey, S.P., Patterson, P.L., Magnussen, S., Næsset, E., McRoberts, R.E. & Gregoire, T.G. (2016). Use of models in large-area forest surveys: comparing model-assisted, model-based and hybrid estimation. *Forest Ecosystems*, 3 (1). https://doi.org/10.1186/s40663-016-0064-9

Stoklosa, J., Blakey, R.V. & Hui, F.K.C. (2022). An Overview of Modern Applications of Negative Binomial Modelling in Ecology and Biodiversity. *Diversity*, 14 (5). https://doi.org/10.3390/d14050320

Swindel, B.F. (1983). Choice of size and number of quadrats to estimate density from frequency in Poisson and binomially dispersed populations. *Biometrics*, 39 (2), 455–464. https://doi.org/10.2307/2531016

Takashina, N., Kusumoto, B., Beger, M., Rathnayake, S. & Possingham, H.P. (2018). Spatially explicit approach to estimation of total population abundance in field surveys. *J Theor Biol*, 453, 88–95. https://doi.org/10.1016/j.jtbi.2018.05.013

The European Commission (2020). EU Biodiversity Strategy for 2030 (COM/2020/380)

The European Commission (2021). New EU Forest Strategy for 2030 (COM/2021/572)

Thomas, M. (1949). A generalization of Poisson's binomial limit for use in ecology. *Biometrika*, 36 (Pt. 1-2), 18–25. https://doi.org/10.1093/biomet/36.1-2.18

Thompson, S.K. (2012). *Sampling, 3rd Edition*. Wiley.

Tomppo, E., Gschwantner, T., Lawrence, M. & McRoberts, R.E. (2010). Preface. *National Forest Inventories: Pathways for Common Reporting*, v–vi. https://doi.org/10.1007/978-90-481-3233-1

Trijoulet, V., Albertsen, C., Kristensen, K., Legault, C., Miller, T. & Nielsen, A. (2023). Model validation for compositional data in stock assessment models: Calculating residuals with correct properties. *Fisheries Research*, 257. https://doi.org/10.1016/j.fishres.2022.106487

Waagepetersen, R.P. (2007). An estimating function approach to inference for inhomogeneous Neyman-Scott processes. *Biometrics*, 63 (1), 252–258. https://doi.org/10.1111/j.1541-0420.2006.00667.x

Wallerman, J., Axensten, P., Egberth, M., Janzen, J., Sandstrom, E., Fransson, J.E.S. & Nilsson, M. (2021). SLU Forest Map - Mapping Swedish Forests Since Year 2000 In: Proceedings of IGARSS 2021, Crossing Borders, Virtual Symposium, Brussels, Belgium, 11-16 July, 2021, pp. 6056–6059., 2021.

Wintle, B.A., Elith, J. & Potts, J.M. (2005). Fauna habitat modelling and mapping: A review and case study in the Lower Hunter Central Coast region of NSW. *Austral Ecology*, 30 (7), 719–738. https://doi.org/10.1111/j.1442-9993.2005.01514.x

Yee, T. & Dirnböck, T. (2009). Models for analysing species' presence/absence data at two time points. *Journal of Theoretical Biology*, 259 (4), 684–694. https://doi.org/10.1016/j.jtbi.2009.05.004

Popular science summary

As the environment continues to change due to global warming, land use, and other human impacts, keeping an eye on plant populations has become increasingly important. Environmental monitoring programmes, such as the Swedish national forest inventory (NFI) and the national inventory of landscapes in Sweden (NILS), regularly collect large amounts of data pertaining to forests and landscapes that can be used in meaningful environmental analyses.

A particular sampling method that is used in such programmes and that has a large, but not fully exploited potential is the one where only presence or absence of a specific plant species is registered in each sample plot. That method is called presence/absence (P/A) sampling. This method is simple, time- and cost-effective, and easier to carry out compared to many traditional survey methods.

By combining mathematical models with P/A data and environmental covariate data from the NFI or remote sensing, plant density (defined as the number of plants per unit area) is estimated for several forest species, both locally and for entire regions. Different assumptions about the plant populations are considered (whether the plant individuals are randomly scattered or grow in groups). The developed approaches can also account for how environmental factors, such as surrounding trees or soil moisture, might influence the abundance of plants. In short, these techniques help turn simple yes-or-no data into valuable insights about where plants are likely to grow and how they interact with their environment. The methods were applied to both real-world and simulated data and showed promising results.

Nevertheless, the proposed estimates of plant density cannot be trusted blindly. There is some uncertainty at play whenever such values are presented. Errors can emerge from the mathematical models, the remote sensing products, the field measurements, and many more. That is why it is important that a measure of uncertainty is presented in connection with these estimates. In this thesis, it is supposed that the P/A and covariate data are error-free, for instance that there were no measurement errors and that the presences or absences of plants were registered correctly, although this is a simplification of reality.

In most studies, as in Papers I, I and III in this thesis, uncertainty is presented by means of the variance of the estimator. The variance expresses

how an estimator can vary. However, more uncertainty sources can arise when applying mathematical models. The study of the extent of these uncertainty components is the main objective of Paper IV, with a case study focused on biomass based on simulations. The results show that the variance can be used as a suitable approximation of uncertainty when the studies occur on a large area, whereas additional measures of uncertainty need to be taken into account when the study area is small.

Populärvetenskaplig sammanfattning

När miljön förändras på grund av global uppvärmning, markanvändning och annan mänsklig påverkan har övervakning av växtpopulationer blivit allt viktigare. Miljöövervakningsprogram, som Riksskogstaxeringen och Nationella Inventeringar av Landskapet i Sverige (NILS), samlar rutinmässigt in omfattande datamängder relaterade till skogar och landskap som kan användas för värdefulla miljöanalyser.

En specifik inventeringsmetod som används i sådana program och som har stora men relativt outnyttjade fördelar kallas närvaro/frånvaro. Den innebär att det i varje provyta endast registreras om en viss växtart registreras förekommer eller inte. Metoden är enkel, tidseffektiv och med mindre risk för att olika personer gör sinsemellan olika bedömningar än för många andra konventionella inventeringsmetoder.

Genom att kombinera matematiska modeller med data om närvaro/frånvaro samt andra data som beskriver miljön uppskattas planttätheten (definierad som antalet plantor per ytenhet) för flera skogsarter, både lokalt och för stora områden. Miljödata kommer från olika källor som t.ex. Riksskogstaxeringen eller fjärranalys. Olika förhållanden avseende växtpopulationer beaktas, t.ex. om växterna är slumpmässigt utspridda eller grupperade. De utvecklade metoderna kan också ta hänsyn till hur miljöfaktorer, såsom omgivande träd eller markfuktighet, påverkar planttätheten. I korthet kan dessa metoder, baserade på inventeringar som registrerar närvaro/frånvaro av arter, ge värdefulla insikter om planttäthet och hur den påverkas av sin omgivning. Metoderna har tillämpats på både faktiska fältdata och simulerade data och har gett lovande resultat.

De erhållna skattningarna av planttäthet bör dock inte ses som sanningar utan vidare granskning. Det finns osäkerheter i skattningarna och fel kan uppstå från matematiska modeller, kartprodukter framtagna med hjälp av fjärranalysdata, fältmätningar och från andra källor. Det är därför det är viktigt skattningarna också presenteras tillsammans med en uppskattning av osäkerheten, vilket också är en viktig del av avhandlingen. I denna avhandling antas dock att utnyttjade data är utan fel, exempelvis att de inte är behäftade med mätfel och att det inte finns några felregistreringar av frånvaro och närvaro av växtarter, vilket är en förenkling av verkligheten.

För många studier, inklusive papper I, II och III i denna avhandling, presenteras osäkerheten genom skattningars varians. En varians ger ett mått

på hur en skattning kan variera. Dock kan fler osäkerhetskällor förekomma när matematiska modeller tillämpas. Att undersöka omfattningen av dessa är i huvudfokus i papper IV, som är en fristående studie med fokus på biomassa och som bygger på simuleringar. Den studien visar att variansen för t.ex. en uppskattad mängd biomassa ger en rätt god approximation av osäkerhet vid storskaliga undersökningar, medan andra osäkerhetskomponenter kan få större betydelse ifall studieområdet är mindre.

Acknowledgements

To start with, a big thank you to my main supervisor Magnus Ekström. I really think you've been the best supervisor I could have thought of. Thanks for your patience, your help, your understanding, your amazing pedagogical skills, but also for the fascinating non-work related discussions. Of course, this big thank you includes my other supervisors, Göran Ståhl, Saskia Sandring and Bege Jonsson, for the constant help with my studies. My thanks go also to Jörgen Wallerman, who wasn't officially part of the supervising team but was definitely considered as part of the team. This wouldn't have been possible without you all! You were always available for me, gave me lots of insights (and comments) and I gained invaluable knowledge thanks to you all. We also had fun during the field excursions. Thanks as well to Lucy, my cat supervisor, for being present at (almost) all our supervision meetings.

There have been many people helping me at SLU, with my studies as well as morally, along the way. I'd like to thank some people in particular. Thanks to Hilda, for the tremendous musical discussions we've had (and discussions about our favourite musical genres… you still haven't converted me to "1-minute" punk music, sorry!); thanks to the "metal club" at SRH, especially Sabina and Mateusz (let's go to more gigs together, and expand the metal culture at SLU and worldwide!); thanks to Cornelia, for the possibility to speak my mother tongue once in a while; thanks to Olivia, for making me play the greatest video game ever (you know which one I'm referring to ☺); thanks to Emanuele, for being always so funny; thanks to Mariana for the varied discussions (and for being the first person that likes Visual Kei I meet in real life!); thanks to Felix, for being my only queer ally at the department; thanks to Kohsuke, for the practice in Japanese; thanks to Svetlana, for keeping in touch even after you left SLU; thanks to the remainder of the statistics team: Wilmer, Fabio and Anton (Oh, by the way, did you know that there's a strong correlation between being a statistician and playing the bass? Hilda, Felix, Wilmer and I proved it). Thanks to Carl for the last-minute help with the kappa (aaah, these cursed programmes that are always up to mischief at the worst moments…). Thanks to my co-authors that aren't included in my supervision group. And I guess thanks to some of my other PhD student colleagues. Thanks to all the people that have helped me with my studies, the logistics (for the field study), the courses, the programming, the administration (I promise I'll settle on a first name soon enough… I

already decided on my pronoun)… The list goes on and on, it's difficult to name everyone…

Luckily, I also got moral support from people outside of SLU. If it weren't for them, I probably wouldn't have survived in this dark, snowy, remote place (just joking… or not?). A gigantic thank you to my band mates Jakob, Nicklas, Olof, Jonathan, Karo, Lisa, Gena, Natalia and Tony. Music is my life, and playing with you guys has been a blast. I hope our adventures keep on going forever! Look out for our next gigs and releases (shameless self-promotion detected). Thanks to solitude, for giving me inspiration… I also thank my family for the support and for having put up with me during all these years…

Finally, thanks to the fuel of my life, music (wasn't it clear already?). Thanks to (old-school) Visual Kei, Japanese Rock/Metal, but also non-Japanese Metal (not Nu-metal tho). Special mention to Black Metal, which I started listening to while staying here (the environment sure helped: endless forests, the darkness, the harsh and cold winters…). It's an acquired taste…

II

Ecological Informatics 80 (2024) 102377

Contents lists available at ScienceDirect

Ecological Informatics

journal homepage: www.elsevier.com/locate/ecolinf

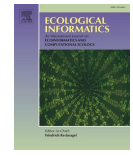

Estimation of plant density based on presence/absence data using hybrid inference

Léna Gozé [a,*], Magnus Ekström [a,b], Saskia Sandring [a], Bengt-Gunnar Jonsson [c], Jörgen Wallerman [a], Göran Ståhl [a]

[a] Department of Forest Resource Management, Swedish University of Agricultural Sciences, Skogsmarksgränd, 901 83 Umeå, Sweden
[b] Department of Statistics, USBE, Umeå University, Stastistics, 901 87 Umeå, Sweden
[c] Department of Natural Sciences, Design and Sustainable Development, Mid Sweden University, 851 70 Sundsvall, Sweden

ARTICLE INFO

Keywords:
Binary regression
Forest inventory data
Inhomogeneous Poisson point processes
Plant monitoring
Vegetation survey

ABSTRACT

Monitoring of plant populations has become more and more important, especially in the current context of environmental change. In this paper, we propose methods to estimate plant density from presence/absence surveys, wherein the presence or absence of each species is recorded on sample plots. Presence/absence sampling is a useful and relatively simple method for monitoring state and change of plant communities. Moreover, it has advantages compared to traditional plant cover assessment, the latter being more prone to observer bias. We present a hybrid estimation framework, that combines model- and design-based inference features, in which a generalised linear model (for binary presence/absence data) and an inhomogeneous Poisson model (for plant locations) are used to estimate plant density in a region of interest. We look at two different cases, the first one with a known area and the second one where the area is unknown and must be estimated. Our methods are applied to real data on *Vaccinium vitis-idaea* from the Swedish National Forest Inventory as well as simulated data to assess the performance of our estimators of plant density and corresponding variance estimators. The results obtained are promising and indicate that this method has a potential to add considerable analytic strength to monitoring programmes that collect presence/absence data.

1. Introduction

Collecting data on ground vegetation in forests is an important part of environmental monitoring, e.g., as part of initiatives for assessing trends in biodiversity (e.g., Pain et al. 2020; CBD 2002) or reporting within international agreements, such as the EU's Habitats Directive (Commission of the European Communities 2003). The demands for such monitoring programmes are currently increasing (e.g. O'Connor et al. 2020). However, monitoring plant populations is far from trivial. The methods applied should preferably be cost-efficient, easy to apply, and use protocols that avoid assessment errors. Methods based on assessing plant cover fulfil the first two requirements, but they tend to be prone to observer bias and variability due to phenology (e.g., Gallegos Torell & Glimskär 2009; Futschik et al. 2020; Kennedy & Addison 1987; Kercher et al. 2003).

In some cases, especially if the sample plots are not too large, methods based on presence/absence (P/A) sampling are less prone to errors of the kinds mentioned above (e.g., Ringvall et al. 2005; Kercher et al. 2003), since only the presence or absence of target species within plots needs to be registered. Some studies also suggest that P/A-data could be more useful than cover data in characterizing plant communities (e.g., Bastow Wilson 2012). On the other hand, whereas state and change in terms of vegetation cover or plant density are straightforward to interpret, state and change in terms of presence or absence frequencies are vaguer measures, which depend on sample plot size (e.g., Ståhl et al. 2017). However, if plant spatial occurrences are modelled, large-area estimates in terms of state and change of plant density or vegetation cover can be derived from P/A data (Ekström et al. 2020; Ståhl 2003) through application of model-based inference (e.g., Cassel et al. 1977; Warton et al. 2015). In addition, if a model for the probability that at least one plant will occur on a given plot (or pixel) depends on one or more auxiliary variables, then the model-based inferential framework assumes the availability of wall-to-wall auxiliary variables (cf. Fortin et al. 2023).

Auxiliary information is becoming increasingly available through different remote sensing techniques (e.g., Olsson 2020; Baena et al.

* Corresponding author.
E-mail address: lena.goze@slu.se (L. Gozé).

https://doi.org/10.1016/j.ecoinf.2023.102377
Received 12 July 2023; Received in revised form 10 November 2023; Accepted 11 November 2023
Available online 21 November 2023

2018; Dubayah et al. 2022) and so are data about presence of species through citizen science data collection programs (e.g., the Species Observation System in Sweden (Artdatabanken 2022) or the Atlas of Living Australia and its citizen science data portal (Belbin 2011)), which can be combined with P/A data (Fithian et al. 2015). Thus, opportunities for modelling plant occurrence are much better today compared to some decades ago. This type of modelling, with the availability of wall-to-wall auxiliary information from, e.g., remote sensing, can offer information in terms of both estimates and maps. Estimates are needed, e.g., for trend analysis and reporting to agreements such as the Habitats Directive mentioned above. Maps are useful for implementing management plans related to preserving threatened species (Baena et al. 2018) or limiting the impact of invasive species.

As the degree of detail in the auxiliary data increases, it will be possible to develop better models for plant occurrences, thus facilitating model-based estimation of plant density with higher precision. Dense networks of field plots from National Forest Inventories (NFI, e.g., Fridman et al. 2014; Tomppo et al. 2010) could provide such auxiliary data, because very detailed descriptions of biotic and abiotic conditions, including soil variables, are made on such plots. However, with sample plot data alone, i.e. without wall-to-wall data, it is not possible to apply the standard theory of model-based inference. Instead, hybrid inference can be an alternative (e.g., Corona et al. 2014; Ståhl et al. 2016), where features of model-based and design-based inference are combined.

Examples of applications of hybrid inference include biomass surveys based on LiDAR sample data in Norway (Ståhl et al. 2011) and North America (Margolis et al. 2015), biomass prediction for temperate and pan-tropical regions in the context of the Global Ecosystem Dynamics Investigation project (Saarela et al. 2022), comparison of forest biomass estimates based on coarse and fine resolution data in the USA (McRoberts et al. 2019), and estimation of growing stock volume in Italy (Corona et al. 2014), Finland (Saarela et al. 2015), and Spain (Condés and McRoberts 2017). It has been applied to a broad variety of models, such as mixed-effect models (Fortin et al. 2016) and more complex models where variance estimation requires resampling methods such as the parametric bootstrap (Fortin et al. 2018).

Using conventional model-based inference, Ekström et al. (Unpublished results) investigated the use of P/A data for regional estimation of plant density for a selection of plant species occurring mainly in forests. The main components of the study were inhomogeneous Poisson point processes for modelling the spatial locations of plants and generalised linear models (GLMs) with a complementary log-log link function for associating P/A data with the intensity of the point process, taking auxiliary remotely sensed data into account. As will be described in detail later, a similar modelling approach is used in the present study, with the important difference that auxiliary data were obtained from a large probability sample rather than from wall-to-wall remote sensing. A GLM with a complementary log-log link function for modelling P/A data has also been used in other studies, such as Yee & Mitchell (1991), Royle & Dorazio (2008), Lindenmayer et al. (2009), Baddeley et al. (2010) or Fithian et al. (2015). However, contrary to these articles, which focus on pixel-wise estimation for, e.g., producing maps, our study focuses on obtaining large-area estimates of plant density based on data collected exclusively from sample plots. To our knowledge, no previous studies that make use of hybrid inference have been conducted based on GLMs.

A complementary log-log link function has also been used for modelling of presence-only data (e.g., Phillips et al. (2017); Wan et al. (2017); Sreekumar & Nameer (2022)), although none of them make use of hybrid inference. In addition, it should be mentioned that the standard logit link is frequently used in studies analysing P/A data of species occurrences (e.g., Foody 2008; Ekström et al. 2018; Esseen et al. 2022; Esseen & Ekström 2023). However, for the case where the locations of plants are regarded as a realisation of an inhomogeneous Poisson point process, Baddeley et al. (2010) provide an explanation of why the complementary log-log link function should be preferred for modelling P/A data.

The objective of this study is to assess the usefulness of hybrid inference for estimating plant density, where GLMs estimated from a small sample of P/A data (and auxiliary data) were applied to a large sample of auxiliary data from the Swedish NFI. An important part of the study is to develop formal plant density estimators, variances, and variance estimators for this approach, because no previous studies are available where hybrid inference has been applied in this modelling context. The performance of our estimators and corresponding variance estimators was examined through Monte Carlo simulations and the use of empirical NFI data on a common dwarf shrub, *Vaccinium vitis-idaea*.

We choose to focus our study on estimating the expected plant density (we refer to (13) for a precise definition) rather than on predicting the actual plant density (which is a random quantity in our study setting). The main reason is that this approach simplifies the analyses to some extent meanwhile, for large-area surveys, the relative difference between actual plant density and its expected value is very small, if the models used are approximately correct (cf. Ståhl et al. 2016). The motivation for studying plant density rather than the absolute number of plants is that density is a more relevant measure for plants with large populations (in contrast to many animals), and because the measure allows for comparison between regions of different size.

2. Methods

In this section, we first explain the necessary basis for our derivations, then propose estimators of the expected number of plants in a region of interest U, where U can be, e.g., a municipality, a province or a country. Furthermore, we develop variance formulas and corresponding variance estimators. The estimator of the expected density, defined as the expected number of plants per unit area, is thereafter obtained via the estimator of the expected number of plants and is presented for two cases: one with known area a_U of U and one with unknown area. We also look at the case where we want to estimate the expected density for a specific domain within U, for example the forested part of U. Two different sampling designs are considered. In the first design, plot centres are sampled according to some joint probability density function on U, or rather the union of U and a so-called "buffer" for handling edge effects (Subsections 2.2–2.4). In the second design, centres of clusters of plots are sampled rather than individual plot centres (Subsection 2.5).

2.1. Models

Assume that the plant population is generated by an inhomogeneous Poisson point process with intensity

$$\lambda_{\boldsymbol{\beta}}(\boldsymbol{u}) = \exp\left(\boldsymbol{\beta}^{\mathrm{T}}\boldsymbol{x}(\boldsymbol{u})\right), \boldsymbol{u} \in U \subset \mathbb{R}^2 \tag{1}$$

(Baddeley et al. 2010), where $\boldsymbol{\beta} \in \mathbb{R}^q$ denotes the vector of model parameters and $\boldsymbol{x}(\boldsymbol{u})$ denotes a covariate vector (of length q) at point $\boldsymbol{u}$. The expected number of plants in U is then given by

$$\Lambda(\boldsymbol{\beta}) = \int_U \lambda_{\boldsymbol{\beta}}(\boldsymbol{u}) d\boldsymbol{u}. \tag{2}$$

We consider plots $C(\boldsymbol{u}_i)$, where index i designates plot i, and where the plot centres $\{\boldsymbol{u}_i\}$ are selected according to some specified sampling design. Let N_i denote the number of plants in $C(\boldsymbol{u}_i) \cap U$. Our assumptions imply that N_i is Poisson distributed, and then

$$\mathbb{E}(N_i) = \int_{C(\boldsymbol{u}_i)\cap U} \lambda_{\boldsymbol{\beta}}(\boldsymbol{u}) d\boldsymbol{u} = \int_{C(\boldsymbol{u}_i)\cap U} \exp\left(\boldsymbol{\beta}^{\mathrm{T}}\boldsymbol{x}(\boldsymbol{u})\right) d\boldsymbol{u}.$$

Unless stated otherwise, we assume, as an approximation, that $\boldsymbol{x}(\boldsymbol{u})$ is constant in a sample plot, and thus $\boldsymbol{x}(\boldsymbol{u}) = \boldsymbol{x}(\boldsymbol{u}_i) = \boldsymbol{x}_i$ for all $\boldsymbol{u} \in C(\boldsymbol{u}_i)$, and

$$\mathbb{E}(N_i) = a_i \exp\left(\boldsymbol{\beta}^{\mathrm{T}}\boldsymbol{x}_i\right), \tag{3}$$

with a_i being the area of the intersection of plot $C(\boldsymbol{u}_i)$ and the region of interest U (cf. Baddeley et al. 2010). Since N_i is Poisson-distributed, the probability of presence can be expressed by

$$p_i = 1 - P(N_i = 0) = 1 - \exp\big(-a_i \exp(\boldsymbol{\beta}^{\mathrm{T}}\boldsymbol{x}_i)\big) \tag{4}$$

so that the loglikelihood for the binary response variables (i.e. P/A data from $C(\boldsymbol{u}_i) \cap U$) becomes the loglikelihood of a complementary log-log regression with an offset equal to the log of the plot area, i.e. of the binary regression model given by

$$g(p_i) = \log(a_i) + \boldsymbol{\beta}^{\mathrm{T}}\boldsymbol{x}_i, \text{ where } g(p) = \log(-\log(1-p)). \tag{5}$$

According to Baddeley et al. (2010), the corresponding likelihood may be regarded as an approximation of the likelihood that would have been obtained without the assumption of constant covariate data in a plot.

2.2. Estimation of the expected number of plants in U

Hybrid inference can be used when covariate information is not available everywhere in the region of interest but only at sample plot level, for example for budgetary reasons (Ståhl et al. 2016). As stated in the introduction, this hybrid method includes aspects of both design-based and model-based inference. As in, amongst others, the papers by Ståhl et al. (2011), Nelson et al. (2012), Corona et al. (2014), Saarela et al. (2015) or Saarela et al. (2022) on hybrid inference, we utilise two samples that are readily available, for instance in monitoring programme databases. Our first sample S_1 of size n_1 contains plot centre locations for plots with both binary response data and covariate data, while our second sample S_2 of size n_2 contains plot centre locations for plots with only covariate data. Typically, n_2 is much larger than n_1. Sample S_1 is used only to establish a model and estimate the vector of model coefficients in a GLM (as opposed to, e.g., Ståhl et al. (2011), where a standard linear model is used). Thereafter, the fitted GLM and covariate information from S_2 are used to predict expected numbers of plants on all plots with centres in S_2, and subsequently the expected plant density in the region of interest, using design-based estimation and Horvitz-Thompson-like estimators. Sample plots with centre locations in S_1 and S_2 do not necessarily need to have the same size, and the sampling designs used to obtain the data in S_1 and S_2 are allowed to differ.

When sampling from a finite population, the well-known Horvitz-Thompson estimator (Horvitz & Thompson 1952) is often used for obtaining estimates of population parameters. However, in our case the population is not finite but a continuous set of locations, and therefore we use Cordy's continuous analogue of the Horvitz-Thompson estimator (Cordy 1993), which we introduce next.

Let f be the joint probability density function (pdf) for sample $S_2 = \{\boldsymbol{u}_1, \boldsymbol{u}_2, \cdots, \boldsymbol{u}_{n_2}\}$, and $f_i(\boldsymbol{u})$ the marginal pdf for point $\boldsymbol{u}_i$. The inclusion density function is

$$\pi(\boldsymbol{u}) = \sum_{i=1}^{n_2} f_i(\boldsymbol{u}), \tag{6}$$

and it can intuitively be considered as a local measure of the number of sample points to be selected per unit area (Cordy 1993). If, for example, the points in S_2 are independent and identically distributed (iid), this means that $\pi(\boldsymbol{u}) = n_2 f_1(\boldsymbol{u})$.

The inclusion zone for a point $\boldsymbol{u} \in U$ consists of all points in the frame that would result in the inclusion of $\boldsymbol{u}$ if they were selected to the sample. It may be formally written as $K(\boldsymbol{u}) = \{\boldsymbol{u}' \in U : \boldsymbol{u} \in C(\boldsymbol{u}')\}$, where $C(\boldsymbol{u}')$ is a plot centred around point $\boldsymbol{u}'$. For simplicity purposes, we assume from here on that all plots $C(\boldsymbol{u}_i)$, $i \in S_2$, are circular and have the same area a. The area of the inclusion zone of $\boldsymbol{u} \in U$ is $\widetilde{a_{\boldsymbol{u}}} = \int_U I(\boldsymbol{u} \in C(\boldsymbol{u}'))d\boldsymbol{u}'$. If point $\boldsymbol{u}$ is sufficiently into the interior of U, then its inclusion zone will have the same shape and size as each of the circular plots. On the other hand, if $\boldsymbol{u}$ is close enough to the boundary of U, then its inclusion zone will have a smaller size than a. The Horvitz–Thompson-type estimator presented below has the ability to take this into account, but would require the inclusion zone area to be determined for each point $\boldsymbol{u}_i \in S_2$ near the edge (cf. Gregoire & Valentine 2007). A less labour-intensive way to solve this problem is to use the so-called buffer method, which applies to both the single-plot and cluster-plot designs. Thus, we suppose that a buffer at least as large as the plot radius is used around U (Gregoire & Valentine 2007). This allows sample points $\boldsymbol{u}_i$ to fall outside U, i.e. in some larger region $U^{\bullet}$, defined as the union of U and the buffer. The use of a buffer impacts the definitions of $\widetilde{a_{\boldsymbol{u}}}$ and $K(\boldsymbol{u})$, in which U needs to be replaced by $U^{\bullet}$. The introduction of a buffer implies that all points in U have the same inclusion zone area, and thus $\widetilde{a_{\boldsymbol{u}}} = a_{\boldsymbol{u}} = a$ for all $\boldsymbol{u} \in U$, where $a_{\boldsymbol{u}}$ denotes the area of $C(\boldsymbol{u})$. In this setting, we set $\lambda_\beta(\boldsymbol{u}) = 0$ for all $\boldsymbol{u} \in U$ (cf. Gregoire & Valentine 2007).

The "generalised" Horvitz-Thompson estimator of the expected number of plants in U is then given by

$$\widehat{\Lambda}(\boldsymbol{\beta}) = \sum_{i=1}^{n_2} \frac{\lambda(\boldsymbol{u}_i)}{\pi(\boldsymbol{u}_i)}, \tag{7}$$

where $\pi(\boldsymbol{u})$ is given by (6) and

$$\lambda(\boldsymbol{u}) = \int_{C(\boldsymbol{u})} \frac{\lambda_\beta(\boldsymbol{u}')}{a_{\boldsymbol{u}'}} d\boldsymbol{u}', \boldsymbol{u} \in U^{\bullet},$$

is the average intensity over $C(\boldsymbol{u}_i)$, where $a_{\boldsymbol{u}'} = a$ by our assumptions (Cordy 1993, Grafström et al. 2017). Note that

$$\begin{aligned} \int_{U^{\bullet}} \lambda(\boldsymbol{u}) d\boldsymbol{u} &= \int_{U^{\bullet}} \int_{C(\boldsymbol{u})} \frac{\lambda_\beta(\boldsymbol{u}')}{a_{\boldsymbol{u}'}} d\boldsymbol{u}' d\boldsymbol{u} = \int_{U^{\bullet}} \frac{\lambda_\beta(\boldsymbol{u}')}{a_{\boldsymbol{u}'}} \int_{U^{\bullet}} I(\boldsymbol{u}' \in C(\boldsymbol{u})) d\boldsymbol{u} d\boldsymbol{u}' \\ &= \int_U \frac{\lambda_\beta(\boldsymbol{u}')}{a_{\boldsymbol{u}'}} \int_{U^{\bullet}} I(\boldsymbol{u}' \in C(\boldsymbol{u})) d\boldsymbol{u} d\boldsymbol{u}' = \int_U \lambda_\beta(\boldsymbol{u}') d\boldsymbol{u}' = \Lambda(\boldsymbol{\beta}) \end{aligned} \tag{8}$$

and, according to Theorem 1 in Cordy (1993), this implies that the Horvitz-Thompson estimator of $\Lambda(\boldsymbol{\beta})$ is unbiased if $\pi(\boldsymbol{u}) > 0$ for all $\boldsymbol{u} \in U^{\bullet}$. Hence, with a buffer for handling edge effects, we obtain an unbiased estimator of $\Lambda(\boldsymbol{\beta})$. The price to be paid is that the buffer method tends to inflate the variance of the estimator (Gregoire & Valentine 2007). If the area of the buffer is small relative to the area of U, this increase in variance can be expected to be small. Using (3), $\lambda(\boldsymbol{u}_i)$ can be rewritten as

$$\lambda(\boldsymbol{u}_i) = \int_{C(\boldsymbol{u}_i) \cap U} \frac{\exp(\boldsymbol{\beta}^{\mathrm{T}} x(\boldsymbol{u}))}{a_{\boldsymbol{u}}} d\boldsymbol{u} = \frac{a_i}{a} \exp(\boldsymbol{\beta}^{\mathrm{T}}\boldsymbol{x}_i) = r_i \exp(\boldsymbol{\beta}^{\mathrm{T}}\boldsymbol{x}_i) = \widetilde{\lambda}_\beta(\boldsymbol{u}_i),$$

where r_i is the ratio of the area a_i of $C(\boldsymbol{u}_i) \cap U$ and the area of $C(\boldsymbol{u}_i)$. With $\widetilde{\lambda}_\beta(\boldsymbol{u}_i)$ defined as above, note that if $C(\boldsymbol{u}_i) \subseteq U$, then $\widetilde{\lambda}_\beta(\boldsymbol{u}_i) = \lambda_\beta(\boldsymbol{u}_i)$. This implies that

$$\widehat{\Lambda}(\boldsymbol{\beta}) = \sum_{i=1}^{n_2} \frac{\widetilde{\lambda}_\beta(\boldsymbol{u}_i)}{\pi(\boldsymbol{u}_i)} = \sum_{i=1}^{n_2} \frac{r_i \exp(\boldsymbol{\beta}^{\mathrm{T}}\boldsymbol{x}_i)}{\pi(\boldsymbol{u}_i)}.$$

$\widehat{\Lambda}(\boldsymbol{\beta})$ can also be regarded as a natural predictor of the actual number of plants, given the available information and in the context of the inhomogeneous Poisson point process. As $\boldsymbol{\beta}$ is usually unknown, we will use $\widehat{\Lambda}(\widehat{\boldsymbol{\beta}})$ as our estimator of the expected number of plants, where $\widehat{\boldsymbol{\beta}}$ is an

estimator of $\boldsymbol{\beta}$ obtained using model (5) based on data from S_1.

2.3. Variance estimation

To estimate the variance of the estimator $\widehat{\Lambda}(\boldsymbol{\beta})$ of $\Lambda(\boldsymbol{\beta})$, we use the Sen-Yates-Grundy variance formula defined in Cordy (1993),

$$\mathrm{Var}(\widehat{\Lambda}(\boldsymbol{\beta}))=\frac{1}{2}\int_{U^\bullet}\int_{U^\bullet}\Delta(\boldsymbol{u},\boldsymbol{u}')\left(\frac{\lambda(\boldsymbol{u})}{\pi(\boldsymbol{u})}-\frac{\lambda(\boldsymbol{u}')}{\pi(\boldsymbol{u}')}\right)^2 d\boldsymbol{u}d\boldsymbol{u}',$$

where

$$\Delta(\boldsymbol{u},\boldsymbol{u}')=\pi(\boldsymbol{u})\pi(\boldsymbol{u}')-\pi(\boldsymbol{u},\boldsymbol{u}') \quad \text{and} \quad \pi(\boldsymbol{u},\boldsymbol{u}')=\sum_{i\in I_n}\sum_{j\in J_{n,i}} f_{ij}(\boldsymbol{u},\boldsymbol{u}'), \tag{9}$$

the latter being the pairwise inclusion density function with $I_n=\{1,\dots,n_2\}$, $J_{n,i}=\{1,\dots,n_2\}\backslash\{i\}$, and f_{ij} the joint marginal pdf of $\boldsymbol{u}_i$ and $\boldsymbol{u}_j$. As advised by, e.g., Tillé (2006), the Sen-Yates-Grundy formula should be used in case a fixed sample size is used. By Cordy (1993), if $\pi(\boldsymbol{u})$ and $\pi(\boldsymbol{u},\boldsymbol{u}')$ are strictly positive for all $(\boldsymbol{u},\boldsymbol{u}')\in U^\bullet$, an unbiased estimator of the Sen-Yates-Grundy variance is given by

$$\begin{aligned}\widehat{\mathrm{Var}}(\widehat{\Lambda}(\boldsymbol{\beta}))&=\frac{1}{2}\sum_{i\in I_n}\sum_{j\in J_{n,i}}\frac{\Delta(\boldsymbol{u}_i,\boldsymbol{u}_j)}{\pi(\boldsymbol{u}_i,\boldsymbol{u}_j)}\left(\frac{\lambda(\boldsymbol{u}_i)}{\pi(\boldsymbol{u}_i)}-\frac{\lambda(\boldsymbol{u}_j)}{\pi(\boldsymbol{u}_j)}\right)^2\\&=\frac{1}{2}\sum_{i\in I_n}\sum_{j\in J_{n,i}}\frac{\Delta(\boldsymbol{u}_i,\boldsymbol{u}_j)}{\pi(\boldsymbol{u}_i,\boldsymbol{u}_j)}\left(\frac{r_i\exp(\boldsymbol{\beta}^{\mathrm{T}}\boldsymbol{x}_i)}{\pi(\boldsymbol{u}_i)}-\frac{r_j\exp(\boldsymbol{\beta}^{\mathrm{T}}\boldsymbol{x}_j)}{\pi(\boldsymbol{u}_j)}\right)^2,\end{aligned} \tag{10}$$

and that is in effect the part of the variance due to sampling of the plot centres in S_2, treating the model coefficients as known. With unknown $\boldsymbol{\beta}$, i.e. where $\boldsymbol{\beta}$ needs to be estimated by $\widehat{\boldsymbol{\beta}}$, an estimate of the variance of $\widehat{\Lambda}(\widehat{\boldsymbol{\beta}})$ can be expressed as

$$\begin{aligned}\widehat{\mathrm{Var}}(\widehat{\Lambda}(\widehat{\boldsymbol{\beta}}))&=\frac{1}{2}\sum_{i\in I_n}\sum_{j\in J_{n,i}}\frac{\Delta(\boldsymbol{u}_i\boldsymbol{u}_j)}{\pi(\boldsymbol{u}_i\boldsymbol{u}_j)}\left(\frac{r_i\exp(\widehat{\boldsymbol{\beta}}^{\mathrm{T}}\boldsymbol{x}_i)}{\pi(\boldsymbol{u}_i)}-\frac{r_j\exp(\widehat{\boldsymbol{\beta}}^{\mathrm{T}}\boldsymbol{x}_j)}{\pi(\boldsymbol{u}_j)}\right)^2\\&\quad+\sum_{k=1}^{q}\sum_{l=1}^{q}\widehat{\mathrm{Cov}}_{S_1}(\widehat{\beta}_k\widehat{\beta}_l)\widehat{v}_k\widehat{v}_l,\end{aligned} \tag{11}$$

with

$$\widehat{v}_k=\sum_{i=1}^{n_2}\frac{1}{\pi(\boldsymbol{u}_i)}\widetilde{\lambda}^{(k)}_{\widehat{\boldsymbol{\beta}}}(\boldsymbol{u}_i), \tag{12}$$

where $\widehat{\beta}_k$ denotes the kth component of the $\widehat{\boldsymbol{\beta}}$ vector, and

$$\widetilde{\lambda}^{(k)}_{\widehat{\boldsymbol{\beta}}}(\boldsymbol{u}_i)=\frac{\partial\widetilde{\lambda}_{\widehat{\boldsymbol{\beta}}}(\boldsymbol{u}_i)}{\partial\widehat{\beta}_k}=r_i x_{ik}\exp(\widehat{\boldsymbol{\beta}}^{\mathrm{T}}\boldsymbol{x}_i)$$

with x_{ik} denoting the kth component of $\boldsymbol{x}_i$. The different $\widehat{\mathrm{Cov}}_{S_1}(\widehat{\beta}_k,\widehat{\beta}_l)$ terms can be obtained from statistical software, for example using the *glm* function in R. The derivation of (11) can be found in Appendix A. Another case, where S_2 is a sample of centres of plot clusters, is considered in Subsection 2.5.

2.4. Estimation of the expected plant density

In this section, we utilise our estimator of the total number of plants for estimating the expected plant density. First, we assume that the area of the region of interest is known. In this case, the expected density $R(\boldsymbol{\beta})$ is defined as the expected number of plants in the region divided by the area a_U of U,

$$R(\boldsymbol{\beta})=\frac{\Lambda(\boldsymbol{\beta})}{a_U}, \tag{13}$$

where $\Lambda(\boldsymbol{\beta})$ is defined in (2). This quantity can be estimated by

$$\widehat{R}(\widehat{\boldsymbol{\beta}})=\frac{\widehat{\Lambda}(\widehat{\boldsymbol{\beta}})}{a_U}, \tag{14}$$

where $\widehat{\Lambda}(\boldsymbol{\beta})$ is defined in (7). Its corresponding variance estimator is given by

$$\widehat{\mathrm{Var}}(\widehat{R}(\widehat{\boldsymbol{\beta}}))=\frac{\widehat{\mathrm{Var}}(\widehat{\Lambda}(\widehat{\boldsymbol{\beta}}))}{a_U}, \tag{15}$$

where $\widehat{\mathrm{Var}}(\widehat{\Lambda}(\widehat{\boldsymbol{\beta}}))$ is the same as in (11).

However, information about the area of the region of interest may not be available, or we may wish to estimate expected plant density in a subregion of unknown area, for example in the forested area of a region. In such cases, the area has to be estimated. Thus, $\Lambda(\boldsymbol{\beta})$ needs to be modified as

$$\Lambda^\star(\boldsymbol{\beta})=\int_U\lambda_{\boldsymbol{\beta}}(\boldsymbol{u})I_{\boldsymbol{u}}d\boldsymbol{u},$$

with $I_{\boldsymbol{u}}$ being an indicator function taking the value 1 if $\boldsymbol{u}$ is situated in the target part of the landscape and 0 otherwise; $I_{\boldsymbol{u}}$ is set to 0 outside of U. The area of the target part of the landscape in U can be written as

$$A=\int_U I_{\boldsymbol{u}}d\boldsymbol{u}$$

and the expected plant density in the area of interest is given by

$$R^\star(\boldsymbol{\beta})=\frac{\Lambda^\star(\boldsymbol{\beta})}{A}. \tag{16}$$

This quantity can be estimated by

$$\widehat{R}^\star(\boldsymbol{\beta})=\frac{\widehat{\Lambda}^\star(\boldsymbol{\beta})}{\widehat{A}}, \tag{17}$$

where $\widehat{\Lambda}^\star(\boldsymbol{\beta})$ is defined as

$$\widehat{\Lambda}^\star(\boldsymbol{\beta})=\sum_{i=1}^{n_2}\frac{\lambda^\star(\boldsymbol{u}_i)}{\pi(\boldsymbol{u}_i)}, \tag{18}$$

where

$$\lambda^\star(\boldsymbol{u}_i)=\int_{C(\boldsymbol{u}_i)}\frac{\lambda_{\boldsymbol{\beta}}(\boldsymbol{u})I_{\boldsymbol{u}}}{a_{\boldsymbol{u}}}d\boldsymbol{u},$$

and

$$\widehat{A}=\sum_{i=1}^{n_2}\frac{z(\boldsymbol{u}_i)}{\pi(\boldsymbol{u}_i)} \tag{19}$$

is an estimator of the area A, with

$$z(\boldsymbol{u}_i)=\int_{C(\boldsymbol{u}_i)}\frac{I_{\boldsymbol{u}}}{a_{\boldsymbol{u}}}d\boldsymbol{u}.$$

Note that, if we adopt a reasoning similar to the one in (8), $\widehat{A}$ is an unbiased estimator of A if $\pi(\boldsymbol{u})>0$ for all $\boldsymbol{u}\in U^\bullet$ (Cordy 1993).

In Appendix A, the following estimator of the variance of $\widehat{R}^\star(\widehat{\boldsymbol{\beta}})$ is derived:

$$\widehat{\mathrm{Var}}(\widehat{R}^{\star}(\widehat{\boldsymbol{\beta}}))=\frac{1}{2\widehat{A}^2}\sum_{i\in I_n}\sum_{j\in J_{n,i}}\frac{\Delta(\boldsymbol{u}_i,\boldsymbol{u}_j)}{\pi(\boldsymbol{u}_i,\boldsymbol{u}_j)}\left(\frac{\widehat{\lambda}^{\star}(\boldsymbol{u}_i)-\widehat{R}^{\star}(\widehat{\boldsymbol{\beta}})z(\boldsymbol{u}_i)}{\pi(\boldsymbol{u}_i)}-\frac{\widehat{\lambda}^{\star}(\boldsymbol{u}_j)-\widehat{R}^{\star}(\widehat{\boldsymbol{\beta}})z(\boldsymbol{u}_j)}{\pi(\boldsymbol{u}_j)}\right)^2$$
$$+\frac{1}{\widehat{A}^2}\sum_{k=1}^{q}\sum_{l=1}^{q}\widehat{Cov}_{S_1}(\widehat{\beta}_k,\widehat{\beta}_l)\sum_{i\in I_n}\frac{\widehat{d}_{1,k}(\boldsymbol{u}_i)-z(\boldsymbol{u}_i)\widehat{d}_{2,k}/\widehat{A}}{\pi(\boldsymbol{u}_i)}\sum_{j\in I_n}\frac{\widehat{d}_{1,l}(\boldsymbol{u}_j)-z(\boldsymbol{u}_j)\widehat{d}_{2,l}/\widehat{A}}{\pi(\boldsymbol{u}_j)} \tag{20}$$
$$+\frac{2}{\widehat{A}^2}\sum_{k=1}^{q}\sum_{l=1}^{q}\widehat{\mathrm{Cov}}_{S_1}(\widehat{\beta}_k,\widehat{\beta}_l)\widehat{d}_{2,l}\sum_{i\in I_n}\frac{\widehat{d}_{1,k}(\boldsymbol{u}_i)}{\pi(\boldsymbol{u}_i)}-\frac{1}{\widehat{A}^2}\sum_{k=1}^{q}\sum_{l=1}^{q}\widehat{\mathrm{Cov}}_{S_1}(\widehat{\beta}_k,\widehat{\beta}_l)\widehat{d}_{2,k}\widehat{d}_{2,l},$$

where

$$\widehat{\lambda}^{\star}(\boldsymbol{u}_i)=\int_{C(\boldsymbol{u}_i)}\frac{\lambda_{\widehat{\boldsymbol{\beta}}}(\boldsymbol{u})I_{\boldsymbol{u}}}{a_{\boldsymbol{u}}}d\boldsymbol{u},$$

$$\widehat{d}_{1,k}(\boldsymbol{u}_i)=\int_{C(\boldsymbol{u}_i)}\frac{I_{\boldsymbol{u}}}{a_{\boldsymbol{u}}}\lambda_{\widehat{\boldsymbol{\beta}}}^{(k)}(\boldsymbol{u})d\boldsymbol{u},\quad \widehat{d}_{2,k}=\sum_{i=1}^{n_2}\frac{I_{\boldsymbol{u}_i}\lambda_{\widehat{\boldsymbol{\beta}}}^{(k)}(\boldsymbol{u}_i)}{\pi(\boldsymbol{u}_i)}, \tag{21}$$

$$\widehat{\Lambda}(\widehat{\boldsymbol{\beta}})=\sum_{j\in I_n}\frac{\lambda(\boldsymbol{u}_j)}{\pi(\boldsymbol{u}_j)}=\sum_{j\in I_n}\frac{1/k_j\sum_{i=1}^{k_j}r_i\exp(\widehat{\boldsymbol{\beta}}^{\mathrm{T}}\boldsymbol{x}_i^j)}{\pi(\boldsymbol{u}_j)}. \tag{23}$$

Using the same reasoning that led us to (11), we obtain the following variance estimators for $\widehat{\Lambda}(\widehat{\boldsymbol{\beta}})$;

$$\widehat{\mathrm{Var}}(\widehat{\Lambda}(\widehat{\boldsymbol{\beta}}))=\frac{1}{2}\sum_{j\in I_n}\sum_{j\in J_{n,i}}\frac{\Delta(\boldsymbol{u}_i,\boldsymbol{u}_j)}{\pi(\boldsymbol{u}_i,\boldsymbol{u}_j)}\left(\frac{1}{\pi(\boldsymbol{u}_j)k_j}\sum_{i=1}^{k_j}r_i\exp(\widehat{\boldsymbol{\beta}}^{\mathrm{T}}\boldsymbol{x}_i^j)-\frac{1}{\pi(\boldsymbol{u}_j)k_j}\sum_{l=1}^{k_j}r_l\exp(\widehat{\boldsymbol{\beta}}^{\mathrm{T}}\boldsymbol{x}_l^j)\right)^2+\sum_{k=1}^{p}\sum_{k'=1}^{p}\widehat{Cov}_{S_1}(\widehat{\beta}_k,\widehat{\beta}_{k'})\widehat{v}_k\widehat{v}_{k'}, \tag{24}$$

and

$$\lambda_{\widehat{\boldsymbol{\beta}}}^{(k)}(\boldsymbol{u}_i)=\frac{\partial\lambda_{\widehat{\boldsymbol{\beta}}}(\boldsymbol{u}_i)}{\partial\widehat{\beta}_k}=x_{ik}\exp(\widehat{\boldsymbol{\beta}}^{\mathrm{T}}\boldsymbol{x}_i).$$

It can happen that sample plots are divided into several parts, for example if one part of the plot is in forests and other parts are in other landscape categories. In such cases, some adjustments of the above estimators of the expected plant density and variance are needed. See Appendix B.

2.5. Cluster sampling case

It is also of interest to consider the case where S_2 is a sample of centres of clusters (sometimes called tracts) of plots rather than a sample of centres of individual plots. Indeed, this sampling procedure is used in, e.g., the Swedish NFI (Anon 2014). In this case, $C(\boldsymbol{u}_j)$ denotes a cluster j of k_j plots centred around $\boldsymbol{u}_j$, and we denote the area of the plots within the cluster by $a_{\boldsymbol{u}_j}=k_j s$, where s is the area of a single plot (all plots are assumed to have the same area). A buffer is also used in this case, although it will be larger (at least as large as the radius of the tract, see Grafström et al. 2017). We can still use the Horvitz-Thompson estimator (7) to get our estimator of the expected number of plants in U; the resulting expression will just be slightly different.

Using approximation (3) and if no plot is divided,

$$\lambda(\boldsymbol{u}_j)=\int_{C(\boldsymbol{u}_j)\cap U}\frac{\exp(\boldsymbol{\beta}^{\mathrm{T}}\boldsymbol{x}(\boldsymbol{u}))}{a_{\boldsymbol{u}}}d\boldsymbol{u}=\frac{1}{k_j}\sum_{i=1}^{k_j}r_i\exp(\boldsymbol{\beta}^{\mathrm{T}}\boldsymbol{x}_i^j), \tag{22}$$

where $\boldsymbol{x}_i^j$ denotes the (constant) covariate information in plot i of cluster j, and r_i is the ratio of the area of the intersection of plot i n cluster j and U to the area of a single plot. Then, the Horvitz-Thompson estimator $\widehat{\Lambda}(\boldsymbol{\beta})$ may be written as

with

$$\widehat{v}_k=\sum_{j\in I_n}\frac{1}{\pi(\boldsymbol{u}_j)}\frac{1}{k_j}\sum_{i=1}^{k_j}r_i x_{ik}^j\exp(\widehat{\boldsymbol{\beta}}^{\mathrm{T}}\boldsymbol{x}_i^j),$$

where $\boldsymbol{x}_{ik}^j$ denotes the kth component of vector $\boldsymbol{x}_i^j$. Similar changes are made in case we want to estimate expected plant density in (sub)regions with unknown area.

2.6. Statistical testing

The estimates of the expected plant density and corresponding variance estimators rely on the condition that the binary regression model (5) is realistic. For this reason, it is of importance to assess whether said model, used to estimate $\boldsymbol{\beta}$, holds true. In order to do that, we use a parametric bootstrap test suggested by Ekström et al. (Unpublished results). It should be noted that if model (5) is incorrect, then so is the underlying Poisson model assumption. Details on how to perform the test are given in Appendix C.

3. Real data study

The Swedish NFI (Fridman et al. 2014) is a field sample plot inventory of Swedish forests that consists of both temporary and permanent tracts, each composed of several plots. The temporary plots (which have a radius of 7 m) are only inventoried once, while the permanent plots are inventoried once every 5 years. Moreover, the permanent tracts are separated into two subcategories, "C_1", where both terrain and vegetation inventories are conducted, and "C_2", which denotes all other tracts. At each permanent "C_1" plot, P/A data for a set of plant species are recorded on each of two small circular "vegetation plots"; those small vegetation plots have an area of 0.25 m^2 each and are separated by 5 m and located 2.5 m from the main plot centre, the main plot having a radius of 10 m. Those registrations are not made during each visit, but rather once every two visits (i.e. every tenth year). Vegetation

registrations are not made on temporary plots. The covariates are registered at main plot level for both temporary and permanent plots. Thus, values of the covariates are always the same in each pair of small vegetation plots. The registrations are performed by experienced field workers on plots for which the positions are defined in advance according to the given sampling design.

We chose to study Lingonberry (*Vaccinium vitis-idaea*) data in the Norrbotten Lappmarken region (in northern Sweden) during the years 2008–2012. According to the Swedish NFI, region Norrbotten Lappmarken has a known area of 7,785,748 ha. The particular landscape category we chose for the estimation of $R^\star$ and its corresponding variance is productive forestland (i.e. land that can produce on average at least 1 m^3 of wood per hectare and per year and that is not significantly used for other purposes, according to Anon (2014)), whose area is unknown.

Sample S_1 consists of the centres of the small vegetation plots included in permanent "C_1" plots, in Norrbotten Lappmarken during 2008–2012. Sample S_1 has size $n_1 = 724$, corresponding to 362 pairs of vegetation plots that were used for the parametric bootstrap test. Cluster sampling was used to obtain sample S_2. It originally consists of the centres of the tracts of temporary circular plots. This sample has a size of $n_2 = 111$ tract centres, which corresponds to 1132 sample plots in total. There are one to twelve plots with available data in each (quadratic) tract, and the plots are separated by at least 600 m (Anon 2014).

In Table 1, the fitted binary regression model for *Vaccinium vitis-idaea* is presented for productive forestland in Norrbotten Lappmarken for years 2008–2012. The model was not rejected by the parametric bootstrap test (p-value = 0.184). Its explanatory variables are a transformation of the number of tree stems per hectare, multiplied by 100, and an indicator variable stating whether the soil is humid/wet. It can be seen that *Vaccinium vitis-idaea* seem less likely to be found on humid/wet soil, compared to dry soils. On the other hand, the model suggests that the more tree stems per hectare, the higher the probability of presence of *Vaccinium vitis-idaea*.

Table 2 contains estimated expected densities in two different cases. The first case is cluster sampling, where centres of clusters of plots were assumed to be sampled independently and uniformly on $U^\bullet$. In the second case, the computations were made by (incorrectly) assuming that centres of individual plots were sampled rather than centres of clusters. The densities were estimated using two different estimators (expected density estimator with known area (14) and unknown area (17), and their cluster sampling case counterparts). The corresponding variance estimates, (15) and (20) respectively (as well as their cluster sampling case counterparts), are also given. In both cases, the variance estimate of the expected density estimator in productive forestland is almost twice as high as the variance estimate using the whole region. It can be explained by the relatively small amount of plots that are situated in productive forestland in Norrbotten Lappmarken in the Swedish NFI data (approximately 50% of the total).

Table 1
Estimated model coefficients $\hat{\boldsymbol{\beta}}$ for *Vaccinium vitis-idaea* in productive forestland in Norrbotten Lappmarken. The intercept was offset-adjusted. $\mathbf{1}_{wet}$ is an indicator variable stipulating whether a plot is humid/wet or not. $((\text{No.stems/ha} + 0.6)/1000)^{-0.5}$ is a non-linear transformation of the "number of tree stems per hectare" (in hundreds per hectare) covariate, found by using the mfp R package (Ambler & Benner 2015), which applies multivariable fractional polynomials (Sauerbrei & Royston 1999).

Species	Estimated parameters ($\hat{\boldsymbol{\beta}}$)	
Vaccinium vitis-idaea (Lingonberry)	Offset-adjusted Intercept	2.423
	$\mathbf{1}_{wet}$	−0.667
	$((\text{No.stems/ha} + 0.6)/1000)^{-0.5}$	−0.025

Table 2
Estimated expected plant densities in m^{-2} and corresponding estimates of variance for *Vaccinium vitis-idaea* in Norrbotten Lappmarken. Two cases were considered: one where the computations were made assuming cluster sampling and another where it was (incorrectly) assumed that single plots were sampled. $\widehat{R}(\hat{\boldsymbol{\beta}})$ and $\widehat{\text{Var}}(\widehat{R}(\hat{\boldsymbol{\beta}}))$ are computed for the whole Norrbotten Lappmarken region, while $\widehat{R}^\star(\hat{\boldsymbol{\beta}})$ and $\widehat{\text{Var}}(\widehat{R}^\star(\hat{\boldsymbol{\beta}}))$ are computed for the productive forestland area of Norrbotten Lappmarken only.

Case	$\widehat{R}(\hat{\boldsymbol{\beta}})$	$\widehat{R}^\star(\hat{\boldsymbol{\beta}})$	$\widehat{\text{Var}}(\widehat{R}(\hat{\boldsymbol{\beta}}))$	$\widehat{\text{Var}}(\widehat{R}^\star(\hat{\boldsymbol{\beta}}))$
Tracts	7.61	9.72	0.205	0.406
Single plots	7.49	9.73	0.209	0.411

4. Monte Carlo study

The aim of the Monte Carlo study was to evaluate our estimators of expected plant density and variance estimators and assess whether they performed well. The simulations, all performed in **R** (R Core Team 2022), were conducted as follows.

- We created a quadratic grid of 1024 cells that corresponds to our area frame U, as well as a buffer zone around U. Each grid cell had an area of 1 ha and artificial covariates.
- The created covariates were based on the ones included in the model for *Vaccinium vitis-idaea*. The indicator variable stipulating whether a plot is humid/wet or not was built on actual data in the Norrbotten Lappmarken region between 2008 and 2012, which had approximately 16.85% of plots being considered as humid/wet. This particular covariate was created as realisations of a Bernoulli distribution with parameter $p = 0.1685$ in each cell. As for the number of stems per hectare, we used fitted Weibull distributions as described below. Two cases were considered:
  1. In the first case, we assumed that the whole grid was productive forestland, and the area of the area frame (the cell grid) was assumed to be known. In that case, we supposed that the number of stems per hectare varied only depending on whether the soil was humid/wet or dry. Based on Swedish NFI data in productive forestland, Weibull distributions were fitted using the *fitdist* function from the fitdistrplus package (Delignette-Muller & Dutang 2015). On humid/wet grid cells, the fitted distribution was a Weibull distribution with shape parameter $k = 1.047$ and scale parameter $\lambda = 3898.3$. For the dry grid cells, a two-step procedure was used since 4% of the original data had values equal to 0. Therefore, a random number between 0 and 1 was generated for each grid cell; if this number was smaller than 0.04, the number of stems per hectare for that grid cell was set to 0; otherwise it was a realisation of a Weibull-distributed random variable with parameters $k = 0.903$ and $\lambda = 2076.5$.
  2. In the second case, we created an indicator variable which was assigned the value 1 if the cell was in productive forestland, and 0 otherwise. As 49.8% of the original sample plots are in productive forestland, each cell was assigned the value 1 with a probability of 0.498. The number of stems per hectare was supposed to vary according to both humidity of the soil and type of landscape (productive forestland or not), which means that four different subcases had to be considered. The area of productive forestland in the grid was estimated by (19). The covariates were generated exclusively for the cells that are situated in productive forestland (which means in two of the subscases), and in such case were generated exactly as in case 1.
- Each Monte Carlo simulation consisted of 2000 replicates; P/A data were generated from an inhomogeneous Poisson point process with the *rpoispp* function from the spatstat package (Baddeley et al. 2016) in each replicate; plot centres in S_2 were sampled independently according to a uniform distribution over $U^\bullet$, while a two-step generation procedure was used for S_1: first, plot centres for the

Table 3
Actual expected plant densities $R(\boldsymbol{\beta})$ (resp. $R^{\star}(\boldsymbol{\beta})$), estimated mean values of the estimated expected densities $\widehat{\mathbb{E}}(\widehat{R}(\widehat{\boldsymbol{\beta}}))$ (resp. $\widehat{\mathbb{E}}(\widehat{R}^{\star}(\widehat{\boldsymbol{\beta}}))$), estimated mean value of the variance estimates $\widehat{\mathbb{E}}(\widehat{\mathrm{Var}}(\widehat{R}(\widehat{\boldsymbol{\beta}})))$ (resp. $\widehat{\mathbb{E}}(\widehat{\mathrm{Var}}(\widehat{R}^{\star}(\widehat{\boldsymbol{\beta}})))$) and s^2, the sample variance of the $\widehat{R}(\widehat{\boldsymbol{\beta}})$ (resp. $\widehat{R}^{\star}(\widehat{\boldsymbol{\beta}})$), for simulated *Vaccinium vitis-idaea* data in a grid of 1024 cells, each cell having an area of 1 ha. In the known area case, the area is a_U, the area of the grid. In the unknown area case, the area is estimated according to (19). The variances were estimated using formulas (15) and (20). "/" means that the formula does not apply to the specific case.

Case	$R(\boldsymbol{\beta})$	$R^{\star}(\boldsymbol{\beta})$	$\widehat{\mathbb{E}}(\widehat{R}(\widehat{\boldsymbol{\beta}}))$	$\widehat{\mathbb{E}}(\widehat{R}^{\star}(\widehat{\boldsymbol{\beta}}))$	$\widehat{\mathbb{E}}(\widehat{\mathrm{Var}}(\widehat{R}(\widehat{\boldsymbol{\beta}})))$	$\widehat{\mathbb{E}}(\widehat{\mathrm{Var}}(\widehat{R}^{\star}(\widehat{\boldsymbol{\beta}})))$	s^2
Known area	9.740	/	9.606	/	0.191	/	0.196
Unknown area	/	9.715	/	9.657	/	0.187	0.189

permanent plots were sampled independently according to a uniform distribution over U, and then the small vegetation plots in S_1 were created for each permanent plot as described in Section 3. The value of the vector of coefficients $\boldsymbol{\beta}$ was set equal to the one from the fitted model for *Vaccinium vitis-idaea* in Norrbotten Lappmarken in years 2008–2012 (Table 1). Estimated model coefficients $\widehat{\boldsymbol{\beta}}$ were computed for every replicate using the S_1 data, while the estimated expected plant density and its corresponding variance estimate were computed for every replicate using the S_2 data. The sample sizes were $n_1 = 1500$ and $n_2 = 1500$. The same plot radii as in the Swedish NFI were used (see Section 3). The plots in S_2 were divided when they overlapped different grid cells (see details in Appendix B). In accordance with the Swedish NFI (Jonas Dahlgren, personal communication), the small vegetation plots within S_1 were not divided.

The results for the simulation study are presented in Table 3. The estimator $\widehat{R}(\widehat{\boldsymbol{\beta}})$ was used for Case 1 and $\widehat{R}^{\star}(\widehat{\boldsymbol{\beta}})$ was used for Case 2. In Case 1, the estimator $\widehat{R}(\widehat{\boldsymbol{\beta}})$ was on average close to but a little lower than the real expected plant density. In Case 2, the estimator $\widehat{R}^{\star}(\widehat{\boldsymbol{\beta}})$ was even closer to the true value, but even in that case a slight negative bias occurred. The two variance estimators seem to have a very small bias and have low values. Based on these observations, we can conclude that our estimators performed quite well.

5. Discussion

In this study, we show how P/A data can be used for modelling and monitoring plant population densities. We argue that this approach offers advantages over methods based on visual assessment of vegetation cover, since studies indicate that P/A sampling may not be as prone to observer bias as methods based on assessing vegetation cover, and since P/A sampling is a rapid and thus cheap method to apply (e.g., Ringvall et al. 2005).

Since the auxiliary modelling data are available for both considered samples, but the binary response data are available for only one sample, we apply methods from hybrid inference (e.g., Corona et al. 2014) for estimating the expected value of plant density and the corresponding variance. This concerns taking into account both modelling and sampling uncertainty, and to our knowledge, our study is the first one that involves GLMs in hybrid inference. This type of inference is important in this context since, in many cases, detailed descriptions of environmental conditions, needed for the modelling, may not be available wall-to-wall but only from sampling locations, e.g., from sample plots within environmental monitoring programmes. In this article, we extend the already existing theory on hybrid inference to GLMs with binary response data.

Our method is most suitable when n_2, the sample size of S_2, is much larger than n_1, the sample size of S_1. Indeed, the main purpose in applying this method is to gather a minimum of information to develop a reliable model on the smallest sample possible (principally due to budgetary reasons), to then apply this model in connection with covariates that come from a larger sample whose units do not contain the desired response data. However, with our available data, n_2 was only a little larger than n_1. This shows that our method works even in that particular case.

In regions with high perimeter-to-area ratios, a large or very large proportion of the sampling plots will extend beyond the region's boundary. In such cases, our suggested methodology, which uses a "buffer" to address edge effects, may be unsuitable and could result, for example, in estimators with larger variances than desired.

An important part of the study involves making the proposed hybrid inference framework available for practical application in monitoring programmes, in which case we need to take into account that sample plots are often allocated in clusters and that the area of the domain of study is unknown (e.g., Fridman et al. 2014). This introduces several additional details to the general framework, which are important for the usefulness of the framework in practice.

The Monte Carlo simulations we performed show that our framework for estimating the expected plant density provides accurate estimates when the modelling assumptions are valid. In the study based on empirical data from the Swedish NFI, we obtained estimates of expected Lingonberry (*Vaccinium vitis-idaea*) densities in Northern Sweden that appear to be realistic, although we cannot check them since no reference data are available.

For the sake of simplicity, we assumed that the sampling design of S_1 was non-informative (see Appendix A), i.e. the design was not taken into account during model parameter estimation. Ignoring an informative sampling design may yield biased estimates of regression coefficients. For handling informative designs, methods using probability weighting may be used (e.g., Heeringa et al. 2010; Ekström et al. 2018).

It is possible to generalise the considered hybrid inference framework to other types of GLMs. Instead of P/A data as a response variable, one could use a continuous variable (such as biomass) or a discrete variable such as a count variable (number of trees, birds etc.). The main requirement is to have two samples; one to estimate model coefficients, with both covariate and response data, and another one, with only covariate data, for estimation of, e.g., expected biomass per hectare or expected plant density based on the estimated model coefficients. As long as this requirement is met, then hybrid inference should work, in principle, with any kind of response variable. The statistical developments would, however, be different from the ones derived in the present paper; although with counts instead of P/A, the difference would not be that significant (in both cases, it would be possible to use an inhomogeneous Poisson model). With count data that are not subject to too many errors, it should be possible to obtain better estimators than the ones obtained from P/A data. However, the survey would be more expensive to conduct.

There is one key condition for the developed technique to be applicable; the underlying point process should be, at least approximately, an inhomogeneous Poisson point process. We estimate models that utilise a combination of P/A and auxiliary data to estimate expected plant density, assuming that the spatial distribution of plants follow an inhomogeneous Poisson process, i.e. the plant densities vary due to the environmental conditions. In the article, we check the suitability of the binary regression model implied by the underlying inhomogeneous Poisson point process through a statistical test specifically developed for the purpose (cf. Appendix C). Recognising that plants can occur in clustered spatial patterns, extensions from inhomogeneous Poisson point processes to inhomogeneous cluster point processes serve as an

important topic for further studies. However, if we would like to use a similar methodology as in Ekström et al. (2020), we would need to gather data on more than two subplots for each main plot.

In our paper, the intensity of the inhomogeneous Poisson point process is determined via a log-linear model that involves a number of covariates. This model cannot be fitted directly, since no observed point pattern or observed values of counts of points in plots are available. This problem is circumvented by making use of observable P/A variables. Given that the pattern is a realisation of an inhomogeneous Poisson point process (whose intensity on the ith cell is given by (1)), it follows that the P/A variables satisfy a binary GLM, with complementary log-log link and an offset, with the same parameter vector as that which appears in the intensity of the inhomogeneous Poisson point process. Thus, for extending the current approach to other inhomogeneous point processes than the Poisson, the parameters of their intensities must be estimable from P/A data and corresponding covariate data at plot level. In addition, estimates of covariance matrices of estimators of parameters are also needed. One possibility to achieve this is to extend the intensity estimator in Ekström et al. (2020) from homogeneous cluster point processes such as the Matérn and Thomas processes to corresponding heterogeneous processes, whose intensities are functions of on one or more covariates (Waagepetersen 2007).

When the point pattern is generated by an inhomogeneous Poisson point process, the binary GLM model in (5) will have independent binary (P/A) response variables conditional on the covariates. For other point processes, responses cannot be expected to fulfill this property of conditional independence. Then, instead of using a standard GLM, other estimation methods such as generalised estimating equations (Albert & McShane 1995; Gotway & Stroup 1997) and a composite likelihood approach for spatial binary data (Heagerty & Lele 1998) can be used. However, as mentioned, this is not enough for extending the current approach to more general point processes. Most importantly, the estimable unknown parameters in the regression model for the P/A data must also include all unknown parameters in the intensity function of the point process model.

For a Poisson point process with a homogeneous intensity λ, the species abundance N in a plot C of area a follows a Poisson distribution with mean $a\lambda$, and the probability of presence of at least one plant in the plot C equals $p = 1 - \exp(-a\lambda)$. Rearranging this equation, we can estimate the intensity (plant density) λ from the proportion $\widehat{p}$ of plots with plant occurrences, i.e., by $\widehat{\lambda} = -a^{-1}\log(1-\widehat{p})$ (e.g., Ståhl et al. 2017). A homogeneous spatial Poisson process is synonymous with complete spatial randomness. However, in nature, individuals of many species are typically aggregated (Pielou 1977; He & Gaston 2000). For plot abundance N, the model most commonly used to describe such aggregation is the negative binomial distribution (He et al. 2002), which implies the following relationship between the presence probability p and plant density λ, $p = 1 - \left(1 + k^{-1}\lambda\right)^{-k}$, where k is referred to as a "clumping" parameter, with small $k > 0$ representing strong aggregation (Wright 1991; He & Gaston 2000; He et al. 2002). Under this model, Conlisk et al. (2007) specify the likelihood function and conclude that the clumping parameter cannot be estimated from P/A data, i.e., that it must be specified from outside the model. The suitability of the negative binomial distribution has also been much debated (Holt et al. 2002; Gaston et al. 2011) and only two known homogeneous point processes give the negative binomial distribution for plot abundances, and both are extreme cases (Daley & Vere-Jones 2003). For some further developments of the negative binomial distribution model, we refer to Solow & Smith (2010), Hwang & Huggins (2016), Huggins et al. (2018), Hwang et al. (2022), and Stoklosa et al. (2022). For other suggested models than those based on the Poisson and the negative binomial distributions for describing the relationship between the presence probability p and plant density λ, see, e.g., Holt et al. (2002), He et al. (2002), and the references therein. Extensions of the negative binomial model and other related models to an inhomogeneous setting would be useful for extending the approach presented in the current article to more general settings.

Many monitoring and citizen science programmes already have large amounts of P/A data in their databases (e.g., the Norwegian Biodiversity Information Center in Norway (Hoem 2022); the Global Biodiversity Information Facility GBIF (GBIF 2022)). Therefore, the techniques and estimators developed in the present study can be applied to already available data, especially since new fine-scaled covariate data are becoming increasingly common in such databases. Promising results were obtained in this study, which means that the proposed framework for monitoring plant population density through P/A sampling and modelling holds promise for future practical application, e.g., in national reporting of trends in declining species.

Author contributions

LG wrote the main draft, performed the analyses and simulations and contributed to the theoretical developments; ME conceived the idea, contributed to the theoretical developments and contributed critically to the drafts; SS, BGJ, JW and GS contributed critically to the drafts.

Funding

This work was supported by Kempestiftelserna (SMK-1955).

Declaration of Competing Interest

The authors declare that they have no known competing financial interests or personal relationships that could have appeared to influence the work reported in this paper.

Data availability

The data will be made available upon request.

Acknowledgements

We thank Jonas Dahlgren for having provided the data used in Section 3.

Appendix A. Theoretical developments in the case of single plots

A.1. Case with known area

For simplicity, we assume that the sampling design of S_1 is non-informative, i.e. the vector of model parameters is estimated without taking this sampling design into account. Under this assumption, for large samples and under mild conditions (see for example Sen & Singer 1993),

$$\sqrt{n_2}(\widehat{\boldsymbol{\beta}} - \boldsymbol{\beta}) \sim \mathcal{N}\left(0, I^{-1}(\boldsymbol{\beta})\right), \tag{A.1}$$

where $I(\boldsymbol{\beta})$ denotes the Fisher information matrix and can be estimated by

$$\widehat{I}(\widehat{\boldsymbol{\beta}}) = \frac{1}{n_2}\sum_{i\in I_n}\frac{1}{[g'(p_i(\widehat{\boldsymbol{\beta}}))]^2 v_i(\widehat{\boldsymbol{\beta}})}\ \boldsymbol{x}_i\boldsymbol{x}_i', \tag{A.2}$$

with $\widehat{\boldsymbol{\beta}}$ being the estimate of $\boldsymbol{\beta}$, g defined by (5), p_i defined by (4), and $v_i(\boldsymbol{\beta}) = \mathrm{Var}(Y_i) = p_i(1-p_i)$, where $Y_i = 1$ if there is presence of plants in plot i, and $Y_i = 0$ otherwise.

Using a similar reasoning as in [Ståhl et al. 2011], we start with the decomposition

$$\widehat{\Lambda}(\widehat{\boldsymbol{\beta}}) - \Lambda(\boldsymbol{\beta}) = \sum_{i\in I_n}\frac{\widetilde{\lambda}_{\widehat{\boldsymbol{\beta}}}(\boldsymbol{u}_i)}{\pi(\boldsymbol{u}_i)} - \Lambda = D_1 + D_2, \tag{A.3}$$

where

$$D_1 = \sum_{i\in I_n}\frac{\widetilde{\lambda}_{\boldsymbol{\beta}}(\boldsymbol{u}_i)}{\pi(\boldsymbol{u}_i)} - \Lambda \quad \text{and} \quad D_2 = \sum_{i\in I_n}\frac{\widetilde{\lambda}_{\widehat{\boldsymbol{\beta}}}(\boldsymbol{u}_i) - \widetilde{\lambda}_{\boldsymbol{\beta}}(\boldsymbol{u}_i)}{\pi(\boldsymbol{u}_i)}.$$

Our objective is to compute the variance

$$\mathrm{Var}(D_1 + D_2) = \mathrm{Var}(D_1) + \mathrm{Var}(D_2) + 2\ \mathrm{Cov}(D_1, D_2).$$

Using the Sen-Yates-Grundy formula presented in Cordy (1993), an unbiased estimator of $\mathrm{Var}(D_1)$ is given by (10). If $\boldsymbol{\beta}$ is unknown, we estimate this variance with

$$\widehat{\mathrm{Var}}(D_1) = \frac{1}{2}\sum_{i\in I_n}\sum_{j\in J_{n,i}}\frac{\Delta(\boldsymbol{u}_i,\boldsymbol{u}_j)}{\pi(\boldsymbol{u}_i,\boldsymbol{u}_j)}\left(\frac{r_i\exp(\widehat{\boldsymbol{\beta}}^{\mathrm{T}}\boldsymbol{x}_i)}{\pi(\boldsymbol{u}_i)} - \frac{r_j\exp(\widehat{\boldsymbol{\beta}}^{\mathrm{T}}\boldsymbol{x}_j)}{\pi(\boldsymbol{u}_j)}\right)^2. \tag{A.4}$$

The law of total variance is used in order to compute $\mathrm{Var}(D_2)$, i.e

$$\mathrm{Var}(D_2) = \mathrm{Var}_{S_2}[\mathbb{E}_{S_1}(D_2|S_2)] + \mathbb{E}_{S_2}[\mathrm{Var}_{S_1}(D_2|S_2)]. \tag{A.5}$$

For non-linear models, a Taylor approximation can be applied, i.e.

$$\widetilde{\lambda}_{\widehat{\boldsymbol{\beta}}}(\boldsymbol{u}) \approx \widetilde{\lambda}_{\boldsymbol{\beta}}(\boldsymbol{u}) + \sum_{k=1}^{q}(\widehat{\beta}_k - \beta_k)\widetilde{\lambda}^{(k)}_{\boldsymbol{\beta}}(\boldsymbol{u}), \tag{A.6}$$

where

$$\widetilde{\lambda}^{(k)}_{\boldsymbol{\beta}}(\boldsymbol{u}_i) = r_i x_{ik}\exp(\boldsymbol{\beta}^{\mathrm{T}}\boldsymbol{x}_i).$$

Then,

$$D_2 \approx \sum_{i\in I_n}\sum_{k=1}^{q}\frac{(\widehat{\beta}_k - \beta_k)}{\pi(\boldsymbol{u}_i)}\ \widetilde{\lambda}^{(k)}_{\boldsymbol{\beta}}(\boldsymbol{u}_i) = \sum_{k=1}^{q}(\widehat{\beta}_k - \beta_k)v_k,$$

where

$$v_k = \sum_{i\in I_n}\frac{1}{\pi(\boldsymbol{u}_i)}\widetilde{\lambda}^{(k)}_{\boldsymbol{\beta}}(\boldsymbol{u}_i)$$

and q being the number of model coefficients. Conditioned on S_2, v_k is a constant. Then, by (A.1), $\mathbb{E}_{S_1}(D_2|S_2) \approx \sum_{k=1}^{q}\mathbb{E}_{S_1}(\widehat{\beta}_k - \beta_k|S_2)v_k \approx 0$ for large samples, and thus $Var_{S_2}[\mathbb{E}_{S_1}(D_2|S_2)] \approx 0$. Furthermore,

$$
\begin{aligned}
\mathrm{Var}_{S_1}(D_2|S_2) &\approx \mathrm{Var}_{S_1}\left(\sum_{k=1}^{q}(\widehat{\beta}_k-\beta_k)v_k\,|S_2\right)\\
&\approx \sum_{k=1}^{q}\sum_{l=1}^{q}\mathrm{Cov}_{S_1}(\widehat{\beta}_k,\widehat{\beta}_l)v_k v_l\\
&= \sum_{i\in I_n}\sum_{j\in I_n}\frac{1}{\pi(\boldsymbol{u}_i)\pi(\boldsymbol{u}_j)}\sum_{k=1}^{q}\sum_{l=1}^{q}\mathrm{Cov}_{S_1}(\widehat{\beta}_k,\widehat{\beta}_l)r_i\,r_j\,x_{ik}\,x_{jl}\exp\left(\boldsymbol{\beta}^{\mathrm{T}}(\boldsymbol{x}_i+\boldsymbol{x}_j)\right)\\
&= \sum_{k=1}^{q}\sum_{l=1}^{q}\mathrm{Cov}_{S_1}(\widehat{\beta}_k,\widehat{\beta}_l)\sum_{i\in I_n}\frac{r_i^2}{\pi(\boldsymbol{u}_i)^2}x_{ik}x_{il}\exp\left(2\boldsymbol{\beta}^{\mathrm{T}}\boldsymbol{x}_i\right)\\
&+\sum_{k=1}^{q}\sum_{l=1}^{q}\mathrm{Cov}_{S_1}(\widehat{\beta}_k,\widehat{\beta}_l)\sum_{i\in I_n}\sum_{j\in J_{n,i}}\frac{r_i r_j}{\pi(\boldsymbol{u}_i)\pi(\boldsymbol{u}_j)}x_{ik}\,x_{jl}\,\exp\left(\boldsymbol{\beta}^{\mathrm{T}}(\boldsymbol{x}_i+\boldsymbol{x}_j)\right).
\end{aligned}
$$

From the arguments in the proof of Theorem 2 in Cordy (1993), we get

$$
\begin{aligned}
\mathrm{Var}(D_2) &\approx \mathbb{E}_{S_2}[\mathrm{Var}_{S_1}(D_2|S_2)]\\
&= \sum_{k=1}^{q}\sum_{l=1}^{q}\mathrm{Cov}_{S_1}(\widehat{\beta}_k,\widehat{\beta}_l)\int_{U^\star}\frac{r_{\boldsymbol{u}}^2}{\pi(\boldsymbol{u})}\boldsymbol{x}^k(\boldsymbol{u})\boldsymbol{x}^l(\boldsymbol{u})\exp\left(2\boldsymbol{\beta}^{\mathrm{T}}\boldsymbol{x}(\boldsymbol{u})\right)d\boldsymbol{u}\\
&+\sum_{k=1}^{q}\sum_{l=1}^{q}\mathrm{Cov}_{S_1}(\widehat{\beta}_k,\widehat{\beta}_l)\int_{U^\star}\int_{U^\star}\frac{\pi(\boldsymbol{u},\boldsymbol{u}')}{\pi(\boldsymbol{u})\pi(\boldsymbol{u}')}r_{\boldsymbol{u}}r_{\boldsymbol{u}'}\boldsymbol{x}^k(\boldsymbol{u})\boldsymbol{x}^l(\boldsymbol{u})\exp\left(\boldsymbol{\beta}^{\mathrm{T}}(\boldsymbol{x}(\boldsymbol{u})+\boldsymbol{x}(\boldsymbol{u}'))\right)d\boldsymbol{u}d\boldsymbol{u}',
\end{aligned}
$$

where $\boldsymbol{x}^k(\boldsymbol{u})$ denotes the kth component of the $\boldsymbol{x}$ vector and $r_{\boldsymbol{u}}$ is the ratio of the area of $C(\boldsymbol{u})\cap U$ and the area of $C(\boldsymbol{u})$. Thus, $Var(D_2)$ can be estimated by

$$
\begin{aligned}
\widehat{\mathrm{Var}}(D_2) &= \sum_{k=1}^{q}\sum_{l=1}^{q}\widehat{\mathrm{Cov}}_{S_1}(\widehat{\beta}_k,\widehat{\beta}_l)\sum_{i\in I_n}\frac{r_i^2}{\pi(\boldsymbol{u}_i)^2}\,x_{ik}x_{il}\exp\left(2\widehat{\boldsymbol{\beta}}^{\mathrm{T}}\boldsymbol{x}_i\right)\\
&+\sum_{k=1}^{q}\sum_{l=1}^{q}\widehat{\mathrm{Cov}}_{S_1}(\widehat{\beta}_k,\widehat{\beta}_l)\sum_{i\in I_n}\sum_{j\in J_{n,i}}\frac{r_i r_j}{\pi(\boldsymbol{u}_i)\pi(\boldsymbol{u}_j)}\,x_{ik}x_{jl}\exp\left(\widehat{\boldsymbol{\beta}}^{\mathrm{T}}(\boldsymbol{x}_i+\boldsymbol{x}_j)\right)\\
&= \sum_{k=1}^{q}\sum_{l=1}^{q}\widehat{\mathrm{Cov}}_{S_1}(\widehat{\beta}_k,\widehat{\beta}_l)\sum_{i\in I_n}\sum_{j\in I_n}\frac{r_i r_j}{\pi(\boldsymbol{u}_i)\pi(\boldsymbol{u}_j)}\,x_{ik}x_{jl}\exp\left(\widehat{\boldsymbol{\beta}}^{\mathrm{T}}(\boldsymbol{x}_i+\boldsymbol{x}_j)\right)\\
&= \sum_{k=1}^{q}\sum_{l=1}^{q}\widehat{\mathrm{Cov}}_{S_1}(\widehat{\beta}_k,\widehat{\beta}_l)\widehat{v}_k\widehat{v}_l,
\end{aligned}
\tag{A.7}
$$

where $\widehat{v}_k$ is defined in (12).

The next step is to compute the covariance between D_1 and D_2. According to the law of total covariance,

$$
\mathrm{Cov}(D_1,D_2)=\mathbb{E}_{S_2}[\mathrm{Cov}_{S_1}(D_1,D_2|S_2)]+\mathrm{Cov}_{S_2}[\mathbb{E}_{S_1}(D_1|S_2),\mathbb{E}_{S_1}(D_2|S_2)]. \tag{A.8}
$$

It can be deduced that $\mathrm{Cov}_{S_2}[\mathbb{E}_{S_1}(D_1|S_2),\mathbb{E}_{S_1}(D_2|S_2)]\approx 0$ because, as argued before, $\mathbb{E}_{S_1}(D_2|S_2)\approx 0$. Then, as the stochastic nature of D_1 is determined by sample S_2 and not by sample S_1, $\mathbb{E}_{S_1}(D_1D_2|S_2)=D_1\mathbb{E}_{S_1}(D_2|S_2)\approx 0$. Because of the latter, $\mathbb{E}_{S_2}[\mathrm{Cov}_{S_1}(D_1,D_2|S_2)]\approx 0$. Thus, $\mathrm{Cov}(D_1,D_2)\approx 0$ and we just need to add the variances of D_1 and D_2 to get an approximate variance of D_1+D_2. As a result, setting (A.4) and (A.7) together, the estimate becomes

$$
\begin{aligned}
\widehat{\mathrm{Var}}(\widehat{\Lambda}(\widehat{\boldsymbol{\beta}})) &= \widehat{\mathrm{Var}}(D_1)+\widehat{\mathrm{Var}}(D_2)+2\widehat{\mathrm{Cov}}(D_1,D_2)\\
&= \frac{1}{2}\sum_{i\in I_n}\sum_{j\in J_{n,i}}\frac{\Delta(\boldsymbol{u}_i,\boldsymbol{u}_j)}{\pi(\boldsymbol{u}_i,\boldsymbol{u}_j)}\left(\frac{r_i\exp(\widehat{\boldsymbol{\beta}}^{\mathrm{T}}\boldsymbol{x}_i)}{\pi(\boldsymbol{u}_i)}-\frac{r_j\exp(\widehat{\boldsymbol{\beta}}^{\mathrm{T}}\boldsymbol{x}_j)}{\pi(\boldsymbol{u}_j)}\right)^2+\sum_{k=1}^{q}\sum_{l=1}^{q}\widehat{\mathrm{Cov}}_{S_1}(\widehat{\beta}_k,\widehat{\beta}_l)\widehat{v}_k\widehat{v}_l,
\end{aligned}
$$

with $\widehat{v}_k$ defined in (12).

A.2. Expected density estimator in a specific area of the landscape

Suppose we want to estimate the number of plants exclusively in a certain landscape category, for example forests. Then, the parameter vector $\boldsymbol{\beta}$ will be estimated only from the plots that are situated in this landscape category.

As in Result 5.6.2 in Särndal et al. (1992), for estimating the variance of $\widehat{R}^\star(\boldsymbol{\beta})$ we use a Taylor linearisation by introducing $\widehat{R}_0^\star(\boldsymbol{\beta})$, that is related to $\widehat{R}^\star(\boldsymbol{\beta})$ by the relation

$$
\widehat{R}^\star(\boldsymbol{\beta})\approx\widehat{R}_0^\star(\boldsymbol{\beta})=R^\star(\boldsymbol{\beta})+\frac{1}{A}\sum_{i\in I_n}\frac{\lambda^\star(\boldsymbol{u}_i)-R^\star(\boldsymbol{\beta})z(\boldsymbol{u}_i)}{\pi(\boldsymbol{u}_i)}. \tag{A.9}
$$

Remember that the estimator of $\boldsymbol{\beta}$, $\widehat{\boldsymbol{\beta}}$, is approximately normally distributed with mean $\boldsymbol{\beta}$ (see (A.1)). We estimate $R^{\star}(\boldsymbol{\beta})$ with $\widehat{R}^{\star}(\widehat{\boldsymbol{\beta}})$. The goal here is to derive an estimate of the variance of $\widehat{R}^{\star}(\widehat{\boldsymbol{\beta}})$, or equivalently the variance of $\widehat{R}^{\star}(\widehat{\boldsymbol{\beta}}) - R^{\star}(\boldsymbol{\beta})$, which by the arguments in the proof of Result 5.6.2 in Särndal et al. (1992) is approximately the same as the one for

$$D(\widehat{\boldsymbol{\beta}}) = \widehat{R}_0^{\star}(\widehat{\boldsymbol{\beta}}) - R^{\star}(\widehat{\boldsymbol{\beta}}) = \frac{1}{A}\sum_{i\in I_u}\frac{\widehat{\lambda}^{\star}(\boldsymbol{u}_i) - R^{\star}(\widehat{\boldsymbol{\beta}})z(\boldsymbol{u}_i)}{\pi(\boldsymbol{u}_i)},$$

where

$$\widehat{\lambda}^{\star}(\boldsymbol{u}) = \int_{C(\mathbf{u})}\frac{\lambda_{\widehat{\boldsymbol{\beta}}}(\boldsymbol{u}')I_{\boldsymbol{u}'}}{a_{\boldsymbol{u}'}}d\boldsymbol{u}', \boldsymbol{u}\in U^{\bullet}. \tag{A.10}$$

We can write

$$\widehat{R}_0^{\star}(\widehat{\boldsymbol{\beta}}) - R^{\star}(\boldsymbol{\beta}) = \left(\widehat{R}_0^{\star}(\widehat{\boldsymbol{\beta}}) - R^{\star}(\widehat{\boldsymbol{\beta}})\right) + \left(R^{\star}(\widehat{\boldsymbol{\beta}}) - R^{\star}(\boldsymbol{\beta})\right) = D(\widehat{\boldsymbol{\beta}}) + D_*(\widehat{\boldsymbol{\beta}}),$$

where $D_*(\widehat{\boldsymbol{\beta}}) = R^{\star}(\widehat{\boldsymbol{\beta}}) - R^{\star}(\boldsymbol{\beta})$. By the following Taylor approximation

$$\lambda_{\widehat{\boldsymbol{\beta}}}(\boldsymbol{u}) \approx \lambda_{\boldsymbol{\beta}}(\boldsymbol{u}) + \sum_{k=1}^{q}(\widehat{\beta}_k - \beta_k)\lambda_{\boldsymbol{\beta}}^{(k)}(\boldsymbol{u}), \tag{A.11}$$

where

$$\lambda_{\boldsymbol{\beta}}^{(k)}(\boldsymbol{u}) = \frac{\partial\lambda_{\boldsymbol{\beta}}(\boldsymbol{u})}{\partial\beta_k},$$

we obtain

$$\begin{aligned}\mathbb{E}[R^{\star}(\widehat{\boldsymbol{\beta}})] &= \mathbb{E}_{S_1}[R^{\star}(\widehat{\boldsymbol{\beta}})] = \frac{1}{A}\mathbb{E}_{S_1}[\Lambda^{\star}(\widehat{\boldsymbol{\beta}})] = \frac{1}{A}\int_U \mathbb{E}_{S_1}[\lambda_{\widehat{\boldsymbol{\beta}}}(\boldsymbol{u})]I_{\boldsymbol{u}}d\boldsymbol{u}\\ &\approx \frac{1}{A}\int_U \lambda_{\boldsymbol{\beta}}(\boldsymbol{u})I_{\boldsymbol{u}}d\boldsymbol{u} + \frac{1}{A}\sum_{k=1}^{q}\mathbb{E}_{S_1}[\widehat{\beta}_k - \beta_k]\int_U \lambda_{\boldsymbol{\beta}}^{(k)}(\boldsymbol{u})I_{\boldsymbol{u}}d\boldsymbol{u} \approx \frac{1}{A}\int_U \lambda_{\boldsymbol{\beta}}(\boldsymbol{u})I_{\boldsymbol{u}}d\boldsymbol{u} = R^{\star}(\boldsymbol{\beta})\end{aligned} \tag{A.12}$$

and

$$\begin{aligned}\mathbb{E}\left[(R^{\star}(\widehat{\boldsymbol{\beta}}))^2\right] &= \mathbb{E}_{S_1}\left[(R^{\star}(\widehat{\boldsymbol{\beta}}))^2\right] = \frac{1}{A^2}\mathbb{E}_{S_1}\left[(\Lambda^{\star}(\widehat{\boldsymbol{\beta}}))^2\right]\\ &= \frac{1}{A^2}\int_U\int_U \mathbb{E}_{S_1}[\lambda_{\widehat{\boldsymbol{\beta}}}(\boldsymbol{u})\lambda_{\widehat{\boldsymbol{\beta}}}(\boldsymbol{u}')]I_{\boldsymbol{u}}I_{\boldsymbol{u}'}d\boldsymbol{u}d\boldsymbol{u}'\\ &\approx \frac{1}{A^2}\int_U\int_U \lambda_{\boldsymbol{\beta}}(\boldsymbol{u})\lambda_{\boldsymbol{\beta}}(\boldsymbol{u}')I_{\boldsymbol{u}}I_{\boldsymbol{u}'}d\boldsymbol{u}d\boldsymbol{u}' + \frac{1}{A^2}\sum_{k=1}^{q}\sum_{l=1}^{q}\mathrm{Cov}_{S_1}(\widehat{\beta}_k,\widehat{\beta}_l)d_{2,k}d_{2,l}\\ &= (R^{\star}(\boldsymbol{\beta}))^2 + \frac{1}{A^2}\sum_{k=1}^{q}\sum_{l=1}^{q}\mathrm{Cov}_{S_1}(\widehat{\beta}_k,\widehat{\beta}_l)d_{2,k}d_{2,l},\end{aligned}$$

where

$$d_{2,k} = \int_U I_{\boldsymbol{u}}\lambda_{\boldsymbol{\beta}}^{(k)}(\boldsymbol{u})d\boldsymbol{u} = \frac{\partial\Lambda^{\star}(\boldsymbol{\beta})}{\partial\beta_k}.$$

Thus,

$$\mathbb{E}[D_*(\widehat{\boldsymbol{\beta}})] = \mathbb{E}_{S_1}[D_*(\widehat{\boldsymbol{\beta}})] \approx 0 \tag{A.13}$$

and

$$\mathrm{Var}(D_*(\widehat{\boldsymbol{\beta}})) = \mathrm{Var}_{S_1}(D_*(\widehat{\boldsymbol{\beta}})) \approx \frac{1}{A^2}\sum_{k=1}^{q}\sum_{l=1}^{q}\mathrm{Cov}_{S_1}(\widehat{\beta}_k,\widehat{\beta}_l)d_{2,k}d_{2,l}. \tag{A.14}$$

Let us go further with $D(\widehat{\boldsymbol{\beta}})$. We have

$$\mathrm{Var}(D(\widehat{\boldsymbol{\beta}})) = \mathrm{Var}_{S_2}[\mathbb{E}_{S_1}(D(\widehat{\boldsymbol{\beta}})|S_2)] + \mathbb{E}_{S_2}[\mathrm{Var}_{S_1}(D(\widehat{\boldsymbol{\beta}})|S_2)]. \tag{A.15}$$

We see that

$$\mathbb{E}_{S_1}(D(\widehat{\boldsymbol{\beta}})\,|S_2) = \frac{1}{A}\sum_{i\in I_n}\frac{\mathbb{E}_{S_1}(\widehat{\lambda}^{\star}(\mathbf{u}_i)\,|S_2) - \mathbb{E}_{S_1}(R^{\star}(\widehat{\boldsymbol{\beta}})\,|S_2)z(\boldsymbol{u}_i)}{\pi(\boldsymbol{u}_i)}$$

and, by (A.11), we obtain

$$\begin{aligned}\mathbb{E}_{S_1}[\widehat{\lambda}^{\star}(\boldsymbol{u})\,|S_2] &= \int_{C(\boldsymbol{u})}\frac{1}{a_{\boldsymbol{u}}}E_{S_1}[\lambda_{\beta}(\boldsymbol{u}')]I_{\boldsymbol{u}}d\boldsymbol{u}'\\ &\approx \int_{C(\boldsymbol{u})}\frac{1}{a_{\boldsymbol{u}}}\lambda_{\beta}(\boldsymbol{u}')I_{\boldsymbol{u}}d\boldsymbol{u}' + \sum_{k=1}^{q}E_{S_1}[\widehat{\beta}_k-\beta_k]\int_{C(\boldsymbol{u})}\frac{1}{a_{\boldsymbol{u}}}I_{\boldsymbol{u}}\lambda_{\beta}^{(k)}(\boldsymbol{u}')d\boldsymbol{u}'\\ &\approx \int_{C(\boldsymbol{u})}\frac{1}{a_{\boldsymbol{u}}}\lambda_{\beta}(\boldsymbol{u}')I_{\boldsymbol{u}}d\boldsymbol{u}' = \lambda^{\star}(\boldsymbol{u}).\end{aligned}$$

Thus,

$$\mathbb{E}_{S_1}(D(\widehat{\boldsymbol{\beta}})\,|S_2) \approx \frac{1}{A}\sum_{i\in I_n}\frac{\lambda^{\star}(\boldsymbol{u}_i) - R^{\star}(\boldsymbol{\beta})z(\boldsymbol{u}_i)}{\pi(\boldsymbol{u}_i)} = \widehat{R}_0^{\star}(\boldsymbol{\beta}) - R^{\star}(\boldsymbol{\beta}) \tag{A.16}$$

and, from the Sen-Yates-Grundy formula presented in Cordy (1993),

$$\begin{aligned}&\mathrm{Var}_{S_2}[\mathbb{E}_{S_1}(D(\widehat{\boldsymbol{\beta}})\,|S_2)] \approx \mathrm{Var}_{S_2}\left(\widehat{R}_0^{\star}(\boldsymbol{\beta})\right)\\ &= \frac{1}{2A^2}\int_{U^{\star}}\int_{U^{\star}}\Delta(\boldsymbol{u}_i,\boldsymbol{u}_j)\left(\frac{\lambda^{\star}(\boldsymbol{u}) - R^{\star}(\boldsymbol{\beta})z(\boldsymbol{u})}{\pi(\boldsymbol{u})} - \frac{\lambda^{\star}(\boldsymbol{u}') - R^{\star}(\boldsymbol{\beta})z(\boldsymbol{u}')}{\pi(\boldsymbol{u}')}\right)^2.\end{aligned} \tag{A.17}$$

Then, we can look closer at

$$\mathrm{Var}_{S_1}(D(\widehat{\boldsymbol{\beta}})\,|S_2) = \mathbb{E}_{S_1}\left(D^2(\widehat{\boldsymbol{\beta}})\,|S_2\right) - (\mathbb{E}_{S_1}(D(\widehat{\boldsymbol{\beta}})\,|S_2))^2,$$

which is a part of (A.15), where

$$\mathbb{E}_{S_1}\left(D^2(\widehat{\boldsymbol{\beta}})\,|S_2\right) = \frac{1}{A^2}\sum_{i\in I_n}\sum_{j\in I_n}\mathbb{E}_{S_1}\left[\left(\frac{\widehat{\lambda}^{\star}(\boldsymbol{u}_i) - R^{\star}(\widehat{\boldsymbol{\beta}})z(\boldsymbol{u}_i)}{\pi(\boldsymbol{u}_i)}\right)\left(\frac{\widehat{\lambda}^{\star}(\boldsymbol{u}_j) - R^{\star}(\widehat{\boldsymbol{\beta}})z(\boldsymbol{u}_j)}{\pi(\boldsymbol{u}_j)}\right)\middle|S_2\right]. \tag{A.18}$$

From (A.11), we see that

$$\begin{aligned}\mathbb{E}_{S_1}[\widehat{\lambda}^{\star}(\boldsymbol{u})\widehat{\lambda}^{\star}(\boldsymbol{u}')] &\approx \int_{C(\boldsymbol{u})}\int_{C(\boldsymbol{u}')}a_{\boldsymbol{v}}^{-1}a_{\boldsymbol{v}'}^{-1}\lambda_{\beta}(\boldsymbol{v})\lambda_{\beta}(\boldsymbol{v}')I_{\boldsymbol{v}}I_{\boldsymbol{v}'}d\boldsymbol{v}'d\boldsymbol{v}\\ &\quad+\sum_{k=1}^{q}\sum_{l=1}^{q}\mathrm{Cov}_{S_1}(\widehat{\beta}_k,\widehat{\beta}_l)d_{1,k}(\boldsymbol{u})d_{1,l}(\boldsymbol{u}')\\ &= \lambda^{\star}(\boldsymbol{u})\lambda^{\star}(\boldsymbol{u}') + \sum_{k=1}^{q}\sum_{l=1}^{q}\mathrm{Cov}_{S_1}(\widehat{\beta}_k,\widehat{\beta}_l)d_{1,k}(\boldsymbol{u})d_{1,l}(\boldsymbol{u}'),\end{aligned} \tag{A.19}$$

where

$$d_{1,k}(\boldsymbol{u}) = \int_{C(\boldsymbol{u})}a_{\boldsymbol{u}}^{-1}I_{\boldsymbol{u}}\lambda_{\beta}^{(k)}(\boldsymbol{u}')d\boldsymbol{u}' = \int_{C(\boldsymbol{u})}a_{\boldsymbol{u}}^{-1}I_{\boldsymbol{u}}x(\boldsymbol{u}')_k\exp\left(\boldsymbol{\beta}^{\mathrm{T}}\boldsymbol{x}(\boldsymbol{u}')\right)d\boldsymbol{u}',$$

and that

$$\begin{aligned}&\mathbb{E}_{S_1}[\widehat{\lambda}^{\star}(\boldsymbol{u})R^{\star}(\widehat{\boldsymbol{\beta}})] = \frac{1}{A}\int_{C(\boldsymbol{u})}a_{\boldsymbol{v}}^{-1}\mathbb{E}_{S_1}[\lambda_{\widehat{\beta}}(\boldsymbol{v})\Lambda^{\star}(\widehat{\boldsymbol{\beta}})]I_{\boldsymbol{v}}d\boldsymbol{v} = \frac{1}{A}\int_{U}\int_{C(\boldsymbol{u})}a_{\boldsymbol{v}}^{-1}\mathbb{E}_{S_1}[\lambda_{\widehat{\beta}}(\boldsymbol{v})\lambda_{\widehat{\beta}}(\boldsymbol{v}')]I_{\boldsymbol{v}}I_{\boldsymbol{v}'}d\boldsymbol{v}d\boldsymbol{v}'\\ &\approx\frac{1}{A}\int_{U}\int_{C(\boldsymbol{u})}a_{\boldsymbol{v}}^{-1}\lambda_{\beta}(\boldsymbol{v})\lambda_{\beta}(\boldsymbol{v}')I_{\boldsymbol{v}}I_{\boldsymbol{v}'}d\boldsymbol{v}d\boldsymbol{v}'\\ &\quad+\frac{1}{A}\sum_{k=1}^{q}\sum_{l=1}^{q}Cov_{S_1}(\widehat{\beta}_k,\widehat{\beta}_l)\int_{U}\int_{C(\boldsymbol{u})}a_{\boldsymbol{v}}^{-1}x(\boldsymbol{v})_k\exp\left(\boldsymbol{\beta}^{\mathrm{T}}\boldsymbol{x}(\boldsymbol{v})\right)x(\boldsymbol{v}')_l\exp\left(\boldsymbol{\beta}^{\mathrm{T}}\boldsymbol{x}(\boldsymbol{v}')\right)I_{\boldsymbol{v}}I_{\boldsymbol{v}'}d\boldsymbol{v}d\boldsymbol{v}'\\ &= \lambda^{\star}(\boldsymbol{u})R^{\star}(\boldsymbol{\beta}) + \frac{1}{A}\sum_{k=1}^{q}\sum_{l=1}^{q}Cov_{S_1}(\widehat{\beta}_k,\widehat{\beta}_l)d_{1,k}(\boldsymbol{u})d_{2,l}.\end{aligned} \tag{A.20}$$

From (A.18), (A.19) and (A.20), we obtain

$$\begin{aligned}\mathbb{E}_{S_1}\left[D^2(\widehat{\boldsymbol{\beta}})\,|S_2\right] &\approx \frac{1}{A^2}\sum_{i\in I_n}\sum_{j\in I_n}\left(\frac{\lambda^\star(\boldsymbol{u}_i)-R^\star(\boldsymbol{\beta})z(\boldsymbol{u}_i)}{\pi(\boldsymbol{u}_i)}\right)\left(\frac{\lambda^\star(\boldsymbol{u}_j)-R^\star(\boldsymbol{\beta})z(\boldsymbol{u}_j)}{\pi(\boldsymbol{u}_j)}\right)\\ &+\frac{1}{A^2}\sum_{k=1}^{q}\sum_{l=1}^{q}\mathrm{Cov}_{S_1}(\widehat{\beta}_k,\widehat{\beta}_l)\sum_{i\in I_n}\sum_{j\in I_n}\left(\frac{d_{1,k}(\boldsymbol{u}_i)-z(\boldsymbol{u}_i)d_{2,k}/A}{\pi(\boldsymbol{u}_i)}\right)\left(\frac{d_{1,l}(\boldsymbol{u}_j)-z(\boldsymbol{u}_j)d_{2,l}/A}{\pi(\boldsymbol{u}_j)}\right)\\ &=\left(\widehat{R}_0^\star(\boldsymbol{\beta})-R^\star(\boldsymbol{\beta})\right)^2\\ &+\frac{1}{A^2}\sum_{k=1}^{q}\sum_{l=1}^{q}\mathrm{Cov}_{S_1}(\widehat{\beta}_k,\widehat{\beta}_l)\sum_{i\in I_n}\sum_{j\in I_n}\left(\frac{d_{1,k}(\boldsymbol{u}_i)-z(\boldsymbol{u}_i)d_{2,k}/A}{\pi(\boldsymbol{u}_i)}\right)\left(\frac{d_{1,l}(\boldsymbol{u}_j)-z(\boldsymbol{u}_j)d_{2,l}/A}{\pi(\boldsymbol{u}_j)}\right).\end{aligned}$$

This, together with (A.16), gives

$$\begin{aligned}&\mathrm{Var}_{S_1}(D(\widehat{\boldsymbol{\beta}})\,|S_2)\approx\frac{1}{A^2}\sum_{k=1}^{q}\sum_{l=1}^{q}\mathrm{Cov}_{S_1}(\widehat{\beta}_k,\widehat{\beta}_l)\sum_{i\in I_n}\left(\frac{d_{1,k}(\boldsymbol{u}_i)-z(\boldsymbol{u}_i)d_{2,k}/A}{\pi(\boldsymbol{u}_i)}\right)\sum_{j\in I_n}\left(\frac{d_{1,l}(\boldsymbol{u}_j)-z(\boldsymbol{u}_j)d_{2,l}/A}{\pi(\boldsymbol{u}_j)}\right)\\ &=\frac{1}{A^2}\sum_{k=1}^{q}\sum_{l=1}^{q}\mathrm{Cov}_{S_1}(\widehat{\beta}_k,\widehat{\beta}_l)\sum_{i\in I_n}\frac{1}{\pi(\boldsymbol{u}_i)^2}\left(d_{1,k}(\boldsymbol{u}_i)-z(\boldsymbol{u}_i)d_{2,k}\frac{1}{A}\right)\left(d_{1,l}(\boldsymbol{u}_i)-z(\boldsymbol{u}_i)d_{2,l}\frac{1}{A}\right)\\ &+\frac{1}{A^2}\sum_{k=1}^{q}\sum_{l=1}^{q}\mathrm{Cov}_{S_1}(\widehat{\beta}_k,\widehat{\beta}_l)\sum_{i\in I_n}\sum_{j\in J_{n,i}}\frac{1}{\pi(\boldsymbol{u}_i)\pi(\boldsymbol{u}_j)}\left(d_{1,k}(\boldsymbol{u}_i)-z(\boldsymbol{u}_i)d_{2,k}\frac{1}{A}\right)\left(d_{1,l}(\boldsymbol{u}_j)-z(\boldsymbol{u}_j)d_{2,l}\frac{1}{A}\right).\end{aligned}$$

It follows that

$$\begin{aligned}&\mathbb{E}_{S_2}[\mathrm{Var}_{S_1}(D(\widehat{\boldsymbol{\beta}})\,|S_2)\,]\approx\frac{1}{A^2}\sum_{k=1}^{q}\sum_{l=1}^{q}\mathrm{Cov}_{S_1}(\widehat{\beta}_k,\widehat{\beta}_l)\int_{U^\star}\frac{1}{\pi(\boldsymbol{u})}\left(d_{1,k}(\boldsymbol{u})-z(\boldsymbol{u})d_{2,k}\frac{1}{A}\right)\left(d_{1,l}(\boldsymbol{u})-z(\boldsymbol{u})d_{2,l}\frac{1}{A}\right)d\boldsymbol{u}\\ &+\frac{1}{A^2}\sum_{k=1}^{q}\sum_{l=1}^{q}\mathrm{Cov}_{S_1}(\widehat{\beta}_k,\widehat{\beta}_l)\int_{U^\star}\int_{U^\star}\frac{\pi(\boldsymbol{u},\boldsymbol{u}^{'})}{\pi(\boldsymbol{u})\pi(\boldsymbol{u}^{'})}\left(d_{1,k}(\boldsymbol{u})-z(\boldsymbol{u})d_{2,k}\frac{1}{A}\right)\left(d_{1,l}(\boldsymbol{u}^{'})-z(\boldsymbol{u}^{'})d_{2,l}\frac{1}{A}\right)d\boldsymbol{u}d\boldsymbol{u}^{'}.\end{aligned}\tag{A.21}$$

If we put (A.17) and (A.21) together, we obtain

$$\begin{aligned}&\mathrm{Var}(D(\widehat{\boldsymbol{\beta}})\,)=\mathrm{Var}_{S_2}[\mathbb{E}_{S_1}(D(\widehat{\boldsymbol{\beta}})\,|S_2)\,]+\mathbb{E}_{S_2}[\mathrm{Var}_{S_1}(D(\widehat{\boldsymbol{\beta}})\,|S_2)\,]\\ &\approx\frac{1}{2A^2}\int_{U^\star}\int_{U^\star}\Delta(\boldsymbol{u}_i\boldsymbol{u}_j)\left(\frac{\lambda^\star(\boldsymbol{u})-R^\star(\boldsymbol{\beta})z(\boldsymbol{u})}{\pi(\boldsymbol{u})}-\frac{\lambda^\star(\boldsymbol{u}^{'})-R^\star(\boldsymbol{\beta})z(\boldsymbol{u}^{'})}{\pi(\boldsymbol{u}^{'})}\right)^2d\boldsymbol{u}d\boldsymbol{u}^{'}\\ &+\frac{1}{A^2}\sum_{k=1}^{q}\sum_{l=1}^{q}\mathrm{Cov}_{S_1}(\widehat{\beta}_k,\widehat{\beta}_l)\int_{U^\star}\frac{1}{\pi(\boldsymbol{u})}\left(d_{1,k}(\boldsymbol{u})-z(\boldsymbol{u})d_{2,k}\frac{1}{A}\right)\left(d_{1,l}(\boldsymbol{u})-z(\boldsymbol{u})d_{2,l}\ \frac{1}{A}\right)d\boldsymbol{u}\\ &+\frac{1}{A^2}\sum_{k=1}^{q}\sum_{l=1}^{q}\mathrm{Cov}_{S_1}(\widehat{\beta}_k,\widehat{\beta}_l)\int_{U^\star}\frac{\pi(\boldsymbol{u}\boldsymbol{u}^{'})}{\pi(\boldsymbol{u})\pi(\boldsymbol{u}^{'})}\left(d_{1,k}(\boldsymbol{u})-z(\boldsymbol{u})d_{2,k}\frac{1}{A}\right)\left(d_{1,l}(\boldsymbol{u}^{'})-z(\boldsymbol{u}^{'})d_{2,l}\ \frac{1}{A}\right)d\boldsymbol{u}d\boldsymbol{u}^{'}.\end{aligned}\tag{A.22}$$

Furthermore,

$$\mathrm{Cov}(D(\widehat{\boldsymbol{\beta}})\,,D^*(\widehat{\boldsymbol{\beta}})\,)=\mathrm{Cov}_{S_2}[\mathbb{E}_{S_1}(D(\widehat{\boldsymbol{\beta}})\,|S_2)\,,\mathbb{E}_{S_1}(D^*(\widehat{\boldsymbol{\beta}})\,|S_2)\,]+\mathbb{E}_{S_2}[\mathrm{Cov}_{S_1}(D(\widehat{\boldsymbol{\beta}})\,,D^*(\widehat{\boldsymbol{\beta}})\,|S_2)\,].$$

From earlier calculations, we know that $\mathbb{E}_{S_1}(D(\widehat{\boldsymbol{\beta}})\,|S_2)\approx\widehat{R}_0^\star(\boldsymbol{\beta})-R^\star(\boldsymbol{\beta})$ and $\mathbb{E}_{S_1}(D^*(\widehat{\boldsymbol{\beta}})\,|S_2)\approx 0$, and thus $\mathrm{Cov}_{S_2}[\mathbb{E}_{S_1}(D(\widehat{\boldsymbol{\beta}})\,|S_2)\,,\mathbb{E}_{S_1}(D^*(\widehat{\boldsymbol{\beta}})\,|S_2)\,]\approx 0$. In addition, using (A.16),

$$\begin{aligned}\mathrm{Cov}_{S_1}(D(\widehat{\boldsymbol{\beta}})\,,D^*(\widehat{\boldsymbol{\beta}})\,|S_2) &\approx\mathbb{E}_{S_1}(D(\widehat{\boldsymbol{\beta}})D^*(\widehat{\boldsymbol{\beta}})\,|S_2)=\mathbb{E}_{S_1}(D(\widehat{\boldsymbol{\beta}})R^\star(\widehat{\boldsymbol{\beta}})\,|S_2)-R^\star(\boldsymbol{\beta})\mathbb{E}_{S_1}(D(\widehat{\boldsymbol{\beta}})\,|S_2)\\ &\approx\mathbb{E}_{S_1}(D(\widehat{\boldsymbol{\beta}})R^\star(\widehat{\boldsymbol{\beta}})\,|S_2)-R^\star(\boldsymbol{\beta})\left(\widehat{R}_0^\star(\boldsymbol{\beta})-R^\star(\boldsymbol{\beta})\right)\end{aligned}$$

and, from (A.12) and (A.20),

$$\mathbb{E}_{S_1}(D(\widehat{\boldsymbol{\beta}})R^\star(\widehat{\boldsymbol{\beta}})\,|S_2) = \frac{1}{A}\mathbb{E}_{S_1}\left(\sum_{i\in I_n}\frac{\widehat{\lambda}^\star(\boldsymbol{u}_i)R^\star(\widehat{\boldsymbol{\beta}}) - (R^\star(\widehat{\boldsymbol{\beta}}))^2 z(\boldsymbol{u}_i)}{\pi(\boldsymbol{u}_i)}\,\middle|\,S_2\right)$$

$$\approx R^\star(\boldsymbol{\beta})\frac{1}{A}\sum_{i\in I_n}\frac{\lambda^\star(\boldsymbol{u}_i) - R^\star(\boldsymbol{\beta})z(\boldsymbol{u}_i)}{\pi(\boldsymbol{u}_i)}$$

$$+\frac{1}{A^2}\sum_{k=1}^{q}\sum_{l=1}^{q}Cov_{S_1}(\widehat{\beta}_k,\widehat{\beta}_l)\sum_{i\in I_n}\frac{1}{\pi(\boldsymbol{u}_i)}d_{1,k}(\boldsymbol{u}_i)d_{2,l}$$

$$-\frac{1}{A^3}\sum_{k=1}^{q}\sum_{l=1}^{q}Cov_{S_1}(\widehat{\beta}_k,\widehat{\beta}_l)\sum_{i\in I_n}\frac{z(\boldsymbol{u}_i)}{\pi(\boldsymbol{u}_i)}d_{2,k}d_{2,l}.$$

As a consequence,

$$\begin{aligned}
\mathrm{Cov}(D(\widehat{\boldsymbol{\beta}})\,, D^*(\widehat{\boldsymbol{\beta}})\,) &\approx \mathbb{E}_{S_2}\left(R^\star(\boldsymbol{\beta})(\widehat{R}_0^\star(\boldsymbol{\beta}) - R^\star(\boldsymbol{\beta})\,) + \frac{1}{A^2}\sum_{k=1}^{q}\sum_{l=1}^{q}\mathrm{Cov}_{S_1}\left(\widehat{\beta}_k,\widehat{\beta}_l\right)\sum_{i\in I_n}\frac{1}{\pi(\boldsymbol{u}_i)}d_{1,k}(\boldsymbol{u}_i)d_{2,l}\right.\\
&\quad\left.-\frac{1}{A^3}\sum_{k=1}^{q}\sum_{l=1}^{q}\mathrm{Cov}_{S_1}(\widehat{\beta}_k,\widehat{\beta}_l)\sum_{i\in I_n}\frac{z(\boldsymbol{u}_i)}{\pi(\boldsymbol{u}_i)}d_{2,k}d_{2,l} - R^\star(\boldsymbol{\beta})(\widehat{R}_0^\star(\boldsymbol{\beta}) - R^\star(\boldsymbol{\beta}))\right)\\
&= \frac{1}{A^2}\sum_{k=1}^{q}\sum_{l=1}^{q}\mathrm{Cov}_{S_1}(\widehat{\beta}_k,\widehat{\beta}_l)\mathbb{E}_{S_2}\left(\sum_{i\in I_n}\frac{1}{\pi(\boldsymbol{u}_i)}d_{1,k}(\boldsymbol{u}_i)d_{2,l}\right) - \frac{1}{A^3}\sum_{k=1}^{p}\sum_{l=1}^{p}\mathrm{Cov}_{S_1}(\widehat{\beta}_k,\widehat{\beta}_l)\mathbb{E}_{S_2}\left(\sum_{i\in I_n}\frac{z(\boldsymbol{u}_i)}{\pi(\boldsymbol{u}_i)}d_{2,k}d_{2,l}\right)\\
&= \frac{1}{A^2}\sum_{k=1}^{q}\sum_{l=1}^{q}\mathrm{Cov}_{S_1}(\widehat{\beta}_k,\widehat{\beta}_l)d_{2,l}\int_{U^\bullet}d_{1,k}(\boldsymbol{u})d\boldsymbol{u} - \frac{1}{A^3}\sum_{k=1}^{q}\sum_{l=1}^{q}\mathrm{Cov}_{S_1}(\widehat{\beta}_k,\widehat{\beta}_l)d_{2,k}d_{2,l}\int_{U}z(\boldsymbol{u})d\boldsymbol{u}\\
&= \frac{1}{A^2}\sum_{k=1}^{q}\sum_{l=1}^{q}\mathrm{Cov}_{S_1}(\widehat{\beta}_k,\widehat{\beta}_l)d_{2,l}\int_{U^\bullet}d_{1,k}(\boldsymbol{u})d\boldsymbol{u} - \frac{1}{A^2}\sum_{k=1}^{q}\sum_{l=1}^{q}\mathrm{Cov}_{S_1}(\widehat{\beta}_k,\widehat{\beta}_l)d_{2,k}d_{2,l}.
\end{aligned} \tag{A.23}$$

Finally, putting (A.22), (A.14) and (A.23) together,

$$\begin{aligned}
&\mathrm{Var}\left(\widehat{R}_0^\star(\widehat{\boldsymbol{\beta}}) - R^\star(\boldsymbol{\beta})\,\right) = \mathrm{Var}(D(\widehat{\boldsymbol{\beta}})\,) + \mathrm{Var}(D^*(\widehat{\boldsymbol{\beta}})\,) + 2\,\mathrm{Cov}(D(\widehat{\boldsymbol{\beta}})\,, D^*(\widehat{\boldsymbol{\beta}})\,)\\
&\approx \frac{1}{2A^2}\int_{U^\bullet}\int_{U^\bullet}\Delta(\boldsymbol{u}_i,\boldsymbol{u}_j)\left(\frac{\lambda^\star(\boldsymbol{u}) - R^\star(\boldsymbol{\beta})z(\boldsymbol{u})}{\pi(\boldsymbol{u})} - \frac{\lambda^\star(\boldsymbol{u}') - R^\star(\boldsymbol{\beta})z(\boldsymbol{u}')}{\pi(\boldsymbol{u}')}\right)^2\\
&\quad+\frac{1}{A^2}\sum_{k=1}^{q}\sum_{l=1}^{q}\mathrm{Cov}_{S_1}(\widehat{\beta}_k,\widehat{\beta}_l)\int_{U^\bullet}\frac{1}{\pi(\boldsymbol{u})}\left(d_{1,k}(\boldsymbol{u}) - z(\boldsymbol{u})d_{2,k}\frac{1}{A}\right)\left(d_{1,l}(\boldsymbol{u}) - z(\boldsymbol{u})d_{2,l}\frac{1}{A}\right)d\boldsymbol{u}\\
&\quad+\frac{1}{A^2}\sum_{k=1}^{q}\sum_{l=1}^{q}\mathrm{Cov}_{S_1}(\widehat{\beta}_k,\widehat{\beta}_l)\int_{U^\bullet}\int_{U^\bullet}\frac{\pi(\boldsymbol{u},\boldsymbol{u}')}{\pi(\boldsymbol{u})\pi(\boldsymbol{u}')}\left(d_{1,k}(\boldsymbol{u}) - z(\boldsymbol{u})d_{2,k}\frac{1}{A}\right)\left(d_{1,l}(\boldsymbol{u}') - z(\boldsymbol{u}')d_{2,l}\frac{1}{A}\right)d\boldsymbol{u}d\boldsymbol{u}'\\
&\quad+\frac{2}{A^2}\sum_{k=1}^{q}\sum_{l=1}^{q}\mathrm{Cov}_{S_1}(\widehat{\beta}_k,\widehat{\beta}_l)d_{2,l}\int_{U^\bullet}d_{1,k}(\boldsymbol{u})d\boldsymbol{u} - \frac{1}{A^2}\sum_{k=1}^{q}\sum_{l=1}^{q}\mathrm{Cov}_{S_1}(\widehat{\beta}_k,\widehat{\beta}_l)d_{2,k}d_{2,l}.
\end{aligned}$$

By using Theorem 1 and the variance estimator based on the Sen-Yates-Grundy formula in Cordy (1993), this variance can be estimated by

$$\begin{aligned}
\widehat{\mathrm{Var}}\left(\widehat{R}_0^\star(\widehat{\boldsymbol{\beta}}) - R^\star(\boldsymbol{\beta})\,\right) &= \frac{1}{2\widehat{A}^2}\sum_{i\in I_n}\sum_{j\in J_{n,i}}\frac{\Delta(\boldsymbol{u}_i,\boldsymbol{u}_j)}{\pi(\boldsymbol{u}_i,\boldsymbol{u}_j)}\left(\frac{\widehat{\lambda}^\star(\boldsymbol{u}_i) - \widehat{R}^\star(\widehat{\boldsymbol{\beta}})z(\boldsymbol{u}_i)}{\pi(\boldsymbol{u}_i)} - \frac{\widehat{\lambda}^\star(\boldsymbol{u}_j) - \widehat{R}^\star(\widehat{\boldsymbol{\beta}})z(\boldsymbol{u}_j)}{\pi(\boldsymbol{u}_j)}\right)^2\\
&\quad+\frac{1}{\widehat{A}^2}\sum_{k=1}^{q}\sum_{l=1}^{q}\widehat{\mathrm{Cov}}_{S_1}(\widehat{\beta}_k,\widehat{\beta}_l)\sum_{i\in I_n}\frac{1}{\pi(\boldsymbol{u}_i)^2}\left(\widehat{d}_{1,k}(\boldsymbol{u}_i) - z(\boldsymbol{u}_i)\widehat{d}_{2,k}\frac{1}{\widehat{A}}\right)\left(\widehat{d}_{1,l}(\boldsymbol{u}_i) - z(\boldsymbol{u}_i)\widehat{d}_{2,l}\,\frac{1}{\widehat{A}}\right)\\
&\quad+\frac{1}{\widehat{A}^2}\sum_{k=1}^{q}\sum_{l=1}^{q}\widehat{\mathrm{Cov}}_{S_1}(\widehat{\beta}_k,\widehat{\beta}_l)\sum_{i\in I_n}\sum_{j\in J_{n,i}}\frac{1}{\pi(\boldsymbol{u}_i)\pi(\boldsymbol{u}_j)}\left(\widehat{d}_{1,k}(\boldsymbol{u}_i) - z(\boldsymbol{u}_i)\widehat{d}_{2,k}\frac{1}{\widehat{A}}\right)\left(\widehat{d}_{1,l}(\boldsymbol{u}_j) - z(\boldsymbol{u}_j)\widehat{d}_{2,l}\,\frac{1}{\widehat{A}}\right)\\
&\quad+\frac{2}{\widehat{A}^2}\sum_{k=1}^{q}\sum_{l=1}^{q}\widehat{\mathrm{Cov}}_{S_1}(\widehat{\beta}_k,\widehat{\beta}_l)\widehat{d}_{2,l}\sum_{i\in I_n}\frac{\widehat{d}_{1,k}(\boldsymbol{u}_i)}{\pi(\boldsymbol{u}_i)} - \frac{1}{\widehat{A}^2}\sum_{k=1}^{q}\sum_{l=1}^{q}\widehat{\mathrm{Cov}}_{S_1}(\widehat{\beta}_k,\widehat{\beta}_l)\widehat{d}_{2,k}\widehat{d}_{2,l}\\
&= \frac{1}{2\widehat{A}^2}\sum_{i\in I_n}\sum_{j\in J_{n,i}}\frac{\Delta(\boldsymbol{u}_i,\boldsymbol{u}_j)}{\pi(\boldsymbol{u}_i,\boldsymbol{u}_j)}\left(\frac{\widehat{\lambda}^\star(\boldsymbol{u}_i) - \widehat{R}^\star(\widehat{\boldsymbol{\beta}})z(\boldsymbol{u}_i)}{\pi(\boldsymbol{u}_i)} - \frac{\widehat{\lambda}^\star(\boldsymbol{u}_j) - \widehat{R}^\star(\widehat{\boldsymbol{\beta}})z(\boldsymbol{u}_j)}{\pi(\boldsymbol{u}_j)}\right)^2\\
&\quad+\frac{1}{\widehat{A}^2}\sum_{k=1}^{q}\sum_{l=1}^{q}\widehat{\mathrm{Cov}}_{S_1}(\widehat{\beta}_k,\widehat{\beta}_l)\sum_{i\in I_n}\frac{\widehat{d}_{1,k}(\boldsymbol{u}_i) - z(\boldsymbol{u}_i)\widehat{d}_{2,k}/\widehat{A}}{\pi(\boldsymbol{u}_i)}\sum_{j\in I_n}\frac{\widehat{d}_{1,l}(\boldsymbol{u}_j) - z(\boldsymbol{u}_j)\widehat{d}_{2,l}/\widehat{A}}{\pi(\boldsymbol{u}_j)}\\
&\quad+\frac{2}{\widehat{A}^2}\sum_{k=1}^{q}\sum_{l=1}^{q}\widehat{\mathrm{Cov}}_{S_1}(\widehat{\beta}_k,\widehat{\beta}_l)\widehat{d}_{2,l}\sum_{i\in I_n}\frac{\widehat{d}_{1,k}(\boldsymbol{u}_i)}{\pi(\boldsymbol{u}_i)} - \frac{1}{\widehat{A}^2}\sum_{k=1}^{q}\sum_{l=1}^{q}\widehat{\mathrm{Cov}}_{S_1}(\widehat{\beta}_k,\widehat{\beta}_l)\widehat{d}_{2,k}\widehat{d}_{2,l},
\end{aligned} \tag{A.24}$$

where $\widehat{d}_{1,k}$ and $\widehat{d}_{2,k}$ are as defined in (21).

Appendix B. Case with divided plots

It can happen that sample plots are divided into several parts, for example if one part of the plot is in forests and other parts are in other landscape categories, or if the plot overlaps borders between different regions, strata or forest stands (for example in the Swedish NFI, Anon. 2014). In such cases, the covariate information is not the same in different parts of the plot. Let us consider a case where we want to study expected plant densities in forests, and consider a particular plot $C(\boldsymbol{u}_i)$. Then let $I_{\mathbf{u}}$ be equal to 1 if $\boldsymbol{u}$ is in a forested area in U, and 0 otherwise. If the plot is divided and no part of the plot is in a forested area in U,

$$\lambda^\star(\boldsymbol{u}_i) = \int_{C(\boldsymbol{u}_i)} \frac{\lambda_{\boldsymbol{\beta}}(\boldsymbol{u}) I_{\boldsymbol{u}}}{a_{\boldsymbol{u}}} d\boldsymbol{u} = 0 \quad \text{and} \quad \widehat{\lambda}^\star(\boldsymbol{u}_i) = 0. \tag{B.1}$$

If only one part of the plot is in a forested area in U, and if we denote the area of this part by $a_i^{(s)}$,

$$\lambda^\star(\boldsymbol{u}_i) = \int_{C(\boldsymbol{u}_i)} \frac{\lambda_{\boldsymbol{\beta}}(\boldsymbol{u}) I_{\boldsymbol{u}}}{a_{\boldsymbol{u}}} d\boldsymbol{u} = \lambda_{\boldsymbol{\beta}}(\boldsymbol{u}'_i) \frac{a_i^{(s)}}{a} \quad \text{and} \quad \widehat{\lambda}^\star(\boldsymbol{u}_i) = \lambda_{\widehat{\boldsymbol{\beta}}}(\boldsymbol{u}'_i) \frac{a_i^{(s)}}{a}, \tag{B.2}$$

where $\lambda_{\widehat{\boldsymbol{\beta}}}(\boldsymbol{u}_i) = \exp(\widehat{\boldsymbol{\beta}}^{\mathrm{T}} \boldsymbol{x}(\boldsymbol{u}_i)) = \exp(\widehat{\boldsymbol{\beta}}^{\mathrm{T}} \boldsymbol{x}_i)$ and $\boldsymbol{u}'_i$ is an arbitrary point in the forested part of $C(\boldsymbol{u}_i) \cap U$. If $C(\boldsymbol{u}_i)$ has two parts that are in forests within U (with areas $a_i^{(s_1)}$ and $a_i^{(s_2)}$ respectively), then

$$\lambda^\star(\boldsymbol{u}_i) = \lambda_{\boldsymbol{\beta}}(\boldsymbol{u}'_i) \frac{a_i^{(s_1)}}{a} + \lambda_{\boldsymbol{\beta}}(\boldsymbol{u}''_i) \frac{a_i^{(s_2)}}{a} \quad \text{and} \quad \widehat{\lambda}^\star(\boldsymbol{u}_i) = \lambda_{\widehat{\boldsymbol{\beta}}}(\boldsymbol{u}'_i) \frac{a_i^{(s_1)}}{a} + \lambda_{\widehat{\boldsymbol{\beta}}}(\boldsymbol{u}''_i) \frac{a_i^{(s_2)}}{a} \tag{B.3}$$

where $\boldsymbol{u}'_i$ is an arbitrary point in the first forest part of $C(\boldsymbol{u}_i) \cap U$ and $\boldsymbol{u}''_i$ is an arbitrary point in the second forest part of $C(\boldsymbol{u}_i) \cap U$. And so on with three or more forest parts. Thus, the change of expression of $\widehat{\lambda}^\star(\boldsymbol{u}_i)$ will imply changes when applying formulas (16) and (A.24) for estimating the expected density and its variance estimator. Similar changes need to be done in the cluster sampling case presented in Section 2.5.

Appendix C. Details of the proposed goodness-of-fit test

Assume that there are two disjoint vegetation plots, A_{i1} and A_{i2}, contained in each (main) plot i, where all A_{ij} are of size a_A, $i = 1, \ldots, n$. Each vegetation plot A_{i1} and A_{i2} in a pair is separated by the same distance d. In each A_{ij}, the presence or absence of the plant species of interest is registered. Let M_i be the number of plants in plot A_i, $i = 1, \ldots, n$. Let Y_{ij} be 1 if presence in A_{ij}, and 0 otherwise, $i = 1, \ldots, n$, $j = 1, 2$. In our case, the M_i are not observed, contrary to the Y_{ij}, hence the necessity to develop a test based on the latter. Based on the sample of Y_{ij} data and corresponding covariate data x_i (assumed to be fixed in plot i), an estimator $\widehat{\boldsymbol{\beta}}$ of the parameter vector $\boldsymbol{\beta}$ is obtained using a binary regression with a complementary log-log link function (5). Let Y_i be 1 if there is at least one point in the union of A_{i1} and A_{i2}, and 0 otherwise. Based on a binary regression with a complementary log-log link function, offset $\log(2a_A)$, and the data $\{Y_i, x_i\}$, $i = 1, \ldots, n$, another estimator of $\boldsymbol{\beta}$ is constructed, denoted by $\widetilde{\boldsymbol{\beta}}$.

If the inhomogeneous Poisson point process model assumption is correct, then so is the model for the Y_{ij}. The reverse is not necessarily true. However, if the model for the Y_{ij} is incorrect, then so is the Poisson model for the M_i.

If the inhomogeneous Poisson point process model is correct, Y_{i1} and Y_{i2} will be independent conditional on the covariates, and binary regression model (5) implies the binary regression model based on the data $\{Y_i, x_i\}$. In this case, $\widehat{\boldsymbol{\beta}}$ and $\widetilde{\boldsymbol{\beta}}$ will be close for large n. On the other hand, if Y_{i1} and Y_{i2} are not independent conditional on the covariates, then this implication will not hold and $\widehat{\boldsymbol{\beta}}$ and $\widetilde{\boldsymbol{\beta}}$ will likely differ even if n is large. Based on this idea, Ekström et al. (Unpublished results) suggested the test statistic

$$S = (\widehat{\boldsymbol{\beta}} - \widetilde{\boldsymbol{\beta}})^{\mathrm{T}} \ \widehat{\boldsymbol{\Sigma}}^{-1} (\widehat{\boldsymbol{\beta}} - \widetilde{\boldsymbol{\beta}}), \tag{C.1}$$

where $\widehat{\boldsymbol{\Sigma}}$ is an estimate of the covariance matrix of $\widehat{\boldsymbol{\beta}} - \widetilde{\boldsymbol{\beta}}$ given by

$$\widehat{\boldsymbol{\Sigma}} = n\big(\widehat{\boldsymbol{I}}_1^{-1}(\widehat{\boldsymbol{\beta}}) + \widehat{\boldsymbol{I}}_2^{-1}(\widehat{\boldsymbol{\beta}}) - 2\widehat{\boldsymbol{I}}_1^{-1}(\widehat{\boldsymbol{\beta}}) \widehat{\boldsymbol{C}}(\widehat{\boldsymbol{\beta}}) \widehat{\boldsymbol{I}}_2^{-1}(\widehat{\boldsymbol{\beta}})\big),$$

where

$$\widehat{\boldsymbol{I}}_1(\boldsymbol{\beta}) = \frac{1}{n} \sum_{i=1}^{n} \frac{2}{[g'(q_{i1}(\boldsymbol{\beta}))]^2 t_{i1}(\boldsymbol{\beta})} \boldsymbol{x}_i \boldsymbol{x}_i^{\mathrm{T}},$$

$$\widehat{\boldsymbol{I}}_2(\boldsymbol{\beta}) = \frac{1}{n} \sum_{i=1}^{n} \frac{1}{[g'(q_i(\boldsymbol{\beta}))]^2 t_i(\boldsymbol{\beta})} \boldsymbol{x}_i \boldsymbol{x}_i^{\mathrm{T}},$$

$$\widehat{\boldsymbol{C}}(\boldsymbol{\beta}) = \frac{2}{n} \sum_{i=1}^{n} \frac{1}{g'(q_i(\boldsymbol{\beta})) t_i(\boldsymbol{\beta})} \frac{1}{g'(q_{i1}(\boldsymbol{\beta})) t_{i1}(\boldsymbol{\beta})} q_{i1}(\boldsymbol{\beta})(1 - q_i(\boldsymbol{\beta})) \boldsymbol{x}_i \boldsymbol{x}_i^{\mathrm{T}},$$

$q_{ij}(\boldsymbol{\beta}) = 1 - \exp(-a_A \exp(\boldsymbol{\beta}^{\mathrm{T}} \boldsymbol{x}_i))$, $t_{ij}(\boldsymbol{\beta}) = q_{ij}(1 - q_{ij})$, $q_i(\boldsymbol{\beta}) = 1 - \exp(-2a_A \exp(\boldsymbol{\beta}^{\mathrm{T}} \boldsymbol{x}_i))$, $t_i(\boldsymbol{\beta}) = q_i(1 - q_i)$, and $g(p) = \log(-\log(1 - p))$.

If the Poisson model is valid, S is asymptotically distributed according to a chi-squared distribution with q degrees of freedom, where q is the length of $\boldsymbol{\beta}$. The binary model (5),and hence the Poisson model, is rejected if S is improbably large according to this chi-squared distribution. For small or

moderately large sample sizes, a better option might be to use parametric bootstrap (Davison and Hinkley, 1997). The bootstrap algorithm for computing the *p*-value of the test is given below.

For $b = 1,\ldots,B$, where B is a large integer:

i) For A_{ij}, generate points according to a Poisson point process with log intensity $\log\widehat{\lambda}_i = \widehat{\boldsymbol{\beta}}^{\mathrm{T}}\boldsymbol{x}_i$, $i = 1,\ldots,n$, $j = 1,2$.

ii) Based on the point data obtained in i), let Y^*_{ijb} be 1 if presence in A_{ij} and 0 otherwise, and let $Y^*_{ib} = max\left\{Y^*_{i1b}, Y^*_{i2b}\right\}$, $i = 1,\ldots,n$.

iii) Let S^* be defined as in (C.1), but based on $\left\{Y^*_{ijb}\right\}$ and $\left\{Y^*_{ib}\right\}$ rather than $\left\{Y_{ij}\right\}$ and $\{Y_i\}$.

The p-value of the test is given by the proportion of times S^* is larger than or equal to S.

References

Albert, P.S., McShane, L.M., 1995. A Generalized Estimating Equations Approach for Spatially Correlated Binary Data: Applications to the Analysis of Neuroimaging Data. Biometrics 51 (2), 627–638. https://doi.org/10.2307/2532950.

Ambler, G., Benner, A., 2015. mfp: Multivariable Fractional Polynomials. R Pack. Vers. 1 (5), 2. https://CRAN.R-project.org/package=mfp.

Anon, 2014. Fältinstruktion 2014, RIS, Riksinventeringen av skog [Field Instructions for the Swedish National Forest Inventory and the Swedish Forest Soil Inventory]. The Swedish University of Agricultural Sciences, Umeå, Sweden (In Swedish).

Artdatabanken, 2022. Artportalen. https://www.artdatabanken.se/sok-art-och-miljodata/artportalen/. Retrieved 17 August 2022.

Baddeley, A., Berman, M., Fisher, N.I., Hardegen, A., Milne, R.K., Schuhmacher, D., Turner, R., 2010. Spatial logistic regression and change-of-support for Poisson point processes. Electron. J. Stat. 4, 1151–1201. https://doi.org/10.1214/10-EJS581.

Baddeley, A., Rubak, E., Turner, R., 2016. Spatial Point Patterns: Methodology and Applications with R. CRC Press, Boca Raton. https://doi.org/10.1201/b19708.

Baena, S., Boyd, D.S., Moat, J., 2018. UAVs in pursuit of plant conservation-real world experiences. Eco. Inform. 47, 2–9. https://doi.org/10.1016/j.ecoinf.2017.11.001.

Bastow Wilson, J., 2012. Species presence/absence sometimes represents a plant community as well as species abundances do, or better. J. Veg. Sci. 23 (6), 1013–1023. https://doi.org/10.1111/j.1654-1103.2012.01430.x.

Belbin, L., 2011. The Atlas of Living Australia's Spatial Portal. In: Jones, M.B., Gries, C. (Eds.), Proceedings of the Environmental Information Management Conference 2011 (EIM 2011), pp. 39–43 (Santa Barbara).

Cassel, C., Särndal, C.E., Wretman, J.H., 1977. Foundations of inference in survey sampling. Wiley, New York. https://doi.org/10.2307/3314835.

CBD, 2002. Global Strategy for Plant Conservation. The Secretariat of the Convention on Biological Diversity, Montreal, Canada.

Commission of the European Communities, 2003. Council directive 92/43/EEC of 21 May 1992 on the conservation of natural habitats and of wild fauna and flora. Official Journal of the European Union 1. 236 99 23.9.2003, Brussels. European Commission 1992/95/2003.

Condés, S., McRoberts, R.E., 2017. Updating national forest inventory estimates of growing stock volume using hybrid inference. For. Ecol. Manag. 400, 48–57. https://doi.org/10.1016/j.foreco.2017.04.046.

Conlisk, E., Conlisk, J., Harte, J., 2007. The impossibility of estimating a negative binomial clustering parameter from presence-absence data: a comment on He and Gaston. Am. Nat. 170 (4), 651–659. https://doi.org/10.1086/521339.

Cordy, C.B., 1993. An extension of the Horvitz-Thompson theorem to point sampling from a continuous universe. Stat. Probab. Lett. 18 (5), 353–362. https://doi.org/10.1016/0167-7152(93)90028-H.

Corona, P., Fattorini, L., Franseschi, S., Scrinzi, G., Torresan, C., 2014. Estimation of standing wood volume in forest compartments by exploiting airborne laser scanning information: model-based, design-based and hybrid perspectives. Can. J. For. Res. 44 (11), 1303–1311. https://doi.org/10.1139/cjfr-2014-0203.

Daley, D.J., Vere-Jones, D., 2003. An introduction to the theory of point processes: volume I: elementary theory and methods. Springer. https://doi.org/10.1007/b97277.

Davison, A., Hinkley, D., 1997. Bootstrap Methods and their Application (Cambridge Series in Statistical and Probabilistic Mathematics). Cambridge University Press. https://doi.org/10.1017/CBO9780511802843.

Delignette-Muller, M.-L., Dutang, C., 2015. fitdistrplus: An R Package for Fitting Distributions. J. Stat. Softw. 64 (4), 1–34. https://doi.org/10.18637/jss.v064.i04.

Dubayah, R., Armston, J., Healey, S.P., Bruening, J.M., Patterson, P.L., Kellner, J.R., Duncanson, L., Saarela, S., Ståhl, G., Yang, Z., Tang, H., Bryan Blair, J., Fatoyinbo, L., Goetz, S., Hancock, S., Hansen, M., Hofton, M., Hurtt, G., Luthcke, S., 2022. GEDI launches a new era of biomass inference from space. Environ. Res. Lett. 17 (9), 095001 https://doi.org/10.1088/1748-9326/ac8694.

Ekström, M., Esseen, P.-A., Westerlund, B., Grafström, A., Jonsson, B.G., Ståhl, G., 2018. Logistic regression for clustered data from environmental monitoring programs. Eco. Inform. 43, 165–173. https://doi.org/10.1016/j.ecoinf.2017.10.006.

Ekström, M., Sandring, S., Grafström, A., Esseen, P.-A., Jonsson, B.G., Ståhl, G., 2020. Estimating density from presence-absence data in clustered populations. Methods Ecol. Evol. 11 (3), 390–402. https://doi.org/10.1111/2041-210X.13347.

Ekström, M., Gozé, L., Wallerman, J., Dahlgren, J., Jonsson, B.-G., Sandring, S., Ståhl, G., 2023. Model-based estimation and mapping of plant density based on remote sensing and presence/absence data.

Esseen, P.-A., Ekström, M., 2023. Influence of canopy structure and microclimate on three-dimensional distribution of the iconic lichen Usnea longissimi. For. Ecol. Manag. 529, 120667 https://doi.org/10.1016/j.foreco.2022.120667.

Esseen, P.-A., Ekström, M., Grafström, A., Jonsson, B.G., Palmqvist, K., Westerlund, B., Ståhl, G., 2022. Multiple drivers of large-scale lichen decline in boreal forest canopies. Glob. Chang. Biol. 28 (10), 3293–3309. https://doi.org/10.1111/gcb.16128.

Fithian, W., Elith, J., Hastie, T., Keith, D.A., 2015. Bias correction in species distribution models: pooling survey and collection data for multiple species. Methods Ecol. Evol. 6 (4), 424–438. https://doi.org/10.1111/2041-210X.12242.

Foody, G.M., 2008. Refining predictions of climate change impacts on plant species distribution through the use of local statistics. Eco. Inform. 3 (3), 228–236. https://doi.org/10.1016/j.ecoinf.2008.02.002.

Fortin, M., Manso, R., Calama, R., 2016. Hybrid estimation based on mixed-effects models in forest inventories. Can. J. For. Res. 46 (11), 1310–1319. https://doi.org/10.1139/cjfr-2016-0298.

Fortin, M., Manso, R., Schneider, R., 2018. Parametric bootstrap estimators for hybrid inference in forest inventories. Forestry 91 (3), 354–365. https://doi.org/10.1093/forestry/cpx048.

Fortin, M., Lier, O.V., Côté, J.-F., 2023. Combining forest growth models and remotely sensed data through a hierarchical model-based inferential framework. Can. J. For. Res. 53, 1–13. https://doi.org/10.1139/cjfr-2022-0168.

Fridman, J., Holm, S., Nilsson, M., Nilsson, P., Ringvall, A.H., Ståhl, G., 2014. Adapting National Forest Inventories to changing requirements – the case of the Swedish National Forest Inventory at the turn of the 20th century. Silva Fennica 48 (3). https://doi.org/10.14214/sf.1095.

Futschik, A., Winkler, M., Steinbauer, K., Lamprecht, A., Rumpf, S.B., Barančok, P., Palaj, A., Gottfried, M., Pauli, H., 2020. Disentangling observer error and climate change effects in long-term monitoring of alpine plant species composition and cover. J. Veg. Sci. 31 (1), 14–25. https://doi.org/10.1111/jvs.12822.

Gallegos Torell, Å., Glimskär, A., 2009. Computer-aided calibration for visual estimation of vegetation cover. J. Veg. Sci. 20 (6), 973–983. https://doi.org/10.1111/j.1654-1103.2009.01111.x.

Gaston, K.J., He, F., Maguran, A., McGill, B., 2011. Species occurrence and occupancy. Biol. Divers. 141–151.

GBIF, 2022. What Is GBIF? Available from. https://www.gbif.org/what-is-gbif.

Gotway, C.A., Stroup, W.W., 1997. A Generalized Linear Model Approach to Spatial Data Analysis and Prediction. J. Agric. Biol. Environ. Stat. 2 (2), 157–178. https://doi.org/10.2307/1400401.

Grafström, A., Schnell, S., Saarela, S., Hubbell, S.P., Condit, R., 2017. The continuous population approach to forest inventories and use of information in the design. Environmetrics 28 (8). https://doi.org/10.1002/env.2480.

Gregoire, T.G., Valentine, H.T., 2007. Sampling Strategies for Natural Resources and the Environment. Chapman & Hall/CRC. https://doi.org/10.1201/9780203498880.

He, F., & Gaston, K.J. (2000). Estimating species abundance from occurrence. Am. Nat., 156 (5). 553–559. ISSN 0003–0147.

He, F., Gaston, K., Wu, J., 2002. On species occupancy-abundance models. Écoscience 9 (1), 119–126. https://doi.org/10.1080/11956860.2002.11682698.

Heagerty, P.J., Lele, S.R., 1998. A Composite Likelihood Approach to Binary Spatial Data. J. Am. Stat. Assoc. 93 (443), 1099–1111. https://doi.org/10.2307/2669853.

Heeringa, S.G., West, B.T., Berglund, P.A., 2010. Applied Survey Data Analysis. Chapman and Hall/CRC, Boca Raton. https://doi.org/10.1201/9781420080674.

Hoem, S., 2022. Norwegian Biodiversity Information Centre - Other Datasets. Version 13.236. The Norwegian Biodiversity Information Centre (NBIC). https://doi.org/10.15468/tm56sc. Occurrence dataset.

Holt, A.R., Gaston, K.J., He, F., 2002. Occupancy-abundance relationships and spatial distribution: a review. Basic Appl. Ecol. 3 (1), 1–13. https://doi.org/10.1078/1439-1791-00083.

Horvitz, D.G., Thompson, D.J., 1952. A generalization of sampling without replacement from a finite universe. J. Am. Stat. Assoc. 47 (260), 663–685. https://doi.org/10.1080/01621459.1952.10483446.

Huggins, R., Hwang, W.-H., Stoklosa, J., 2018. Estimation of abundance from presence–absence maps using cluster models. Environ. Ecol. Stat. 25, 495–522. https://doi.org/10.1007/s10651-018-0415-5.

Hwang, W.-H., Huggins, R., 2016. Estimating abundance from presence–absence maps via a paired Negative-Binomial Model. Scand. J. Stat. 43 (2), 573–586. https://doi.org/10.1111/sjos.12192.

Hwang, W.-H., Huggins, R., Stoklosa, J., 2022. A model for analyzing clustered occurrence data. Biometrics 78 (2), 598–611. https://doi.org/10.1111/biom.13435.

Kennedy, K.A., Addison, P.A., 1987. Some considerations for the use of visual estimates of plant cover in biomonitoring. J. Ecol. 151-157 https://doi.org/10.2307/2260541.
Kercher, S.M., Frieswyk, C.B., Zedler, J.B., 2003. Effects of sampling teams and estimation methods on the assessment of plant cover. J. Veg. Sci. 14 (6), 899–906. https://doi.org/10.1111/j.1654-1103.2003.tb02223.x.
Lindenmayer, D.B., Welsh, A., Donnelly, C., Crane, M., Michael, D., Macgregor, C., McBurney, L., Montague-Drake, R., Gibbons, P., 2009. Are nestboxes a viable alternative source of cavities for hollow-dependent animals? Long-term monitoring of nest box occupancy, pest use and attrition. Biol. Conserv. 142, 33–42. https://doi.org/10.1016/j.biocon.2008.09.026.
Margolis, H., Nelson, R., Montesano, P., Beaudoin, A., Sun, G., Andersen, H.-E., Wulder, M., 2015. Combining Satellite lidar, Airborne lidar and Ground Plots to Estimate the Amount and Distribution of Aboveground Biomass in the Boreal Forest of North America. Can. J. For. Res. 45 (7), 838–855. https://doi.org/10.1139/cjfr-2015-0006.
McRoberts, R.E., Næsset, E., Liknes, G.C., Chen, Q., Walters, B.F., Saatchi, S., Herold, M., 2019. Using a Finer Resolution Biomass Map to Assess the Accuracy of a Regional, Map-Based Estimate of forest Biomass. Surv. Geophys. 40 (4), 1001–1015. https://doi.org/10.1007/s10712-019-09507-1.
Nelson, R., Gobakken, T., Næsset, E., Gregoire, T.G., Ståhl, G., Holm, S., Flewelling, J., 2012. Lidar sampling - using an airborne profiler to estimate forest biomass in Hedmark County, Norway. Remote Sens. Environ. 123, 563–578. https://doi.org/10.1016/j.rse.2011.10.036.
O'Connor, B., Bojinski, S., Röösli, C., Schaepman, M.E., 2020. Monitoring global changes in biodiversity and climate essential as ecological crisis intensifies. Eco. Inform. 55, 101033 https://doi.org/10.1016/j.ecoinf.2019.101033.
Olsson, B., 2020. National Land Cover Database. Swedish Environmental Protection Agency, Stockholm. https://www.naturvardsverket.se/en/services-and-permits/maps-and-map-services/national-land-cover-database/.
Pain, D.J., Bardin, P., Hutchinson, N., Pénzesné Kónya, E., Krause, M., 2020. A review of European progress towards the Global Strategy for Plant Conservation 2011-2020. Planta Eur. Plantlife Int. XXXpp.
Phillips, S.J., Anderson, R.P., Dudík, M., Schapire, R.E., Blair, M.E., 2017. Opening the black box: an open-source release of Maxent. Ecography 40, 887–893. https://doi.org/10.1111/ecog.03049.
Pielou, E.C., 1977. Mathematical Ecology. Wiley.
R Core Team, 2022. R: A Language and Environment for Statistical Computing. R Foundation for Statistical Computing, Vienna, Austria. URL. https://www.R-project.org/.
Ringvall, A., Petersson, H., Ståhl, G., Lämås, T., 2005. Surveyor consistency in presence/absence sampling for monitoring vegetation in a boreal forest. For. Ecol. Manag. 212 (1–3), 109–117. https://doi.org/10.1016/j.foreco.2005.03.002.
Royle, J.A., Dorazio, R.M., 2008. Hierarchical modeling and inference in ecology: the analysis of data from populations, metapopulations and communities. Academic Press, London. https://doi.org/10.1016/B978-0-12-374097-7.50001-5.
Saarela, S., Schnell, S., Grafström, A., Tuominen, S., Nordkvist, K., Hyyppä, J., Kangas, A., Ståhl, G., 2015. Effects of sample size and model form on the accuracy of model-based estimators of growing stock volume. Can. J. For. Res. 45 (11), 1524–1534. https://doi.org/10.1139/cjfr-2015-0077.
Saarela, S., Holm, S., Healey, S.P., Patterson, P.L., Yang, Z., Andersen, H.-E., Dubayah, R. O., Qi, W., Duncanson, L.I., Armston, J.D., Gobakken, T., Næsset, E., Ekström, M., Ståhl, G., 2022. Comparing frameworks for biomass prediction for the global ecosystem dynamics investigation. Remote Sens. Environ. 278 https://doi.org/10.1016/j.rse.2022.113074.
Särndal, C.-E., Swensson, B., Wretman, J., 1992. Model Assisted Survey Sampling. Springer. https://doi.org/10.1007/978-1-4612-4378-6.
Sauerbrei, W., Royston, P., 1999. Building multivariable prognostic and diagnostic models: transformation of the predictors by using fractional polynomials. J. R. Stat. Soc. Ser. A 162 (1), 71–94. https://doi.org/10.1111/1467-985X.00122.
Sen, P.K., Singer, J.M., 1993. Large Sample Methods in Statistics: An Introduction with Applications. Chapman & Hall, New York.
Solow, A.R., Smith, W.K., 2010. On predicting abundance from occupancy. Am. Nat. 176 (1), 96–98. https://doi.org/10.1086/653077.
Sreekumar, E.R., Nameer, P.O., 2022. A MaxEnt modelling approach to understand the climate change effects on the distributional range of white-bellied Sholakili Sholicola albiventris (Blanford, 1868) in the Western Ghats, India. Ecol. Inform. 70 https://doi.org/10.1016/j.ecoinf.2022.101702.
Ståhl, G., 2003. Presence/absence sampling as a substitute for cover assessment in vegetation monitoring. In: Corona, P., Köhl, M., Marchetti, M. (Eds.), Advances in Forest Inventory for Sustainable Forest Management and Biodiversity Monitoring. Kluwer Academic Publishers, pp. 137–142. https://doi.org/10.1007/978-94-017-0649-0_11.
Ståhl, G., Holm, S., Gregoire, T.G., Gobakken, T., Næsset, E., Nelson, R., 2011. Model-based inference for biomass estimation in a LiDAR sample survey in Hedmark County, Norway. Can. J. For. Res. 41 (1), 96–107. https://doi.org/10.1139/X10-161.
Ståhl, G., Saarela, S., Schnell, S., Holm, S., Breidenbach, J., Healey, S.P., Patterson, P.L., Magnussen, S., Næsset, E., McRoberts, R.E., Gregoire, T.G., 2016. Use of models in large-area forest surveys: comparing model-assisted, model-based and hybrid estimation. Forest Ecosyst. 3 (5) https://doi.org/10.1186/s40663-016-0064-9.
Ståhl, G., Ekström, M., Dahlgren, J., Esseen, P.-A., Grafström, A., Jonsson, B.G., 2017. Informative plot sizes in presence-absence sampling of forest floor vegetation. Methods Ecol. Evol. 8 (10), 1284–1291. https://doi.org/10.1111/2041-210X.12749.
Stoklosa, J., Blakey, R.V., Hui, F.K.C., 2022. An Overview of Modern Applications of Negative Binomial Modelling in Ecology and Biodiversity. Diversity 14 (5), 320. https://doi.org/10.3390/d14050320.
Tillé, Y., 2006. Sampling Algorithms. Springer, New York. ISBN 0-387-30814-8.
Tomppo, E., Gschwantner, T., Lawrence, M., McRoberts, R.E. (Eds.), 2010. National Forest Inventories. Pathways for Common Reporting, 1. European Science Foundation, pp. 541–553. https://doi.org/10.1007/978-90-481-3233-1.
Waagepetersen, P., 2007. An estimating function approach to inference for inhomogeneous Neyman–Scott processes. Biometrics 63, 252–258. https://doi.org/10.1111/j.1541-0420.2006.00667.x.
Wan, J.-Z., Wang, C.-J., Yu, F.-H., 2017. Wind effects on habitat distributions of wind-dispersed invasive plants across different biomes on a global scale: assessment using six species. Eco. Inform. 42, 38–45. https://doi.org/10.1016/j.ecoinf.2017.09.002.
Warton, D.I., Foster, S.D., De'ath, G., Stoklosa, J., Dunstan, P.K., 2015. Model-based thinking for community ecology. Plant Ecol. 216, 669–682. https://doi.org/10.1007/s11258-014-0366-3.
Wright, D.H., 1991. Correlations Between Incidence and Abundance are Expected by Chance. J. Biogeogr. 18 (4), 463–466. https://doi.org/10.2307/2845487.
Yee, T.W., Mitchell, N.D., 1991. Generalized additive models in plant ecology. J. Veg. Sci. 2, 587–602. https://doi.org/10.2307/3236170.

Acta Universitatis Agriculturae Sueciae

Doctoral Thesis No. 2025:40

This thesis presents new methods to estimate plant abundance from presence/absence data assuming different types of spatial point processes for modelling the plant locations. Model-based and hybrid inference frameworks are applied. In addition, variance estimates are provided, and a broadened analysis of uncertainty is performed in a model-based inference context.

Léna Gozé received xer doctoral education at the Department of Forest Resource Management at the Swedish University of Agricultural Sciences (SLU), Umeå. In 2020, xe was awarded a Master of Science in Statistics from the University of Lille, France.

Acta Universitatis Agriculturae Sueciae presents doctoral theses from the Swedish University of Agricultural Sciences (SLU).

SLU generates knowledge for the sustainable use of biological natural resources. Research, education, extension, as well as environmental monitoring and assessment are used to achieve this goal.

ISSN 1652-6880
ISBN (print version) 978-91-8046-475-8
ISBN (electronic version) 978-91-8046-525-0